Faculty of Science & Engineering
Department of Petroleum Engineering

A Novel CO_2 Flooding Based EOR for Sandstone Reservoirs

Xingguang Xu

This thesis is presented for the Degree of
Doctor of Philosophy
of Petroleum Engineering
Curtin University

October 2016

Declaration

To the best of my knowledge and belief this thesis contains no material previously published by any other person except where due acknowledgment has been made.

This thesis contains no material which has been accepted for the award of any other degree or diploma in any university.

Signature:

Date: 06/10/2016

Acknowledgement

This thesis would not have been possible without the kind support and assistance of a number of people to whom I am greatly indebted.

Foremost, I would like to express my heartiest gratitude to my respected main supervisor, **Senior Lecturer Ali Saeedi** and co-supervisors, **Professor Reza Rezaee** and **Professor Keyu Liu** for their guidance and encouragement. The knowledge, insights and thoughtful suggestions they brought to me truly contribute to the completion of this work. It is absolutely a great honour to work under their supervision which also will benefit my career in the future. I feel tremendously fortunate to have their company during this fantastic journey.

I also place my sincere gratitude to the entire staff and faculty members in the Department of Petroleum Engineering for their unceasing help. Special thanks go to **Technical Officer**, **Bob Webb** for his professional support and wise advise that expedites my research. Thank you, also to **Head of Department**, **Mofazzal Hossain** who serves on the academic committee despite his tight schedule. I am equally grateful for colleagues in Department of Chemical Engineering, Research Institute of Petroleum Exploration and Development (RIPED) and Commonwealth Scientific and Industrial Research Organisation (CSIRO) for the technique supports they provided that was critical for the thesis's development.

Last but not the least, I would take this opportunity to express my deepest and heartfelt gratitude to my **fiancée Shican Liu** and our family members for their unconditional love, constant encouragement and tremendous support that empower me to reach the finish line of this circuitous but beautiful journey. Although my father and grandfather are now in heaven, I can always feel their company and the power they pass on me. I also dedicate this work to the beloved them.

Parts of this work have been published in the following articles:

- Xu, X., Saeedi, A., and Liu, K. (2016) *Laboratory studies on CO_2 foam flooding enhanced by a novel amphiphilic ter-polymer*. Journal of Petroleum Science and Engineering, 138, 153-159
- Xu, X., Saeedi, A., and Liu, K. (2017) *Experimental study on a novel foaming formula for CO_2 foam flooding*. Journal of Energy Resources Technology, in press, 139, 02229021-02229029
- Xu, X., Saeedi, A., and Liu, K. (2017) *Bulk phase behaviour and displacement performance of CO_2 induced by a combined foaming formulation*. Journal of Petroleum Science and Engineering, 147, 864-872
- Xu, X., Saeedi, A., and Liu, K. (2017) An experimental study of combined foam/surfactant polymer (SP) flooding for carbon dioxide-enhanced oil recovery (CO2-EOR), Journal of Petroleum Science and Engineering, 149, 603-611
- Xu, X., Saeedi, A., Rezaee, R., and Liu, K. (2015*) Investigation on a novel polymer with surface activity for polymer enhanced CO_2 foam flooding*. SPE 2015 International Symposium on Oilfield Chemistry, Houston, US
- Xu, X., Saeedi, A., and Liu, K., (2016) *Laboratory Investigation of CO_2 foam flooding for mature fields in Western Australia*. SPE 2016 OTC Conference, Kuala Lumpur, Malaysia

Table of Contents

Executive Summary

An effective and viable way to considerably reduce the CO_2 emission is to inject the CO_2 captured from industrial sources into the depleted oil reservoirs where the unwanted gas can be used as a displacing fluid for the purpose of enhancing oil recovery (EOR). To be more specific, this technique is normally referred to as the CO_2 flooding which can be primarily divided into either immiscible or miscible flooding. Despite its exceptional advantages and broad potential of application, the recovery factor of a typical CO_2 flooding is far below 40% even in the best scenario due to the adverse mobility ratio and the density contrast of the flood resulting in low sweep efficiency.

Over the past several decades, a number of mitigating approaches such as the water-alternating-gas (WAG) flooding, CO_2 thickeners and CO_2 foams have been extensively employed to improve the displacement performance of the CO_2 flooding. Among these techniques, the CO_2 foams are highly recognized due to their remarkable ability to modify the mobility ratio. In turn, the successful application of a foam flooding is strongly dependent on the generation of robust foams in a target porous medium. However, gravity drainage tends to undermine the creation of foam under reservoir condition. Additionally, crude oil is capable of spreading and entering the foams lamellae and thus greatly affecting the foam longevity, leading to the lower than expected displacement efficiency of the CO_2 foam flooding.

In an attempt to maximize the potential of the CO_2-EOR, this research develops and then examines the effectiveness of a novel CO_2-EOR method which combines the advantages of surfactant/polymer (SP), WAG and CO_2 foam flooding. Generally, slugs containing surfactant/polymer and CO_2 foam are injected alternatively; hence the name of this proposed technique is Chemical-Alternating-Foams (CAF) flooding. On one hand, the CO_2 foam is more robust and reliable due to the existence of polymers in the SP slug while the adsorbed and lost surfactant from the foam slugs can be compensated by the SP solution through material exchange. As a result, to some extent, the foaming ability of the CO_2 foam flooding can be maintained if not enhanced. On the other hand, from a micro-scale perspective, instead of being blocked in the pores, the residual oil would be mobilized by the SP solution and with

the improved mobility ratio on a macro reservoir scale, the displacement profile may be controlled to the most extent.

From a broader perspective, two aspects are included in this work: 1) the discovery of a novel foaming formulation that brings together a surfactant with polymer and additives for the use in CO_2 foam flooding; 2) the evaluation and optimization of the chemicals-alternating-foam (CAF) flooding that utilises the above proposed new formulation.

Through a comprehensive and systematic investigation, a new foaming formulation that is able to significantly improve the foam stability without greatly compromise the foaming ability has been identified: 0.5 wt % AOS + 0.15 wt% AVS + 0.5 wt% N70k-T, where AOS, AVS and N70K-T are the surfactant, polymer and chemical additive, respectively. It is found that this proposed formulation results in remarkable resistance factor (RF), residual resistance factor (RRF) and mobility reduction factor (MRF) and thus higher oil recovery factor than that of the conventional CO_2 foam flooding. Besides, the core flooding experiments demonstrate that the CAF flooding that applies this new formulation possesses greater displacement efficiency than either of the CO_2 foam flooding or gas-alternating-solution flooding with the same amount of chemicals and gas employed and conducted at identical testing conditions. It is therefore believed that a CAF flooding using this new formulation might be a promising candidate for CO_2-EOR.

Chapter 1 Introduction

1.1 Background and Problem Description

As a naturel and crucial component of the atmosphere, the CO_2 gas is colourless and odourless at standard conditions (0.1 MPa and 25 °C), and its density and viscosity are 1.98 kg/m^3 and 0.015 cp, respectively (Zondervan et al. 2001). Fig. 1.1 shows the CO_2 phase diagram under a range of temperature and pressure values. Obviously, it maintains its gaseous state at pressure below 0.52 MPa, above which, the CO_2 is able to be liquefied. Referring to Fig. 1.1, the triple point at which the three possible phases of CO_2 can coexist is identified to be around 0.52 MPa at – 56.56 °C. The critical point, which is the end point of the phase equilibrium curve, is found at 7.38 MPa and 31.10 °C above which CO_2 would exist in the supercritical state which exhibits unique properties midway between the gas and liquid phases (Nediljko and Dirk, 2014). The supercritical or dense CO_2 has been broadly applied for the aerogel production, sterilization of biomedical materials, extraction of essential oil and enhanced oil recovery (EOR) (Yeo and Kiran, 2005; Pint and Keiser, 2014; Bolmatov et al., 2014).

Apart from its wide useful industrial and scientific applications, CO_2 is also the primary greenhouse gas that plays a critical role in increasing the global temperatures. This phenomenon is known as the “global warming” which is believed to impose detrimental impact on the climate and ecological systems. Especially in the recent decades, global warming has caused a number of severe and negative environmental effects (Dimento and Doughman, 2007; Lu et al. 2007; England 2014; Scheffer et al. 2006).

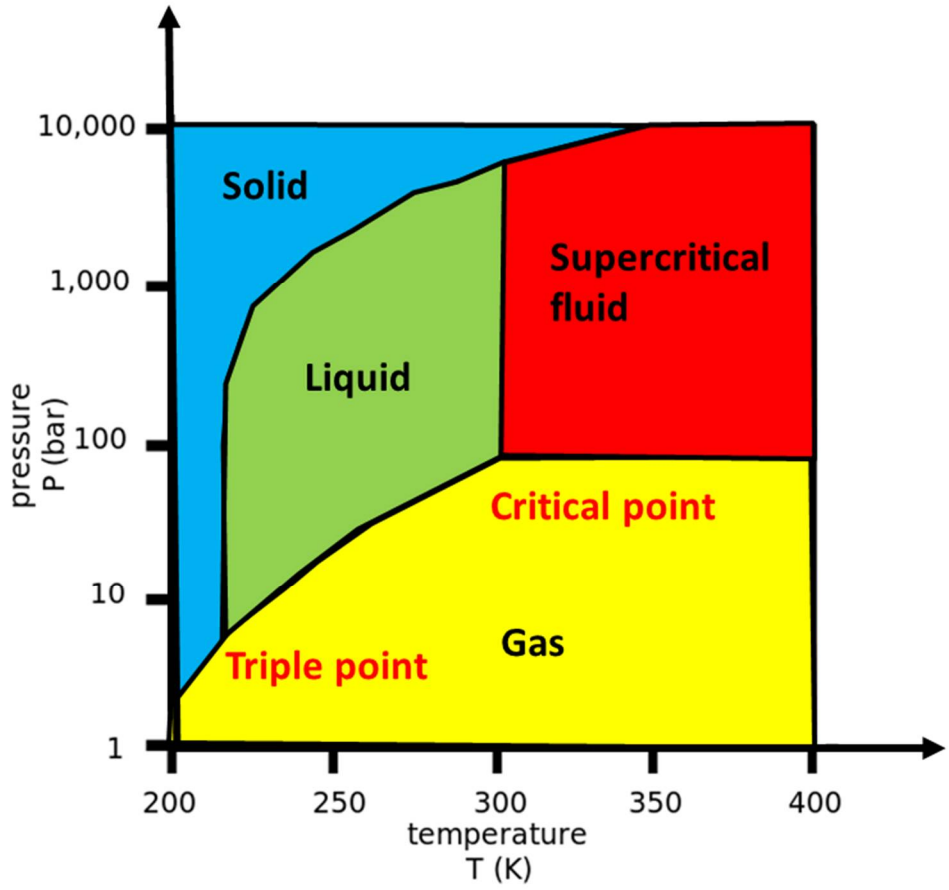

Fig. 1.1 Carbon dioxide pressure-temperature phase diagram (modified after Finney and Jacobs, 2010)

Perhaps the most efficient and viable way to deal with the greenhouse gas effect is to inject the CO_2 into the depleted reservoirs where it can be used as a displacing fluid for the purpose of enhancing oil recovery (EOR). To be more specific, this technique is referred to as CO_2-EOR (Fig. 1.2). Based on the entirely different phase behaviours between the injected CO_2 fluid and crude oil under reservoir condition, CO_2 flooding can be primarily divided into immiscible flooding and miscible flooding (Holm 1982; Fulop et al. 1997). Under immiscible conditions, CO_2 is capable of lowering the crude oil viscosity dramatically as well as swelling the in-situ oil (Hao et al. 2004). In particular, above the so called minimum miscibility pressure (MMP), CO_2 miscible flooding is extraordinary effective in mobilizing the trapped oil at the microscopic level through extracting light components out of the crude oil (Salem and Moawad, 2013). With the completion of the EOR process, parts of the injected CO_2 are permanently stored in the depleted and abandoned oil reservoir. CO_2-EOR, thereby, mitigates the energy crisis and global warming at the same time, which aids the energy security and

environmental sustainability accordingly (US National Energy Technology Laboratory, 2011; Godec, 2010). It is also worth mentioning the injection of CO_2 for the enhanced gas recovery (EGR) has been discussed for 15 years, but has not been practiced and commercially applied.

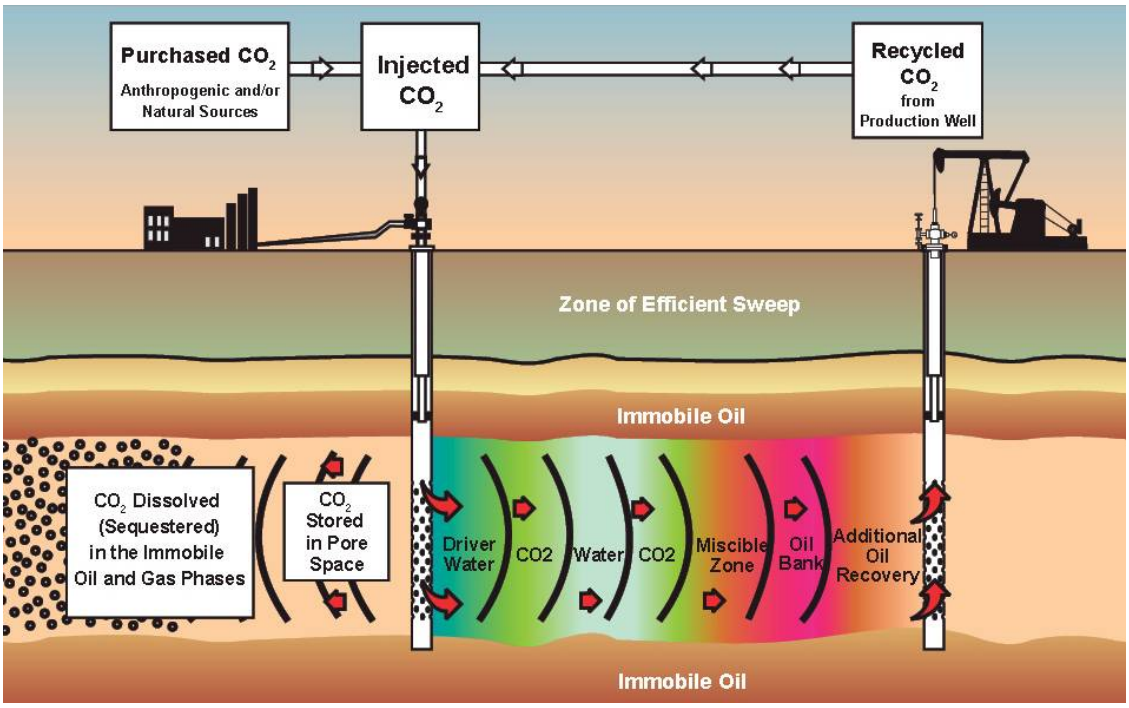

Fig. 1.2 Illustration of CO_2-EOR process **(**Advanced Resources International and Melzer Consulting, prepared for UK Department of Energy & Climate Change, 2010)

Since the successful implementation of the first field test in 1972 (Texas, US), CO_2 flooding has been applied to improve oil production from depleted oil formations worldwide. A few examples include the application of CO_2 from industrial sources in Croatia for a CO_2 flooding pilot test at Ivanic Field (Novosel, 2005); the active CO_2-EOR projects operating since mid-1970s in Trinidad (Moritis, 2008); a number of CO_2 floods in the Rio Pojuca fields and Mirange Field for the purpose of improved oil recovery (IOR) and carbon control strategy in Brazil (Guedes, 2008). Hungary also has decades of experience in CO_2 flooding projects among which Budafa Field and Lovvaszi Field were the two cases have been well documented (Remenyi et al. 1995). A number of field operators and organizations in Canada has been also very active assessing the CO_2-EOR potential over the past decades (Bachu et al. 2000). Petroleum Technology Alliance of Canada (PTAC) estimated the CO_2-EOR potential in Alberta region could reach 3.6 billion barrels in the near future (Byfield et al. 2009). The cases mentioned above represent the popularity of the CO_2 floods which are applicable to a

wide variety of reservoirs, either onshore or offshore, either sandstone or carbonate, either mature or water flooded, either conventional or unconventional.

Despite its exceptional advantages and broad applications, CO_2 flooding is not able to reach 100 % oil recovery factor even in the best scenario. Typically, 10-20% of the original oil in place (OOIP) is recovered by the miscible CO_2 flooding after the secondary recovery which is capable of displacing 20-40% OOIP on its own, while the immiscible CO_2 flooding is only able to recovery an additional 5-10% of the oil in the formation (Moritis, 2002). Consequently, a large portion of the OOIP still remains unrecovered even after ample CO_2 is introduced into the target reservoir. The chief cause of this unsatisfactory displacement performance of CO_2 flooding is the low viscosity of dense or supercritical CO_2, as shown in Fig. 1.3. As can be seen, the CO_2 viscosity increases with the density, but its typical values (0.05-0.1 cP) are far lower than that of most of the formation brines or crude oils. This large viscosity contrast between CO_2 and reservoir fluids can result in adverse mobility ratio which leads to frontal instability of CO_2 flooding and thus low sweep efficiency. Fig. 1.4 clearly demonstrates the effect of the mobility ratio on the areal sweep efficiency. Accordingly, problems such as viscous fingering, early CO_2 breakthrough, low oil production rate and high CO_2 utilization ratios take place during a typical CO_2 flooding (Lescure and Claridge, 1986; Rogers and Grigg, 2011; Dugstad et al. 2011). The second cause of the low recovery factor of CO_2 flooding is the low density of the CO_2 even in its dense supercritical state, as shown in Fig. 1.5. The relatively low density of CO_2 compared to the crude oil results in the gravity segregation and poor oil recovery in the base of the reservoir.

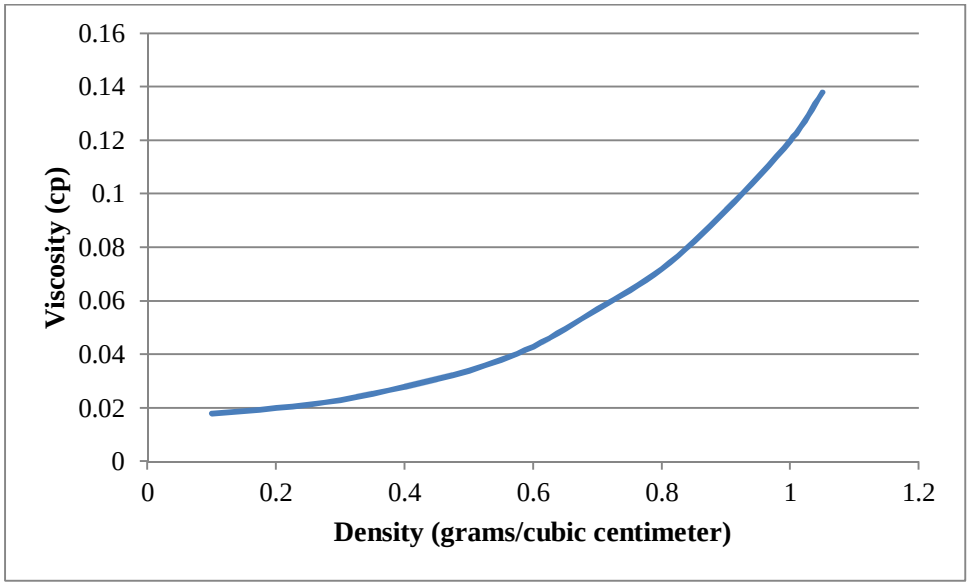

Fig. 1.3 Viscosity of CO_2 at 32°C and ambient pressure (modified after Chung and Nguyen, 1985)

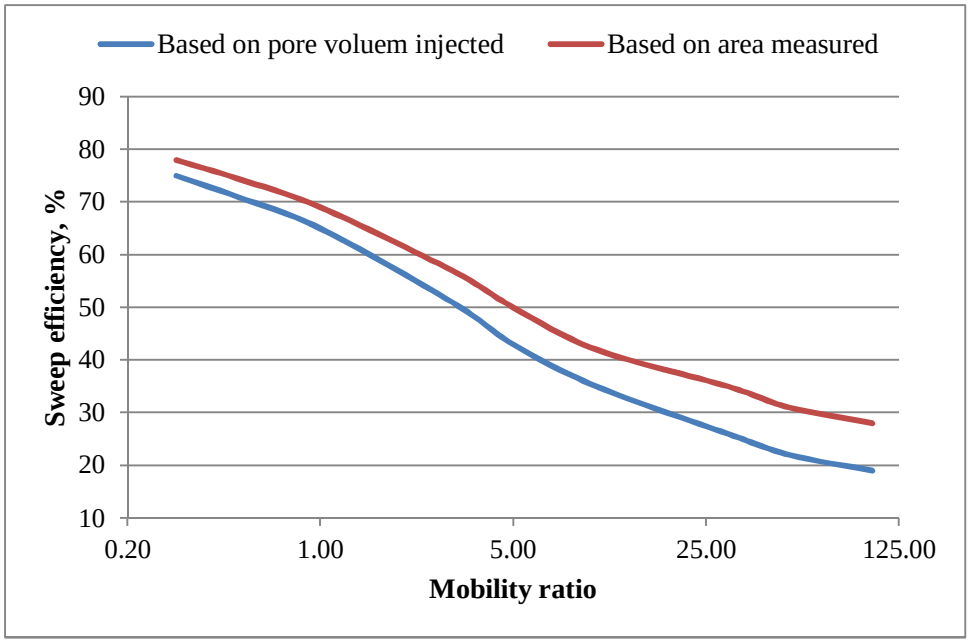

Fig. 1.4 Effect of mobility ratio on sweep efficiency at breakthrough for CO_2 miscible floods (modified after Habermann, 1960)

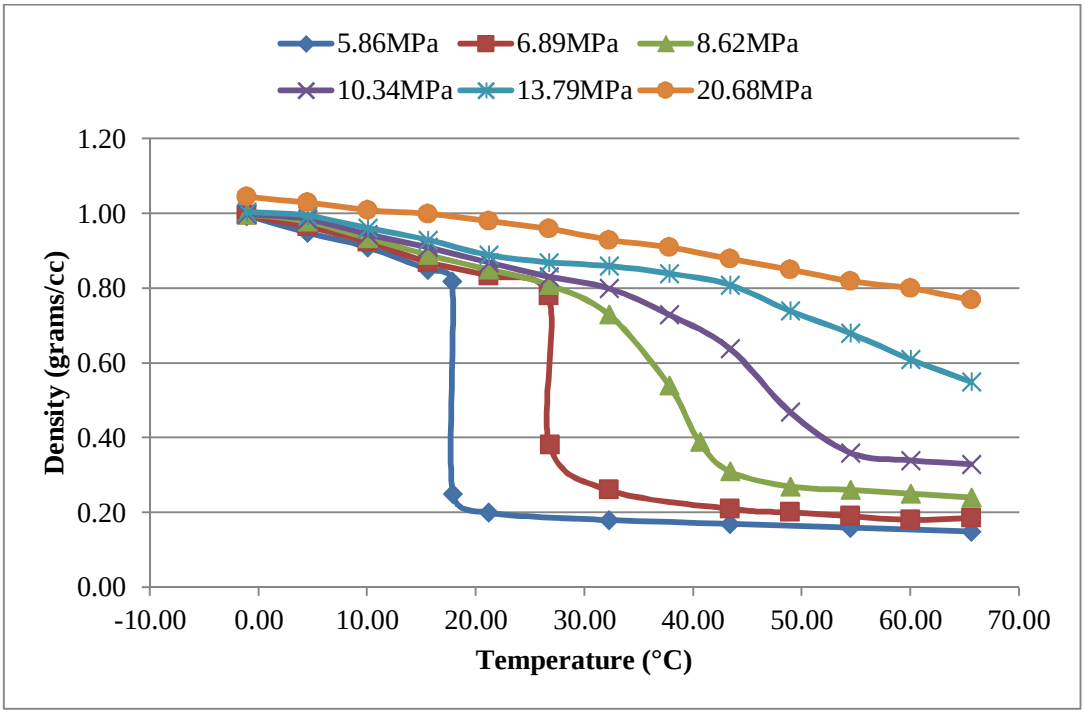

Fig. 1.5 Dense of CO_2 under various temperature and pressure (modified after Ely and Hanley, 1987)

It is also noted that there are other issues that can compromise the effectiveness of a CO_2 flooding as means of EOR. For instance, sometimes the CO_2 flooding is not completely miscible because of the oil composition and reservoir conditions, resulting in an unsatisfactory ultimate recovery factor. However, compared to viscous fingering and gravity override, these problems seem to be less significant, and this is basically why the mobility control and profile modification are considered to be the most serious concerns when CO_2 flooding is performed (Bae and Irani 1993; Borchardt et al. 1985; Dugstad et al. 2011). Mobility control generally tends to tackle the CO_2 early breakthrough that stems from the viscosity and density variance between CO_2 and formation water/crude oil, while profile modification technique attempts to mitigate the either naturally controlled or man-made reservoir heterogeneity. To date, there have been extensive studies conducted by various researchers trying to address these two issues. The various technologies examined are as follows. It is worth noting that extensive details of the studies listed below will be presented in subsequent chapters of this dissertation. The aim of this introductory chapter is to present a brief description of them only.

- *Water-alternating-gas flooding (WAG)*: Dyes and Caudle (1958) developed the idea of injecting water in alternation with the gas which drives the miscible slug. This injected water reduces the relative permeability to gas and thus lowers the total mobility (Caudle and Dyes 1958). As explained earlier, due to the density and viscosity contrast, it is hard for CO_2 and water to move evenly, thus WAG injection has been widely accepted since 1970's based on the theory that alternating gas and water is necessary to implement mobility control (Merchant 2010). Oil recovery by CO_2 WAG injection has been attributed to contact of unswept zones, especially recovery of attic or cellar oil, which is usually achieved by taking advantage of the segregation of gas to the top and the accumulation of water toward the bottom (Christensen et al. 2001).
- *CO_2 thickeners*: Some approaches attempt to increase the in-situ bulk viscosity of CO_2 by the use of a polymer that is sufficiently soluble in dense CO_2. Generally, a more viscous displacing phase results in a more favourable mobility ratio. Polymers thereby can serve as mobility control agents or thickeners. There have been a wide range of studies conducted evaluating the effectiveness of this process. Heller et al. (1985) pointed out that more than a dozen polymers were found to be soluble at least in the parts-per-thousand (ppt) range in the liquid and dense CO_2. Moreover, the solubilities of these polymers generally increased with increase in the CO_2 density. Terry et al. (1987) successfully increased CO_2 viscosity by in-situ polymerization of monomers which are miscible with CO_2. In another study, Bae and Irani (1993) presented a thickened CO_2 process utilizing a commercial silicone polymer and toluene as a co-solvent, and it was measured that the CO_2 viscosity was increased by two orders in magnitude; Xu et al. (2001) synthesized a fluoroacrylate-styrene copolymer (polyFAST) which was reportedly able to increase the in-situ CO_2 viscosity by 10 folds in dilute concentration without the presence of a co-solvent.
- *CO_2 foams*: By injecting foamed CO_2 stabilized by surfactants or nanoparticles, both the aerial and vertical sweep efficiencies can be significantly improved no matter the CO_2 is in the gas phase or dense/supercritical state (Ren et al. 2013). This benefit stems from the reduction of gas mobility by the presence of thin foam film, named lamellae. Foaming ability and foam stability are the two most essential variables when designing and implementing a foam flooding (Permadi, et al. 2013). The creation and coalescence of lamellae have remarkable effect on the foaming ability in porous

media while foam stability is generally determined by both the molecular structure of foaming agents and the formation in-situ condition. Studies conducted on the CO_2 foam floods have been focusing on several aspects of the foods: (1) Synthesis and evaluation of the foaming agents (Borchardt, et al. 1985, Tortopidis, 1994, Kang et al. 2010); (2) Foam creation and coalescence mechanisms (Kam et al. 2004); (3) Modelling foam in porous media (Zhou and Rossen, 1995, Kam and Mayberry, 2006), and (4) Foam injection schemes (Bogdanovic, et al. 2009).

- *Other techniques*: Apart from the conventional mobility and conformance control techniques stated above, a number of trials have also been conducted trying to maximize the EOR potential of the CO_2 floods. Hild et al., (1999) presented the application of a chromic-acetate-acrylamie gel to modify the injection profile of the CO_2 flooding in north-western Colorado and found this technique to be more effective in very high permeability area; Majidaie, et al. (2012) proposed the chemically enhanced water-alternating-gas flooding (CWAG) technique which used alkaline, surfactant and polymer as the chemical slug during a WAG process and simulated the performance of CWAG using a commercial software (CMG-STAR); Zhang, et al. (2010) investigated the oil recovery of coupled CO_2 and polymer injection and compared the results with those of polymer flooding alone and the WAG process; Behzadi and Towler (2009) developed the process of alkaline-surfactant-gas (ASG) injection which replaced the alkaline-surfactant-polymer (ASP) flooding by using foam rather than polymer as a mobility control agent.

Nearly each of the proposed CO_2-EOR methods named above possesses its own deficiencies. Regarding the WAG technique, injected water blocks the oil in pores and impedes the contact of dense CO_2 with the crude oil, causing the typical recovery factor for WAG injection, as reported in the literature, to be only 5-8% of OOIP (Christensen et al. 2001; Mirkalaei, et al. 2011); the primary impediment to employ the CO_2 thickeners is unaffordable cost as well as the potential negative effect on the environment. Furthermore, the poor injectivity of the thickened CO_2 is another major concern in the process engineering of field operation of such technique; when it comes to CO_2 foam flooding, the first issue requiring to be addressed is the foam stability (Schramm et al. 1990). Currently, foams cannot be well stabilized in heterogeneous reservoirs or the reservoir with harsh conditions during the field test. This may suggest a great mount of CO_2 may leak through the open flow channels to the production wellbore or to the surface. The second problem that affects the displacement performance of

the CO_2 foam flooding is the adsorption loss which greatly reduces the amount of the surfactant that employed in the foam generation and regeneration in porous rocks (Falcone et al. 1982). Besides, most of the new techniques mentioned above for mobility and conformance control are in their infancies or investigated only by conducting desktop numerical simulation research techniques; their viabilities, thereby, have not been validated yet.

1.2 Research Objectives

From a broader perspective, the objective of this research is twofold. One objective is to help the current efforts made in the scientific community to find a way to reduce the global CO_2 emissions as an effective way to combat global warming. The main specific objective of this work is to find an efficient way through which CO_2 could be used for EOR purposes.

Therefore, primarily, this research aims to develop and examine the effectiveness of a novel CO_2-EOR method which combines the advantages of surfactant/polymer (SP) flooding, WAG and CO_2 foam flooding. Slugs containing surfactant/polymer and CO_2 foam are injected alternatively; hence the name of this proposed technique is Chemical-Alternating-Foams (CAF) flooding. On one hand, CO_2 foams are more robust and reliable due to the existence of polymers in the SP slug while the adsorbed surfactant in the foam slugs can be compensated by SP solution through material exchange, then to some extent, the foaming ability of the CO_2 foam flooding can be maintained if not enhanced On the other hand, from a micro-scale perspective, instead of being blocked in the pores, the residual oil would be mobilized by the SP solution and with the improved mobility ratio, on a macro reservoir scale, the displacement profile may be controlled to the most extent.

In order to achieve the above stated primary objective of this study a purpose built experimental approach was employed with following main objectives:

- Finding and screening suitable chemicals and formulations including surfactants, polymers and additives in order to establish the CO_2 foam system which is endowed with appropriate foaming ability and foam durability.
- Validating the effectiveness of the developed foaming formulation in porous media and comparing its displacement performance with that of the conventional CO_2 foam flooding at miscible and immiscible conditions.

- Evaluating the effect of critical operation parameters such as the foam quality, chemical concentrations, foam/chemicals slug size ratio as well as the injection scheme on the chemical alternating foam (CAF) performance by carrying out extensive core flooding experiments.

1.3 Organization of Thesis

This thesis is organized in five chapters. Following this short introductory chapter, Chapter 2 presents a comprehensive review of the previously developed and examined CO_2-EOR techniques. The first part in this chapter describes the mechanisms, strengths and faults of the widely acknowledged CO_2 flooding while the second part focuses mainly on the promising alternatives of CO_2 flooding which contribute to modifying the mobility ratio and controlling the injection profile. In this part, special attention has been given to the CO_2 foam flooding technique. The impediments to the broad application of these reviewed techniques are also included in this part. Chapter 3 presents the experimental materials and methods which are applied in this research. Detailed experimental procedures for each method used are also provided here. The Chapter 4 presents the assessment the results along with the interpretation, analysis and discussion of these results. Lastly, Chapter 5 summarizes the research outcomes, and based on the experimental findings, several conclusions are made. This chapter ends with a few recommendations for any similar research to be conducted in the future in the area of CO_2-EOR.

References

Bachu S, Brulotte M, Grobe M, Stewart S, (2000). Suitability of the Alberta Subsurface for Carbon-Dioxide Sequestration in Geological Media. Alberta Energy and Utilities Board: Calgary, Canada.

Bae JH, and Irani CA, (1993). A laboratory investigation of viscosified CO_2 process." SPE Advanced Technology Series 1(1): 166-17.

Behzadi S, Towler BF, (2009). A New EOR Method. SPE Annual Technical Conference and Exhibition. New Orleans, Louisiana, USA.

Bogdanovic M, Gajbhiye RN, and Kam SI, (2009). Experimental study of foam flow in horizontal pipes: Two flow regimes and its implications. Colloids Surf A Physicochem Eng Asp 344(1–3): 56-71.

Bolmatov D, Zavyalov D, Gao M, Zhernenkov M, (2014). Structural evolution of supercritical CO_2 across the Frenkel Line. J. Phys. Chem. Lett., 5 (16): 2785–2790.

Borchardt, JK, Bright DB, Dickson MK, and Wellington SL, (1985). Surfactants for CO_2 foam flooding. SPE Annual Technical Conference and Exhibition. Las Vegas, Nevada, USA.

Byfield M, Husky and PTAC, (2009). Propose A Game-Changing CO_2 EOR Project. Oil Gas Inquirer, 5.

Caudle BH, and Dyes AB, (1958). Improving Miscible Displacement by Gas-Water Injection. SPE-911-G.

Christensen JR, Stenby EH, Skauge A, (2001). Review of WAG field experience. SPE Reservoir Eval Eng 4(2): 97-106

Chung E, Nguyen H, (1985). Carbon Dionde Thermodynamic Properties [Computer] Program; National Institute for Petroleum and Energy Research: Bartlesville, OK.

DiMento JFC, Doughman, PM, (2007). Climate Change: What It Means for Us, Our Children, and Our Grandchildren. The MIT Press. p. 68

Dugstad O, Opel K, Fjelde I, (2011). Improved understanding of CO_2/foam EOR techniques by aid of tracer technology. SPE EUROPEC/EAGE Annual Conference and Exhibition. Vienna, Austria.

Ely JF, Hanley JM, (1987). TRAPP—Transport Properties Prediction [Computer] Program; Thermophysical Properties Division, National Institute of Standardsand Technology: Boulder, CO.

England M, (2014). Recent intensification of wind-driven circulation in the Pacific and the ongoing warming hiatus. 227–Change 4: 222 .Nat. Clim

Falcone JS, Krumrine PH, Schweiker GC, (1982). The use of inorganic sacrificial agents in combination with surfactants in enhanced oil recovery. J. Am. Oil Chem. Soc. 59(10): 826A-832A.

Finney B, Jacobs M (2010). Carbon dioxide pressure-temperature phase diagram. https://en.wikipedia.org/wiki/File:Carbon_dioxide_pressure-temperature_phase_diagram.svg

Fulop R, Biro Z, Gombos Z, Papay J, Tramboczky (1997). Enhanced oil recovery by CO_2 flooding. 15th World Petroleum Congress. Beijing, China., World Petroleum Congress.George K, Ziska LH, Bunce JA, Quebedeaux B, (2007). Elevated atmospheric CO2 concentration and temperature across an urban–rural transect. Atmospheric Environment 41 (35): 7654–7665.

Godec ML, (2010). Advanced Resources International. U.S. Oil Production Potential From Accelerated Deployment of Carbon Capture and Storage.

Guedes S, (2008) 70% Recovery Factor: Petrobras Perspective. Rio Oil & Gas Exposition and Conference. Rio de Janeiro, Brazil.

Hao Y, Wu Z, Ju B, Chen Y, Luo X, (2004). Laboratory investigation of CO_2 flooding. Nigeria Annual International Conference and Exhibition. Abuja, Nigeria.

Heller JP, Dandge DK, Card RJ, and Donaruma LG, (1985). Direct thickeners for mobility control of CO_2 floods. SOC PETROL ENG J 25(5): 679-686.

Hild GP, Wackowski RK, (1999). Reservoir polymer gel treatments to improve miscible CO_2 flood. SPE Reservoir Eval Eng 2 (02): 196-204.

Holm LW, (1982). CO_2 Flooding: Its Time Has Come. J Petrol. Technol. 34 (12).

Kam SI, Mayberry DJ, (2006). The use of fractional flow theory for foam displacement in presence of oil. SPE Asia Pacific Oil & Gas Conference and Exhibition. Adelaide, Australia.

Kam SI, Nguyen QP, Li Q, Rossen WR, (2004). Dynamic simulations with an improved model for foam generation. SPE Annual Technical Conference and Exhibition. Houston, Texas, USA.

Kang W, Liu S, Meng L, Cao D, Fan H, (2010). A novel Uutra-low interfacial tension foam flooding agent to enhance heavy oil recovery. SPE Improved Oil Recovery Symposium. Tulsa, Oklahoma, USA.

Lescure BM, Claridge EL, (1986). CO_2 foam flooding performance vs. rock wettability. SPE Annual Technical Conference and Exhibition. New Orleans, Louisiana

Lu J, Vechhi GA, Reichler T, (2007). Expansion of the hadley cell under global warming. Geophys. Res. Lett. 34 (6): L06805

Majidaie S, Khanifar A, Onur M, Tan IM, (2012). A simulation study of chemically enhanced water alternating Ggas (CWAG) Injection. SPE EOR Conference at Oil and Gas West Asia. Muscat, Oman.

Merchant DH, (2010). Life Beyond 80: A look at conventional WAG recovery beyond 80% HCPV injected in CO_2 tertiary floods. SPE International Conference on CO2 Capture, Storage, and Utilization. New Orleans, Louisiana, USA.

Mirkalaei SMM, Hoseini J, Masoudi R, Ataei A, Demiral B, Karkooti H, (2011). Investigation of eifferent I-WAG schemes toward optimization of displacement efficiency. SPE Enhanced Oil Recovery Conference. Kuala Lumpur, Malaysia.

Moritis G, (2008) Worldwide EOR Survey. Oil Gas J. 106: 41–42.

Moritis G (2002) Special report: enhanced oil recovery-2002 worldwide EOR survey. Oil Gas J 100:43–47

National Energy Technology Laboratory, Advanced Resources International, (2011). Improving Domestic Energy Security and Lowering CO_2 Emissions with “Next Generation” CO_2-Enahanced Oil Recovery (CO_2-EOR).

Nediljko B, Dirk SM, (2014). Supercritical carbon dioxide and its potential as a life-sustaining solvent in a planetary environment. Life 4 (3): 331–340

Novosel D (2005). Initial results of WAG CO_2 IOR pilot project implementation in Croatia. SPE International Improved Oil Recovery Conference in Asia Pacific. Kuala Lumpur, Malaysia.

Permadi A, Efriza I, Bae W, Muslim M, Pham T, Saputra D Gunadi T, (2013). Optimisation of surfactant concentration to the foam generation and swelling ratio of CO_2 foam flooding in light oil reservoir. SPE Asia Pacific Oil & Gas Conference and Exhibition. Jakarta, Indonesia.

Pint BA, Keiser JR, (2014). The effect of temperature on the sCO_2 compatibility of conventional structural alloys. The 4th International Symposium - Supercritical CO_2 Power Cycle, Pittsburgh, Pennsylvania

Remenyi I, Szittar A, Udvardi G, (1995). CO_2 IOR in the Szank Field using CO_2 from sweetening plant. 8th European Symposium on Improved Oil Recovery. Vienna, Austria.

Ren G, Zhang H, Nguyen Q, (2013). Effect of surfactant partitioning on mobility control during carbon-dioxide flooding. SPE J 18(4): 752-765

Rogers JD, Grigg RB, (2001). A literature analysis of the WAG injectivity abnormalities in the CO_2 process. SPE Reservoir Eval Eng 4(05): 375-386

Salem S, Moawad T, (2013). Economic study of miscible CO_2 flooding in a mature waterflooded oil reservoir. SPE Saudi Arabia Section Technical Symposium and Exhibition. Al-Khobar, Saudi Arabia.

Scheffer M, Brovkin V, Cox P, (2006). Positive feedback between global warming and atmospheric CO_2 concentration inferred from past climate change. Geophys. Res. Lett. 33 (10): L10702

Schramm LL, Novosad JJ, (1990). Micro-visualization of foam interaction with a crude oil. Colloids Surf. 46(1): 21-43.

Terry RE, Zaid A, Angelos C, Whitman DL, (1987). Polymerization in supercritical CO_2 to improve CO_2/Oil mobility ratios. SPE International Symposium on Oilfield Chemistry. San Antonio, Texas, USA.

Tortopidis S, (1994). Carbon dioxide foam flood studies under Australian reservoir conditions. SPE Asia Pacific Oil and Gas Conference. Melbourne, Australia.

U.S. Department of Energy (DOE), (2007). Carbon sequestration atlas of the United States and Canada: U.S. Department of Energy, Office of Fossil Energy, National Energy Technology Laboratory. http://www.netl.doe.gov/technologies/carbon_seq/refshelf/atlas

Xu J, Wlaschin A, Enick RM, (2001). Thickening carbon dioxide with the fluoroacrylate-styrene copolymer. SPE Annual Technical Conference and Exhibition. New Orleans, Louisiana, USA.

Yeo S, Kiran E, (2005). Formation of polymer particles with supercritical fluids: A review. J. Supercrit. Fluids 34: 287–308.

Zhang Y, Huang SS, Luo P, (2010). Coupling immiscible CO_2 technology and polymer injection to maximize EOR performance for heavy oils. J. Can. Pet. Technol 49(5): 25-33.

Zhou Z, Rossen WR, (1995). Applying fractional-flow theory to foam processes at the limiting capillary pressure. SPE Advanced Technology Series 3(01): 154-162

Zondervan I, Zeebe RE, Rost B, Rieblesell U (2001). Decreasing marine biogenic calcification: a negative feedback on rising atmospheric CO_2. Global Biogeochemical Cycles 15 (2): 507–516.

2 Literature Review

2.1 Introduction

Carbon dioxide has been broadly applied to improve the oil production in the water flooded formations for a few decades because of its technically and economically attractive features. In spite of the well-known ability of CO_2 flood to increase the oil recovery factor, its effectiveness could be remarkably improved if the existing constraining developmental concerns such as viscous fingering and gravity segregation stemming from low viscosity and density of CO_2 relative to formation fluids are properly resolved.

This chapter firstly describes the mechanism and the unique features of the CO_2 flood that make it an attractive EOR technique as well as the challenges that impede its wider application. Next, the focus of this review chapter will be on the development of CO_2 mobility and conformance control technologies such as WAG, CO_2 thickeners, CO_2 foam and gels. Special interest will be paid to the past successful and discouraging lab-scale efforts and field pilots of CO_2 foam flooding which is widely acknowledged to be the most attainable and effective alternative among these CO_2-EOR game changers.

2.2 Carbon Dioxide as a Displacing Fluid

2.2.1 Properties of Carbon Dioxide

Carbon dioxide is a natural and essential component of the earth's atmosphere at a concentration of about 350 ppm (Deberry and Clark, 1979). Pure CO_2 gas is odourless, colourless, non-toxic and non-combustible and its molecular weight is 44.0 g/mol (Barrage, 1987). Like any other substance, the phase state of CO_2 is largely dependent on the temperature and pressure. As the main points defining the phase diagram of pure CO_2, the triple point temperature (T_{tr}), triple point pressure (P_{tr}), critical pressure (P_c) and critical temperature (T_c) of pure CO_2 are – 56. 5 °C, 0.51 MPa, 7.39 MPa and 31.1 °C (Baviere, 1980), respectively.

Fig. 2.1 shows the compressibility of CO_2 at various temperatures and pressures. As could be seen, the compressibility of gas is largely dependent on the temperature and the mixture composition. Regardless of the gas type, the gas becomes more compressible with the increasing temperature. In the petroleum industry, CO_2 is desirably compressed to its dense supercritical state which makes it, to some extent, attractive as a displacing fluid with

valuable qualities for the EOR applications such as high degree of miscibility with crude oil, low solubility in formation water, low compressibility, high density, etc. (Sweatman et al. 2009; Moritis, 2002). Moreover, CO_2 exists as a dense supercritical fluid over a large portion of temperature and pressure range of many mature oil reservoirs. In fact, for almost all the reservoirs located at depths greater than 800 m the pressure and temperature would be high enough to have CO_2 in its supercritical state (Saeedi, 2012). This dense CO_2 is completely or partially miscible with the crude oil under reservoir conditions. Ideally, CO_2 miscible flooding may have a displacement efficiency approaching 100% (Salem and Moawad, 2013), but in reality the degree of the miscibility is closely dependent on the reservoir conditions and the crude oil composition (Stalkup, 1982; Hoier and Whitson, 1998). Another encouraging factor is that the dense CO_2 has a quite low solubility in the formation water regardless of the brine salinity as shown in Fig. 2.2. This feature prevents excessive amounts of the dense CO_2 from being lost when CO_2 flooding is carried out in the water flooded reservoirs. Besides, the formation water barely vaporises into the dense CO_2, the miscibility of the crude oil and CO_2 thereby would not be affected even in the presence of the water.

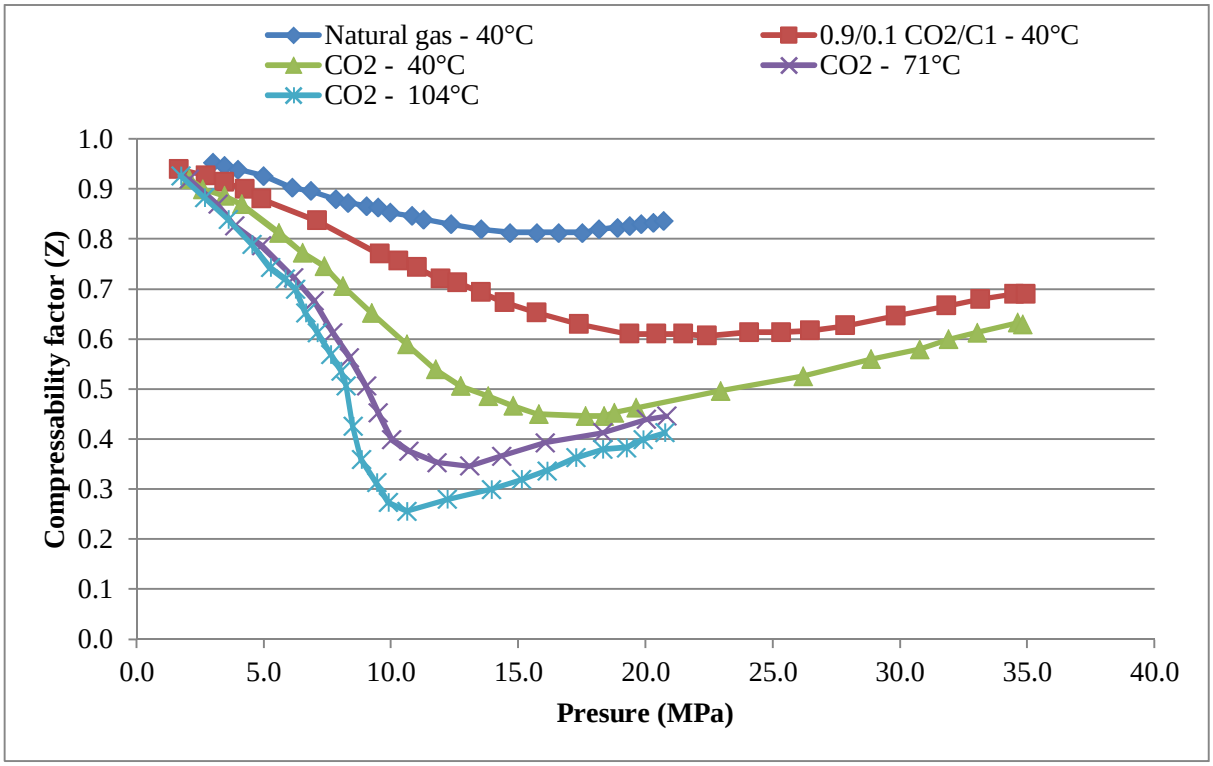

Fig. 2.1 Effect of pressure and temperature on CO_2 compressibility (modified after Macintyre, 1986)

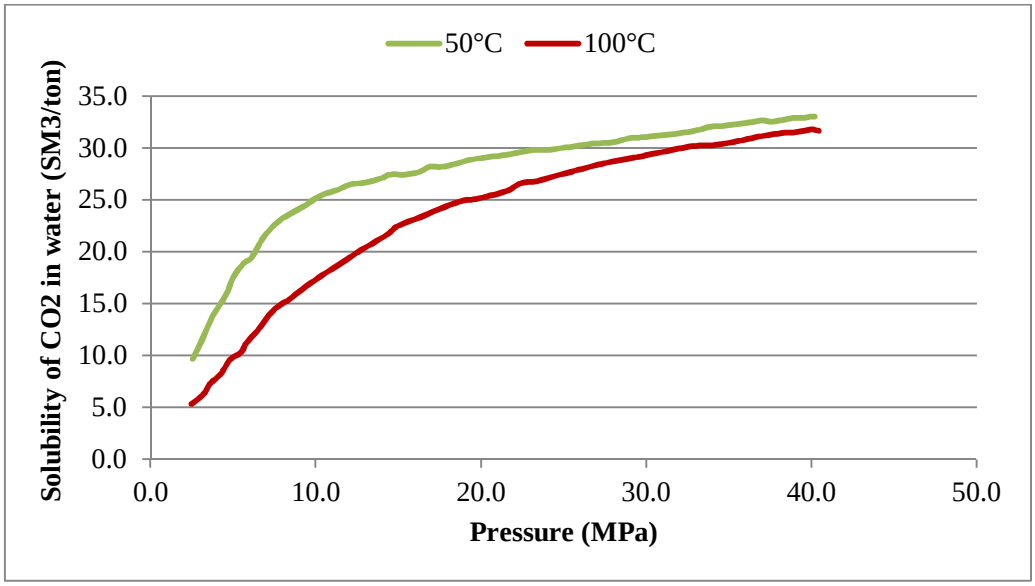

(a)

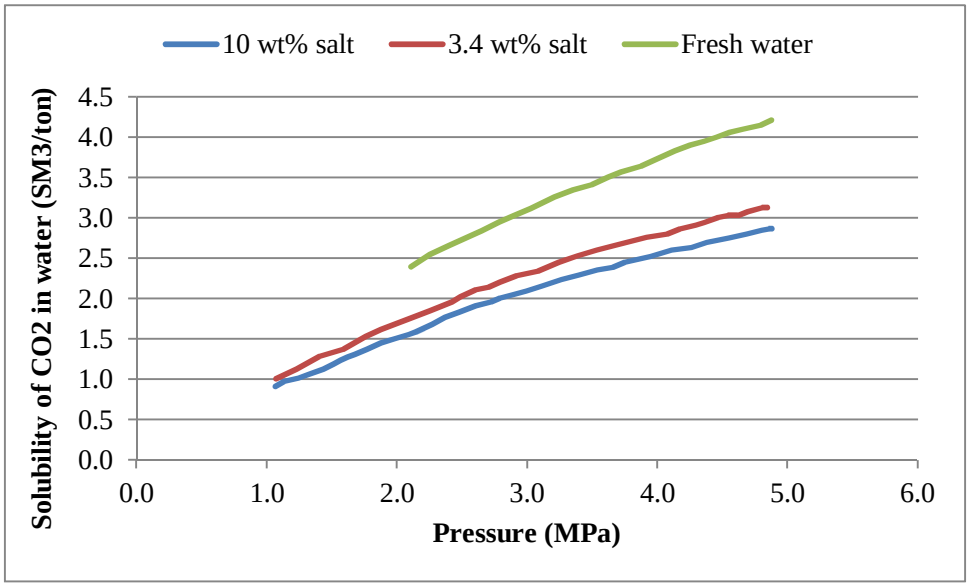

(b)

Fig. 2.2 Effect of temperature and pressure (a) and salinity and pressure (b) on CO_2 solubility (modified after Wiebe and Gady, 1939; Stalkup, 1983)

2.2.2 Interaction between Carbon Dioxide, Rock and Reservoir Fluids

Due to its special qualities as a displacing solvent (a hydrophobic solvent that has a non-polar linear structure), CO_2 actively interacts with the formation rocks, crude oil and brine in a more complex manner than other gases which may be considered for EOR (e.g. natural gas,

N_2). Some of these interactions may be limited to the conditions encountered on the surface but others may occur underground in the reservoir. Of course each of these interactions is expected to impact on the performance and effectiveness of both miscible and immiscible CO_2 flooding in different ways and to different extents. To provide a clearer picture of these complexities, the interactions and their possible consequences are classified in the following groups:

- *CO_2 hydrates*: If water is present, the hydration of CO_2 will take place at temperatures below 10 °C when the pressure is greater than 45 bar (Klauda and Sandler, 2000). Given the favourable pressure and temperature ranges for CO_2 hydrate formation, it is not expected to present any issues downhole or when CO_2 is injected into a formation. However, as also pointed out by Stalkup (1983), the formation of CO_2 hydrates could be a significant concern at chokes and values where a sudden pressure drop may occur in the flow-line. For instance, the North Cross Devonian Unit (located in West Texas) whose wells featured a high gas/oil ratio and CO_2 production did experience the hydrate formation and greatly suffered from this issue (Mizenko, 1992). It is therefore advised that the formation of CO_2 hydrates to be considered as a contributing factor during the decision making process and development planning stages when CO_2 floods are selected as the EOR technique of choice.
- *Scales*: It is well documented that CO_2 injection favours the formation of calcium carbonate scales which greatly reduce the well productivity or productivity (Shuler et al. 1991; Yuan et al. 2001). That is because the bicarbonate concentration in the produced water can increase due to the dissolution of injected CO_2 into the water. Although the scaling problem may not affect the fluid flow in the underground porous formation, it could be a major impediment to maintaining or improving the well injectivity or productivity. Accordingly, appropriate provisions need to be made in the development plan of a CO_2-EOR project so such problems could be avoided as much as possible. Shuler et al. (1991) systematically investigated how to choose an appropriate scale inhibitor which could be used for this purpose. In addition, Yuan et al. (2001) also have provided some insights on approaches used for mineral scale control.
- *Wettability*: Both laboratory studies and pilot tests have indicated that the wettability of the target geological formation plays a vital role in the effectiveness of a CO_2 flooding process. And also, CO_2 is generally considered as a hydrophobic solvent

which affects the wettability. Fig. 2.3 provides an illustration of the pendant drop technique which is based on the measurement of contact angle of CO_2-brine-rock substrate and is one of the most common approaches to determine the wettability in the oil and gas industry. The dissolution of CO_2 leads to reduced pH in the formation brine and alters the rock wettability which is one of the key variables of the operating strategy during a CO_2-EOR process. (Yang et al. 2005; Xu et al. 2005). Rogers et al. (2000) determined that continuous gas injection should be applied in the water-wet formations while WAG technique was suitable for oil-wet formations.

- *Asphaltene precipitation*: Heavy organic components such as asphaltenes are most likely encountered when CO_2 is fed into the underground reservoir in either a immiscible or miscible CO_2 flooding process (OKwen 2006). It is widely believed the magnitude of the asphaltene precipitation largely depends on the composition of crude oil, formation brine and formation rock (Monger and Trujillo, 1991). Without any doubts, asphaltene deposition is unfavourable for the implementation of any CO_2-EOR techniques, because it causes the blockage and plugging of the pores and throats in the underground reservoir (Leontaritis and Ali Mansoori 1988). Accordingly, permeability reduction and decline in production rate take place.
- *Mineral solution and precipitation*: Chemical changes in the deep geologic formation can occur when significant amount of CO_2 is injected (Shao et al. 2010). One change could be the mineral dissolution and the subsequent precipitation of the dissolved mineral phases (Gaus 2010). However, even tiny amount of the mineral deposition can result in noticeable change in the porosity, permeability and rock wettability. For this reason, the transports of CO_2 as well as the integrity of the formation rock are affected to a huge extend (Carroll and Knauss, 2005; Hangx and Spiers, 2009). In recent years, with the assistance of micro-CT and spectroscopic analysis, a large quantity of studies have been conducted to understand the interaction of supercritical CO_2, formation water and minerals during the CO_2 flooding process (Shao et al. 2010; White et al. 2003; Kaszuba et al. 2003).

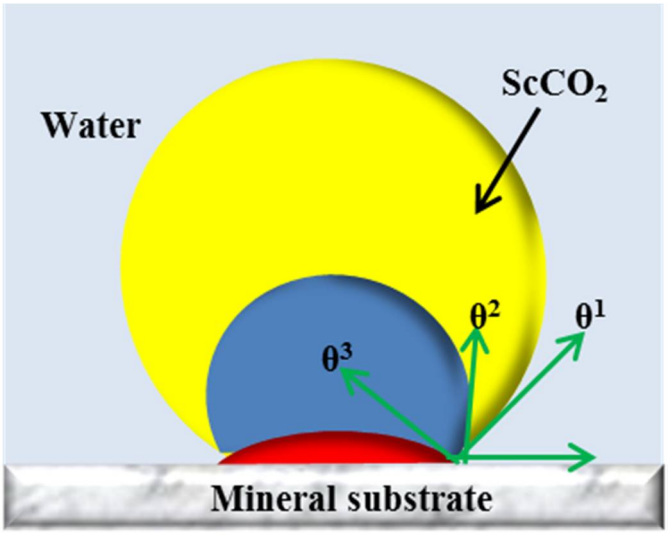

θ^1 Contact angle (water; wetting phase)

θ^2 Contact angle (water; partially wetting)

θ^3 Contact angle (water; non-wetting phase)

Fig. 2.3 Illustration of various wettability stage of supercritical CO_2 (modified after Robin, 2001)

2.2.3 Displacement Mechanisms of Carbon Dioxide Flooding

After primary and secondary recovery stages, an oil field becomes mature and the production rate starts declining sharply, but still leaving a large amount of residual oil behind in the water-flooded formation (Hakiki et al. 2016). Accordingly, with many oil fields nearing their depletion the incentive to increase the oil production through tertiary recovery has grown steeply in the recent decades. CO_2 flooding can be an ideal tertiary recovery technique for the depleted oil reservoirs with depths greater than 800 meters, oil gravity above 22 °API and residual oil saturations more than 25% (Ring and Smith, 1995; Prieditis et al. 1991), since suitable temperature and oil composition are required to maximize the displacement efficiency of the CO_2 flooding. While carbonate formations may present a more complex system in terms of their more pronounced degree of macro- and micro-scale heterogeneities and fluid-rock interactions, both sandstone and carbonate reservoirs are suited for this EOR technology.

On the basis of completely different phase behaviours between CO_2 fluid and crude oil under reservoir condition, CO_2 flooding can be primarily divided into the miscible and immiscible

flooding as the driving mechanisms behind each of these two types of flood are differing (Stalkup, 1978), as outlined in following section of this chapter.

2.2.3.1 Miscibility and Driving Mechanism

The achievable level of miscibility during a CO_2 flood is a strong function of the compositional components of the crude oil. Fig. 2.4 illustrates a typical ternary phase diagram which summarizes various possible driving mechanisms of typical CO_2 flooding. This part of the chapter merely concentrates on describing the miscible CO_2 flooding which is comprised of first contact and multiple contact flooding. The immiscible CO_2 flooding is reviewed in the next part.

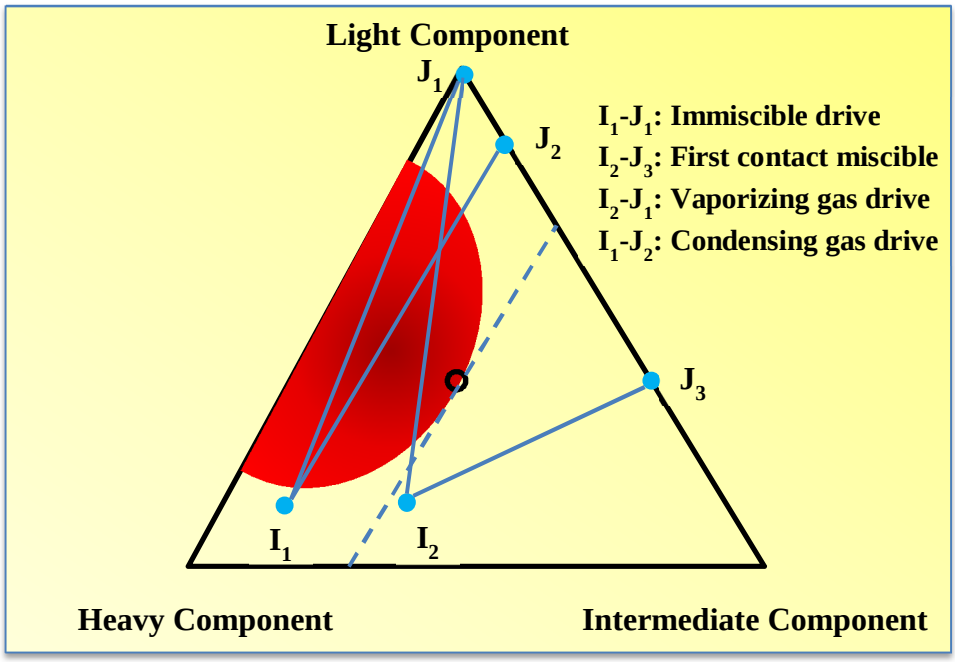

Fig. 2.4 Types of oil displacement by CO_2 flooding (modified after Odd, 2003)

First contact miscible flooding is considered to be the most direct and easiest way to attain miscibility. The injected solvent and crude oil can be mixed in any proportion and form a single phase when they first come in contact with each other at a given reservoir condition (Asar et al. 1989). To achieve the first contact miscible flooding, the injection pressure should be above the first contact minimum miscibility pressure (FCMMP) (Al Wahaibi and Al Hadhrami, 2011). Hydrocarbons such as propane, butane and methane are among the most

common solvents for first contact miscibility (FCM). Though liquid natural gas (LNG) is the most effective solvent, its high cost is a major impediment to its broader application (Al-Shuraiqi et al. 2003). Unfortunately, as for CO_2, it is extremely challenging to reach FCM under the existing condition of a wide spectrum of reservoirs, but CO_2 can relatively readily develop multiple contact miscibility (MCM) which is also known as the dynamic miscibility (Stalkup, 1983).

Apart from enriched natural gas and flue gas, CO_2 is also widely applied as a solvent for the purpose of multiple contact miscible flooding. Two-phase region instead of one-phase region forms when CO_2 and crude oil are mixed directly. In general, the multiple contact miscibility is attained by multiple and repeated processes of mass transfer: the intermediate and heavy components in the crude oil vaporize into the CO_2 phase and CO_2 partially dissolves into the oil (Merchant, 2010). This repeated mass transfer enables the complete miscibility to be achieved and also assists in the development of a transition zone between the displacing and displaced phase which are CO_2 and crude oil, respectively (Jarrell et al. 2002). This transition zone between the injected CO_2 and the oil bank is illustrated in Fig. 2.5. According to the different interaction between CO_2 and oil, there are two primary processes: vaporization gas-drive and condensation gas-drive:

- *Vaporization gas-drive process*: This process specifically refers to vaporization of the intermediate molecular weight hydrocarbons of the crude oil into the bulk phase of CO_2. Usually the vaporization gas drive takes place at the front of the transition zone. Fractions from C_2 to C_{30} are completely extracted by CO_2, therefore, theoretically, nearly 100% of the oil in the formation contacted by CO_2 can be displaced (Orr et al 1981). Compared to other gases, the minimum miscibility pressure (MMP) for CO_2 flood is far lower, which indicates the remarkable achievable injectivity during CO_2 miscible flood process (Orr et al. 1982). Furthermore, as stated above, heavy components of the oil can be extracted by CO_2 miscible flood. Based on the previous research, this process is particularly effective for a reservoir containing oil with a large portion of C_2 to C_6.

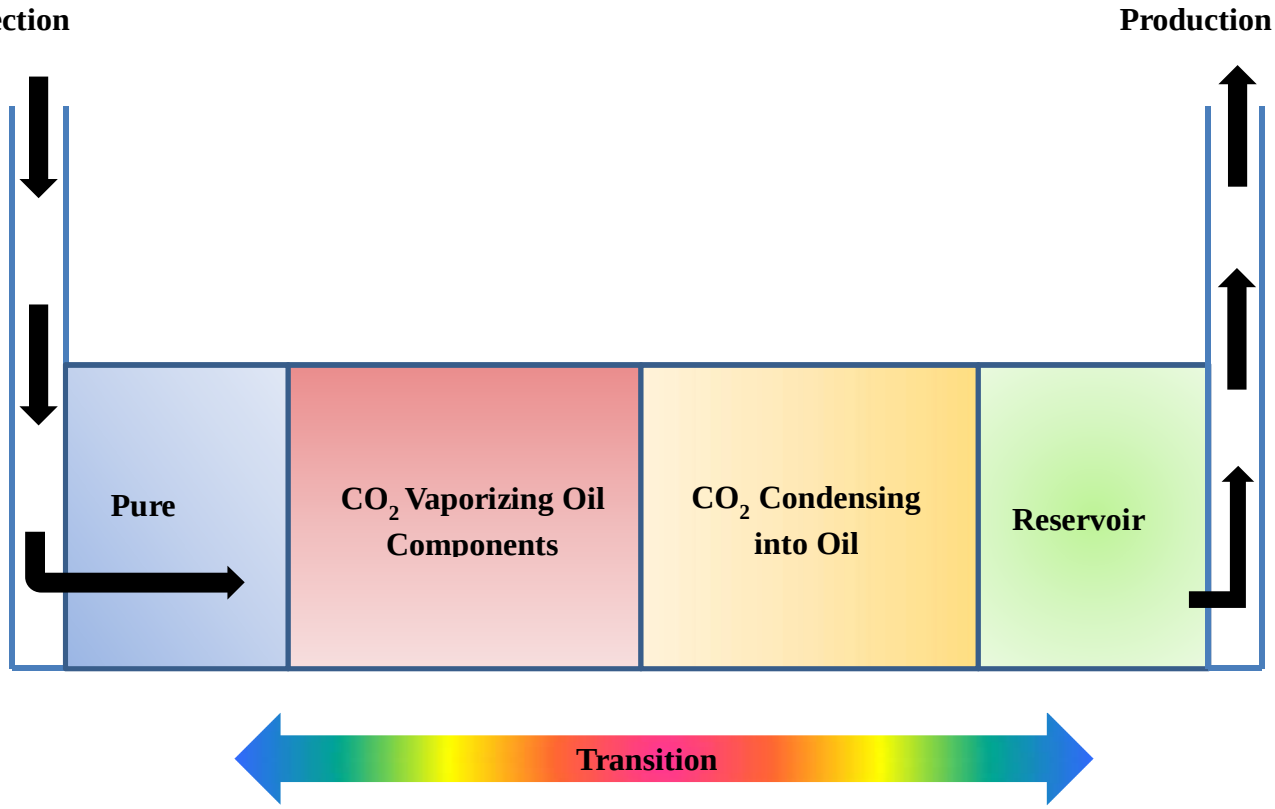

Fig. 2.5 Illustration of the CO_2 miscible flooding with the transition zone (modified after Verma, 2015)

- *Condensation gas-drive process*: When CO_2 is first brought into contact with oil, a two-phase region forms with the oil and solvent being immiscible. The condensation gas drive occurs when a portion of the injected CO_2 dissolves into the oil. Then the oil at the back of the displacement front becomes lighter and more readily mobilized. This will result in the formation of an oil bank behind the zone of pure CO_2. The process then continues until developed miscibility conditions are satisfied.

It is noted that the MMP has to be reached both in case of FCM and MCM (Holm and Josendal, 1974). As a rule-of-thumb, MMP is defined as the pressure where more than 90% of OOIP is recovered at 1.2 HCPC (hydrocarbon pore volume) of CO_2 injection (Yellig and Metcalfe, 1980). MMP is determined by the slim-tube experiment. One typical result of the slim-tube experiment is given in Fig. 2.6 and the MMP is the point where the oil recovery starts to flatten out. Nevertheless, laboratory experiments are costly and time-consuming, so mathematical models and correlations are widely used to estimate MMP. The former generates more accurate and reliable results compared to the latter, but correlations are always easy to use especially when slim-tube test is not available and mathematical models are absent (Lasater, 1958).

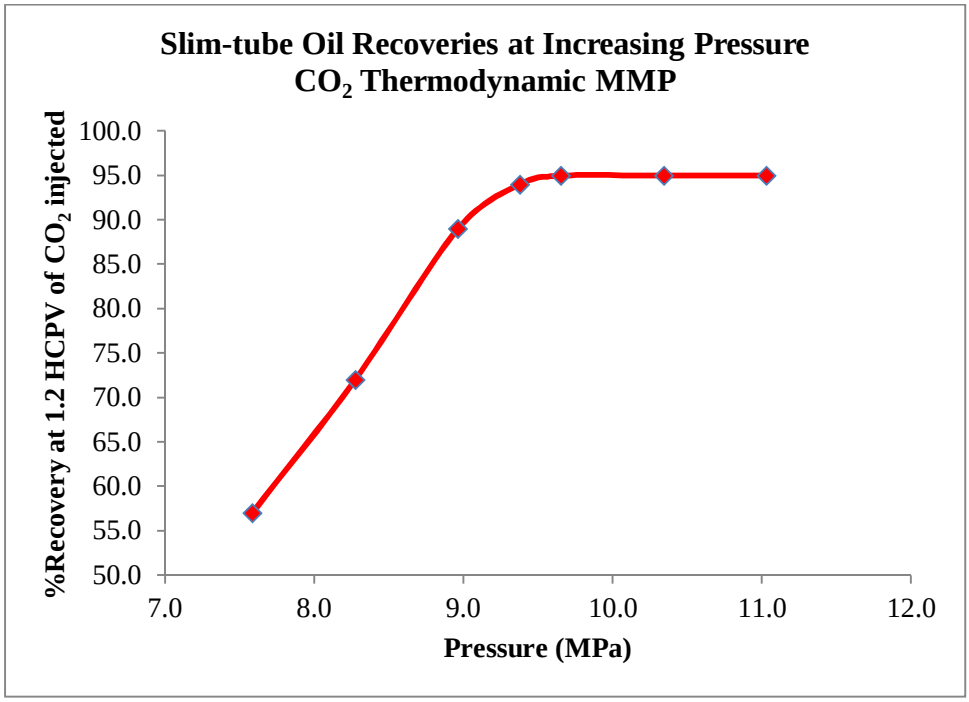

Fig. 2.6 Result of a slim-tube experiment at given oil composition and temperature (modified after Yellig and Metcalfe, 1980)

2.2.3.2 Driving Mechanism of Immiscible Carbon Dioxide Flood

If the slim-tube test or mathematical modelling suggest that the MMP cannot be attained at the given reservoir pressure and oil composition, then CO_2 and oil will not be completely miscible and immiscible CO_2 flood would be expected to take place. Given a particular oil composition, the type of CO_2 flooding that could be achieved generally depends on the reservoir conditions. Ghani (2013) summarized the empirical criteria of reservoir temperature and pressure for CO_2 miscibility as presented in Table 2.1. It is generally acknowledged that the miscible CO_2 flooding is more favourable in terms of mobilizing the residual oil, but CO_2 flooding under immiscible conditions is thought to be attractive for depleted reservoirs with reservoir pressures below the MMP which otherwise would be abandoned due to the discouraging technical and economic feasibility (Mohammed-Singh and Singhal, 2005; Sahin, 2008). The injected CO_2 under immiscible condition dissolves into the crude oil and causes the oil to swell, significantly. The greater the oil swelling, the better the oil recovery would be (Sankur, 1986). Immiscible CO_2 also considerably reduces the oil viscosity and therefore increases the oil mobility. Previous research reported the viscosity reduction is primarily a function of oil composition (Chung, 1988).

Table 2.1 Empirical criteria for CO_2 miscibility (Ghani, 2013)

CO_2 condition	**Criteria Temperature**	**Criteria Pressure**
Immiscibility possible	Less than 30.00°C	Less than 6.90 MPa
Miscibility/Immiscibility (coexist)	Between 30.00 and 32.22°C	Between 6.90 MPa and 8.27 MPa
Miscibility possible	Larger than 32.22°C	Larger than 8.27 MPa

2.2.4 Advantages and Disadvantages of Carbon Dioxide Flooding

Section 2.2.3 outlined in details the main mechanisms through which CO_2 flooding may result in enhanced recovery from depleted oil reservoirs. The laboratory, pilot and full-field scale investigations have all shown the CO_2 flooding to be a viable and encouraging EOR technique. To sum up, the effectiveness and superiority of a CO_2 flooding process is largely dependent on the following characteristics:

- Remarkable ability to swell up the oil.
- Noticeably reducing the oil viscosity and boosting the oil mobility.
- Relatively low MMP compared to the other solvents.
- Extracting heavy components in crude oil up to C_{30}.
- Low solubility in water
- The potential for nearly 100 percent oil recovery under miscible condition.
- Lowering the water/oil interfacial tension.
- Ample natural and anthropogenic gas supply.
- Mitigating greenhouse effect.

There is no doubt that CO_2 flooding is not without challenges. (Stein et al. 1992). Generally, the disadvantages, which mainly stem from the relatively low density and viscosity of dense CO_2 compared to the in-situ reservoir fluids, include:

- Viscous fingering.
- CO_2 early breakthrough.
- Gravity segregation.
- Low areal and vertical sweep efficiency.

2.2.5 Fundamentals of Oil Recovery Factor and Mobility Control Requirement

As mentioned earlier, CO_2, as a displacing fluid, suffers from a number of disappointing qualities which without a doubt would affect the ultimate oil recovery of CO_2 flooding. The recovery factor (R_F) is an indication of the effectiveness of a certain EOR process. It is defined as the product of displacement efficiency (E_D) and volumetric sweep efficiency (E_V) and the mathematical expression used in its calculation is as follows (Ghedan, 2009):

$$R_F = E_D \times E_V \tag{2.1}$$

The displacement efficiency (E_D) is associated with the displacement of the crude oil at microscopic (pore and throat) level. It equals to the fraction of the crude oil that is mobilized by the water flooding (secondary recovery) or an EOR technique (tertiary recovery) in a specific formation once flooded (Ghedan, 2009). Previous studies have demonstrated E_D to be controlled by a number of factors such as reservoir temperature and pressure, rock wettability, fluid properties and production history of the oil formation (Schlumberger, 1998). When it comes to the CO_2 flooding, ideally, the displacement efficiency is considered to be as high as 100% under miscible condition (Holm, 1959). The displacement efficiency thereby is not a concern at all when CO_2 flooding is about to be carried out.

The volumetric sweep efficiency (E_V), on the other hand, indicates the volume fraction of a specific reservoir which in reality is swept and displaced by the injected fluids (e.g. water, solvents or chemicals) at the macroscopic scale. It is believed to be determined by the reservoir heterogeneity, reservoir thickness, injection pattern, formation dip angle, permeability contrast between pay zones, and location of water-oil contact and mobility ratio of the flood (Ghedan, 2009). More specifically, volumetric sweep efficiency can be expressed as:

$$E_V = E_A \times E_I \tag{2.2}$$

Where E_A is the areal sweep efficiency and E_I is the vertical sweep efficiency.

Unfortunately, as stated earlier, CO_2 flooding is accompanied by viscous fingering and gravity override. Modifying the mobility ratio and the density contrast of the flood are the two techniques which may be used to combat the above issues and improve the sweep efficiency in a given oil reservoir, however, the former technique is much more practical than the latter . Consequently, appropriate measures need to be put into place with the purpose of modifying the mobility ratio in CO_2 flooding process to obtain higher recovery factors.

Before proceeding to the next part of this chapter which reviews the common techniques proposed to date for improving the mobility ratio of CO_2 flooding, the potential benefits of mobility control are discussed in details first.

The chief merit of improved mobility ratio is the evident rise in the areal sweep efficiency and relief from the early CO_2 breakthrough (Habermann, 1960), both of which contribute to the increase in total oil recovery. Fig. 2.7 depicts the dependence of oil recovery on the mobility ratio and injected pore volumes of a miscible solvent. Obviously, breakthrough does not occur in the very early times of the flooding, during which one unit of solvent produces one unit of crude oil. Once a certain amount of solvent is injected, the solvent breaks through beyond which, less than one unit of crude oil can be recovered if one unit of solvent is introduced into the system. However, if the mobility ratio is reduced to some extent, the breakthrough timing would be deferred. Furthermore, for any particular amount of solvent applied, oil fraction in the effluent is more than that of the flooding without any mobility controls. Both physical modelling (Lewis et al. 2008) and numerical simulation study have validated the effect of modified mobility ratio on areal sweep efficiency and ultimate oil recovery.

The second advantage of mobility control is the rise in the vertical sweep efficiency of the miscible CO_2 displacement (Craig, 1957). As can be observed in Fig. 2.8, increased mobility of the displacing fluid leads to a decline in the vertical sweep efficiency at breakthrough. For instance, when $(\Delta P_h/(\Delta P_v)$ is 1.0, vertical sweep efficiency increases from 18% to 73% as the mobility ratio decreases from 5.762 to 0.174.

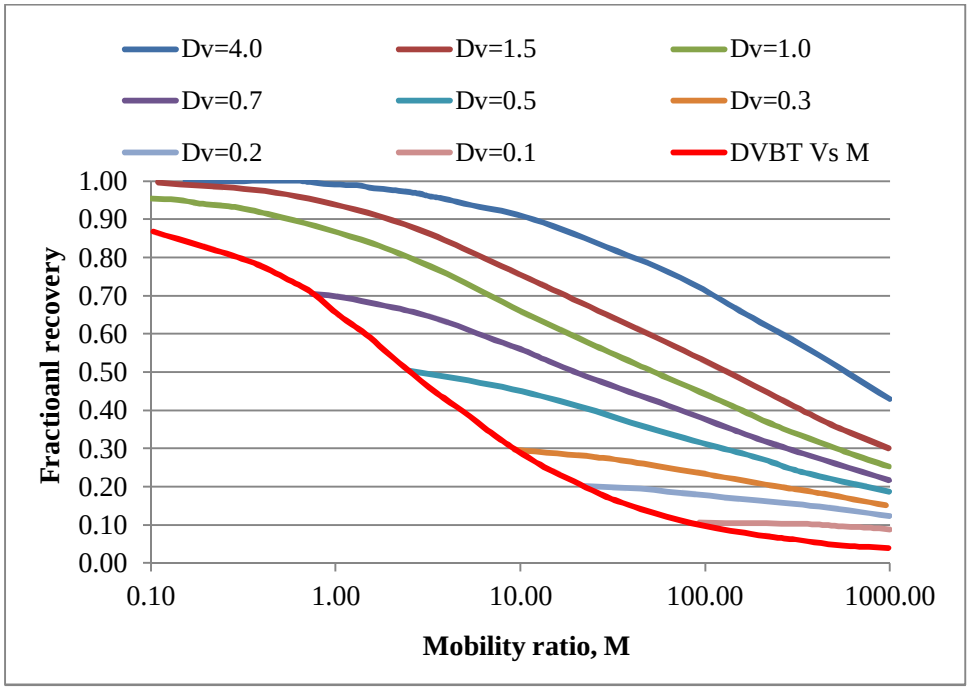

Fig. 2.7 Effect of mobility ratio on oil recovery after breakthrough (Dv stands for the displaceable volume injected while DvBT is the Dv at breakthrough) (modified after Claridge, 1972)

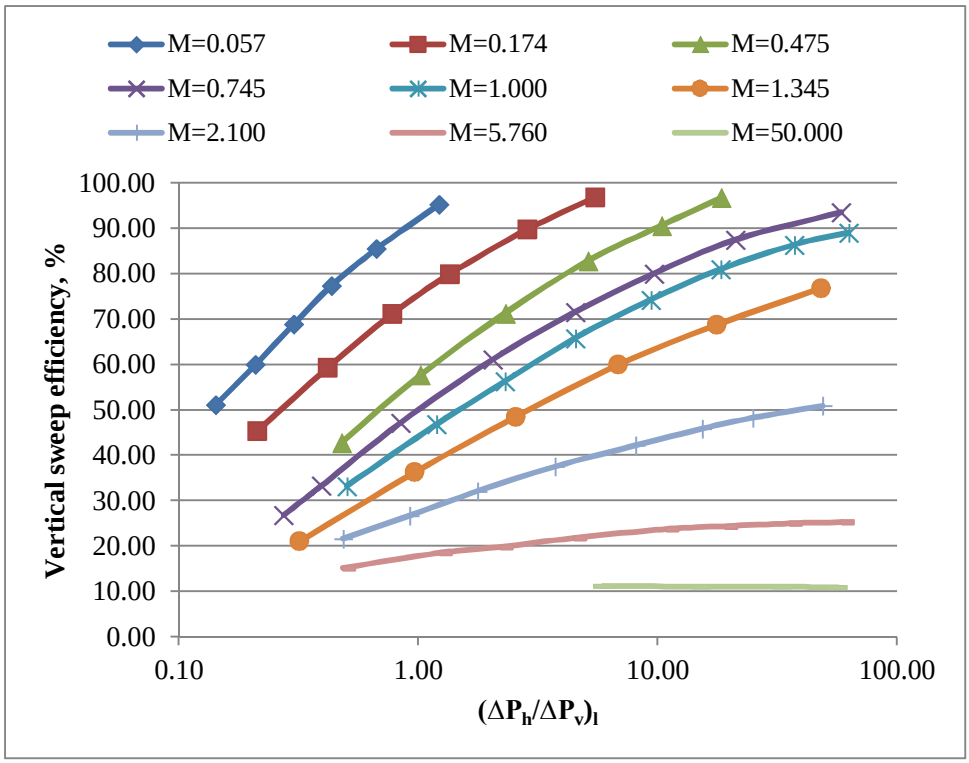

Fig. 2.8 Effect of the viscous/gravity force ratio to the vertical sweep efficiency ($(\Delta P_h/\Delta P_v)_l$

is the ratio of viscous force to gravity force at a linear uniform system) (modified after Craig, 1971)

2.2.6 Mobility Control and Conformance Modification

The intention of mobility control and conformance modification of CO_2 flooding is to ease the negative effects brought in by fingers and channels (Heller, 1994). Fingers of CO_2 occur as a result of the unstable flood front, while the permeability variation leads to the formation of CO_2 channels and associated problems. Generally, fingers and channels would not be a large issue for the close well spacing, since the so called "transverse dispersion" hinders the growth of fingers and channels. Nonetheless, in the case of widely spaced wells, fingers and channels are problematic and would keep growing during the displacement process. In this scenario, mobility and conformance control must be given the priority. A few of the commonly applied modification techniques are reviewed below.

2.2.6.1 Water-Alternating-Gas (WAG)

The mobility control technique attempts to reduce the mobility of the displacing fluid by suppressing fingers and channels, so that mobility ratio is less or equal to 1.0 (Gauglitz et al. 2002; Grane et al. 1981). WAG, which injects CO_2 and water into the target pay zone in an alternating sequence, is regarded as a state-of-the-art technology for mobility control (Huang and Holm, 1988). The first reported WAG field test which was performed by Mobil in 1957 was applied to the North Pembina Field in Alberta, Canada (Van Poollen, 1980). Since then, around 60 field applications have been conducted worldwide and most of the involved fileds have been onshore with sandstone reservoirs, as shown in Fig. 2.9.

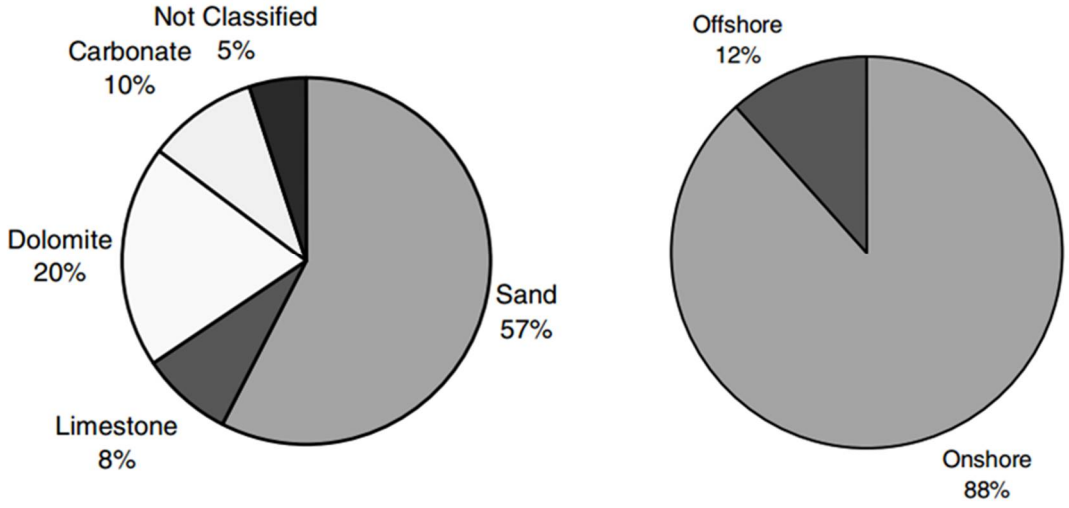

Fig 2.9 WAG field application (Christensen et al. 2001)

A common way to classify the WAG processes is to divide them into two groups as follows:

- *Miscible WAG displacement:* Majority of the WAG projects worldwide are reported to be of miscible injection type and most of them are found onshore (Graham and Bowen, 1980; Hsie and Moore, 1986; Prieditis et al. 1991; Genrich et al. 1986; Brownlee and Sugg, 1987). Nearly all of these miscible WAG projects included the process of reservoir re-pressurization in order to reach their respective MMPs. However, it is extremely challenging to maintain the boosted pressure, a typical real field case thereby can be a mixed process of miscible and immiscible WAG.
- *Immiscible WAG displacement:* The immiscible WAG injection gained wide application in reservoirs where gravity override was a major concern due to either the low dip or pronounced heterogeneity (Ma and Youngren, 1994; Grigg and Schechter, 1997; Robie et al. 1995; Ma et al. 1995). Due to the influence of cycle-dependent relative permeability, the recovery factor of the immiscible WAG injection is higher than that of water flooding or gas flooding alone (Skauge and Aarra, 1993; Skauge and Larsen, 1994).

In a WAG process, it is vital to balance the amount of the injected gas and water to achieve the best possible displacement performance. Too much gas leads to disappointing vertical sweep efficiency while too much water can compromise the microscopic displacement efficiency (Birarda et al. 1990; Reinbold et al. 1992). The cycle timing of WAG injection typically ranges from several months to one year, and the gas/liquid ratio is normally determined to be 1:1 in a conventional WAG flood (Jackson et al. 1985). However, tapering injection is applied sometimes to increase the water/gas ratio even if it is not planned at the very beginning. In this situation, increasing amount of water is injected at the later stages to reduce the gas usage. Tapering thereby is economically attractive if sourcing the gas is costly (Masoner et al. 1996; Fullbright et al. 1996; Attanucci et al. 1993).

WAG injection is an extremely complicated process which involves changes in numerous physical and chemical properties of the gaseous, aqueous, and oil phases in the porous rock. It is believed that its main contributing EOR mechanisms include the followings:

- *Microscopic displacement efficiency*: Gas flooding noticeably increases the displacement efficiency by oil swelling, viscosity reduction and lowering the IFT between the solvent and the oil. A detailed description of this mechanism has been included in the earlier sections of this chapter.
- *Macroscopic sweep efficiency*: As mentioned earlier, only a portion of the reservoir may be flooded by the injected gas due to the low density and viscosity of an injected gaseous phase. WAG greatly improves the sweep efficiency without affecting other advantages of gas flooding.
- *Relative permeability*: A study conducted by Braun and Holland (1995) revealed that the relative permeability hysteresis effect was more evident for a non-wetting phase than the wetting phase. In WAG process, three phases coexist and interact with each other, which make the hysteresis effect much more pronounced (Larsen and Skauge, 1998). Reduced water mobility is observed in intermediate wet WAG injection process (Skauge and Larsen, 1994). Injectivity reduction (huge injection pressure) during WAG displacement was also reported by Shneider and Owens (1976). Despite its inability to thicken the dense CO_2, WAG significantly promotes water saturation and thus reduction in CO_2 saturation in the formation, which, as a result, leads to the decrease in relative permeability of the dense CO_2 as shown in Fig. 2.10. Take the Viking Sandstone in Fig 2.10 for example, the relative permeability of CO_2 decreases from 0.37 to 0.06 as the CO_2 saturation decrease from 0.4 to 0.2. Since the reduction in relative permeability lowers the mobility ratio, the viscous fingering is relieved to a large extent by the alternating injection of water and dense CO_2.
- *Residual oil saturation*: Researchers have demonstrated that there is a strong link between the gas saturation and residual oil saturation in water wet reservoir, i. e., the presence of trapped gas facilitated the reduction in residual oil saturation (Element et al. 2003). For intermediate wet and oil wet reservoir, however, the link is far weaker or does not exist at all (Kralik et al. 2000). The decline in the residual oil saturation apparently contributes to the increase in accumulative oil recovery.

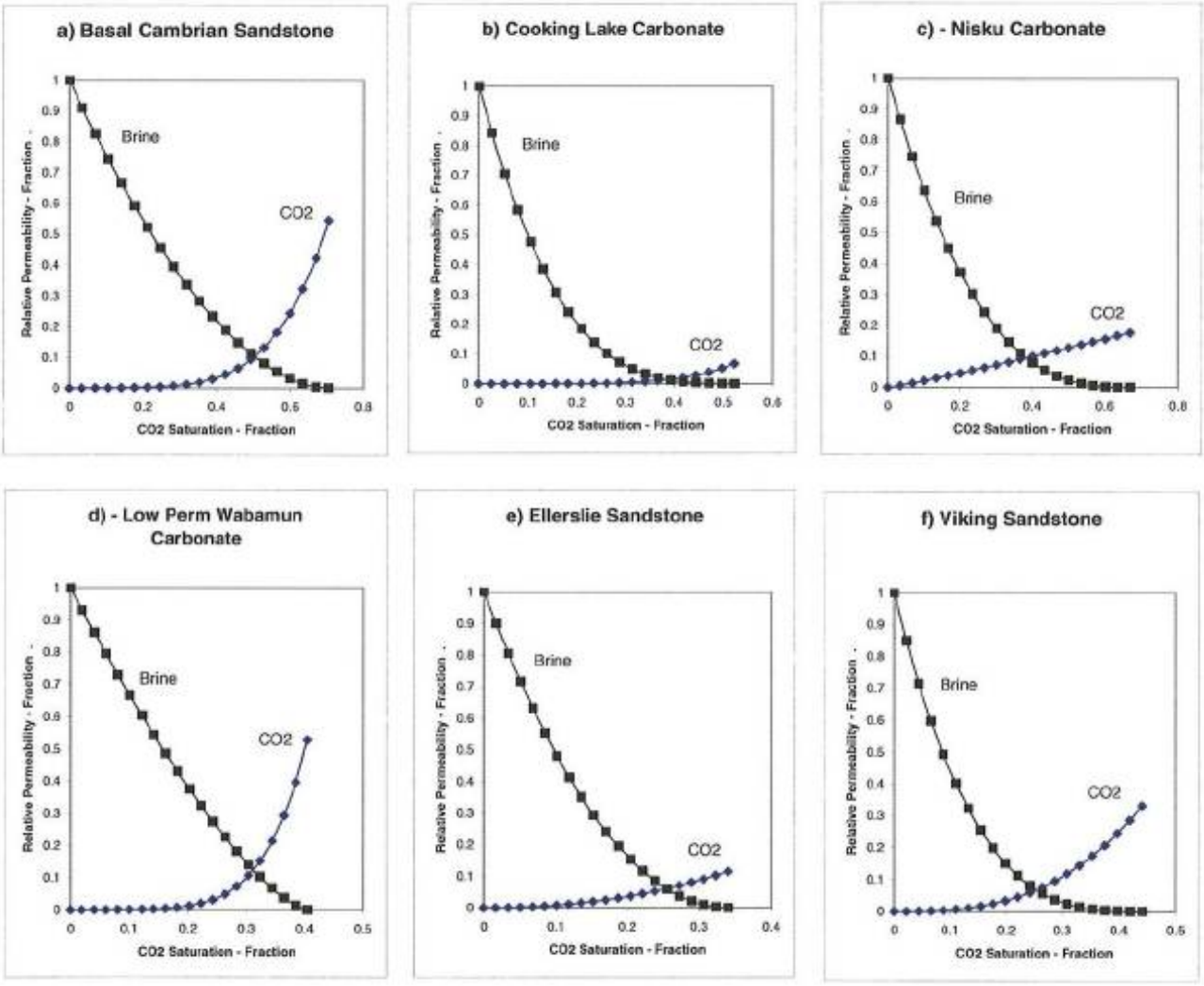

Fig. 2.10 Effect of CO_2 saturation and brine on the relative permeability of dense CO_2 (Bennin and Bachu, 2005)

As a consequence of its outstanding capacity to improve macroscopic sweep efficiency as well as microscopic displacement efficiency, WAG technique is employed in more than 90% of the tertiary CO_2 injection projects worldwide (Merchant, 2010). Nevertheless, it is believed that around half of the oil left behind by water floods still resides in the formations treated by some kinds of WAG injection. Moreover, design and installation of a number of WAG-related facilities may delay the injection of a given amount of CO_2, which prolongs the entire lifetime of the project. Meanwhile, the introduction of a substantial volume of water into the gas flood hampers the close contact of oil and CO_2 in the porous rock and significantly increase the water cut in the production wells. Besides, WAG technique suffers from numerous problems which are reported in the literature (Holloway and Fitch, 1964;

Holm, 1972; Jensen et al. 1996; Skauge and Berg, 1997; Goodrich, 1980; Hadlow, 1992; Grigg and Schechter, 1997) a list of which is provided below:

- Early breakthrough in the production wells.
- Water blockage leading to rise in trapped gas saturation.
- Stress-related tubing failure caused by differing temperatures of injected gas and water.
- Asphaltene precipitation and hydrate formation.
- Scale formation that can damage the protection coating of the casings.
- Corrosion problems associated with the application of acidic gases like CO_2.

2.2.6.2 Carbon Dioxide Thickener for Mobility Control

Probably, the most obvious and direct solution to combat the high CO_2 mobility is to use a viable and effective CO_2 thickener which would increase the viscosity of the dense CO_2 high enough so that a favourable or at least a less problematic mobility ratio can be obtained (Dandge and Heller, 1987; Eastoe et al. 1992; Enick, 1991). In an ideal situation, the designed CO_2 thickener is readily dissolved in the dense CO_2 with only marginal dissolution in both brine and oil. Therefore, it would not partition into these formation fluids (Xu et al. 2003; Terry et al. 1987). Meanwhile, thickeners are expected to be shear-thinning which facilitates the motion of CO_2 thickener near the wellbore and induces substantial increase in CO_2 viscosity in the formation only.

Currently, CO_2 thickeners, regardless of their molecular structure, are normally difficult to dissolve at ambient conditions (Shi et al. 1999), such as PFA, PDMS and PVAc. This is reasonable because the intermolecular interactions that enhance the CO_2 viscosity can also prohibit the dissolution of the thickener. The intermolecular attraction is so strong that stirring alone is not enough to attain the desirable dissolution and additional heat energy thereby is required to weaken the interaction. However, when the mixture is cooled off, the intermolecular network would form again and solid micro-fibre may appear in the solution, which is obviously inappropriate for the flow in porous rocks. This is primarily why the solution of CO_2 thickeners is required to be clear, single-phase and viscous when moving in the formation (Potluri et al. 2002; Llave et al. 1990).

A CO_2 thickener is typically a natural or synthetic polymer with extraordinarily high molecular weight. Alternatively, it can be a relatively small molecule compound with both CO_2-phobic and CO_2-philic segments in the molecular chain. Brief reviews of various types of CO_2 thickeners are provided below.

2.2.6.2.1 Carbon Dioxide Thickener: Polymeric Compound

It is generally recognized that thickening CO_2 by using polymers would be quite challenging, since CO_2 is a fairly poor solvent for polymers with an ultra-high molecular weight. Although in the literature the details of several polymers which have been designed and prepared as CO_2 thickeners could be found, the required pressure for their dissolution falls in the range of 68.95 MPa to 275.79 MPa which is considerably higher than typical CO_2 MMP values (10.3 MPa-27.6 MPa) (Enick, 1998). In an attempt to make these polymeric thickeners more applicable and economical, extensive studies have been performed over the past few decades. One of the earliest attempts was conducted by Heller et al. (1985). They evaluated scores of polymer candidates and picked 18 of them that displayed encouraging solubility in CO_2 with the temperature and pressure in the range of 25-58°C and 11.7 MPa-21.4MPa, respectively. Unfortunately, none of the selected polymers induced noticeable viscosity enhancement. Subsequent work by the same researchers (Dandge and Heller, 1987) concentrated on the preparation of poly α-olefins in an effort to further increase the thickener solubility in CO_2. Although some progresses were made, a very small number of the evaluated polymers were considered to be viable CO_2 thickeners. They also concluded that the molecular weight should be fairly low to achieve the satisfactory level of solubility. Based on this guideline, researchers tried to synthesize CO_2-soluble polymer in the bulk phase of the dense CO_2, but the many experiment ended with polymer precipitation out of the dense CO_2 (Terry et al. 1987).

In order to obtain high molecular weight polymers as CO_2 thickeners, other researchers have assessed numerous other candidates with the Hildebrand solubility parameter no more than 7$(cal/cc)^{0.5}$ (Bae and Irani, 1990; Harrris et al. 1990). Later on, it was pointed out that identifying polymer candidates with good electron/acceptor interaction could be a benifical solution (Williams, et al. 2004). Furthermore, the finding that high molecular weight Polydimethylsiloxane (PDMS) was not capable of dissolving and viscosifying CO_2 without the use of a co-solvent agreed with the results obtained from Williams at al. study (Bayraktar and Kiran, 2000). Nevertheless, the first reported high molecular weight CO_2 thickener

capable of improving CO_2 viscosity in the absence of a co-solvent is poly (1-, 1-, dihydroperfluorooctyl acrylate) or PFOA or PFA (McClain et al. 1996). McClain et al. (1996) discovered that the addition of PFOA could remarkably enhance the CO_2 viscosity as shown Fig. 2.11. For instance, the viscosities of 3.4 wt./vol% PFOA in CO_2 and pure CO_2 at 27 MPa are 0.19 cP and 0.07 cP, respectively, with the former being 2.7 times greater than the latter. To date, PFOA is still recognised as the most promising candidate for CO_2 viscosity enhancement, but the high concentration is not practical for real field operations if the overall cost is considered.

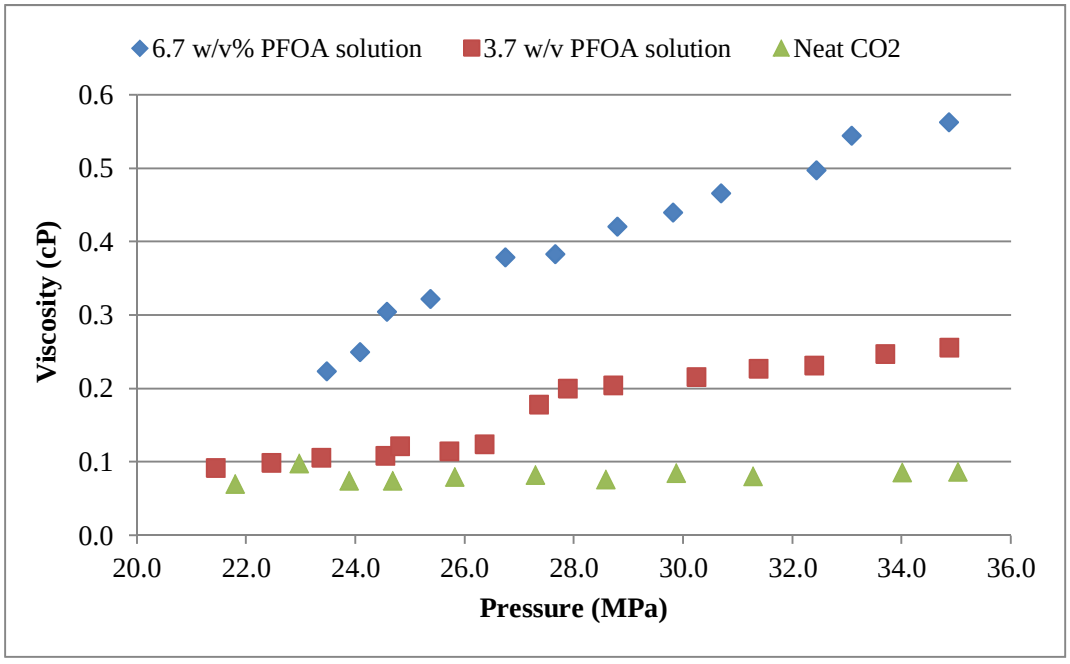

Fig. 2.11 Effect of pressure and concentration on the viscosifying performance of PFOA (modified after McClain et al. 1996)

Some researchers have tried to reduce the required amount of the thickener without affecting its outstanding performance (Xu et al. 2003; Huang et al. 2000). Among them, polyFAST prepared by (Xu, et al. 2003) is believed to be the most effective polymeric thickener as shown in Fig. 2.12. It remains the only viable thickener that properly functions in diluted concentrations at typical CO_2-EOR reservoir condition and low superficial velocity.

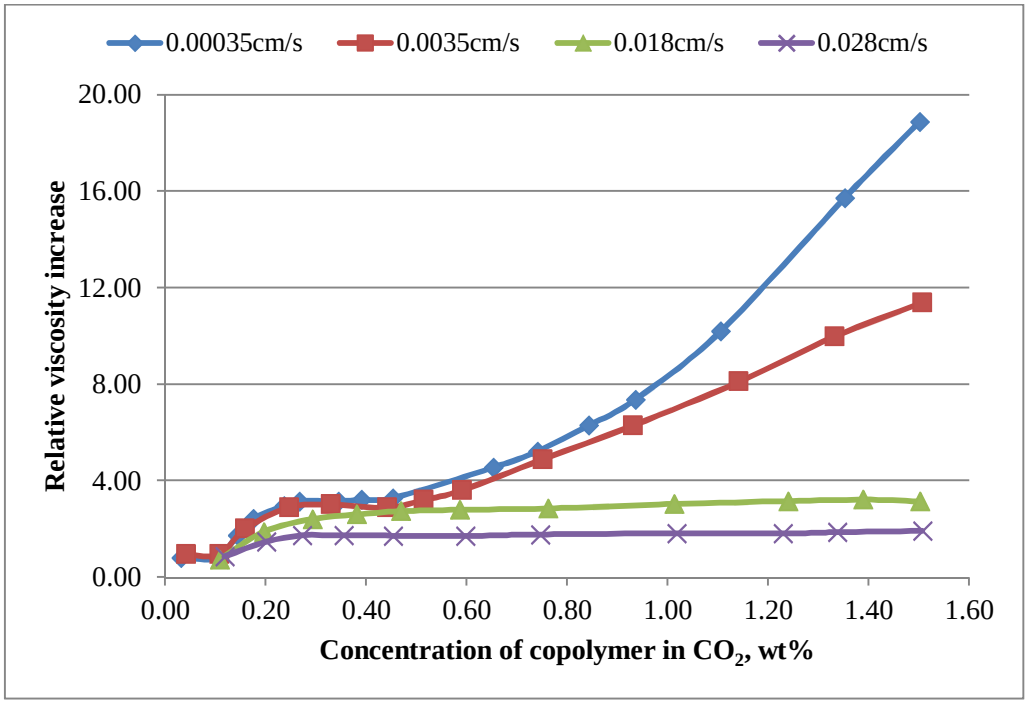

Fig. 2.12 Effect of superficial velocity and concentration on the CO_2 viscosity (modified after Xu et al. 2003)

Another promising route to obtain a high-performance CO_2 thickener is to introduce associating groups into molecular chains. This type of product is considered to be extraordinarily effective for non-polar solvents since the introduced ionic groups are able to aggregate into pairs (Martin et al. 1991). Given the high cost and environmental concern of the fluoroacrylate substances, the strategy of designing and synthesizing CO_2-philic non-fluorous thickeners seems to be attractive. The interest in such a product therefore has grown quickly and thus hydrocarbon-based polymers are in the spotlight. Unlike the extensive screening and testing on existing polymers that had been conducted in 1980s, polymers most of the time have been designed and tailed to contain specific functional groups and favourable properties that assist its dissolution in CO_2 since then (Enick et al. 2005; Potluri et al. 2002; Erick et al. 2003). Some of the most attractive CO_2-philic polymers are polyvinyl acetate (PVAc), poly [(1-O-(vinyloxy) ethyl-2, 3, 4, 6-tetra-O-acetyl-β-D-glucopyranoside)] (PAcGIcVE), oligo (3-acetoxy oxetane) (OAO) and amorphous polylactic acid (Wang et al. 2009; Tapriyal and Enick, 2008). Other less CO_2-philic polymers include: polyvinyl methoxy methylether (PVMME), oligomers of cellulose triacetate (OCTA), polymethyl acrylate (PMA), per-acetylated cyclodextrin rings (PACD) and the oligo (3-acetoxy oxetane) (OAO). The molecular structures of a fraction of these polymers are illustrated in Fig 2.13.

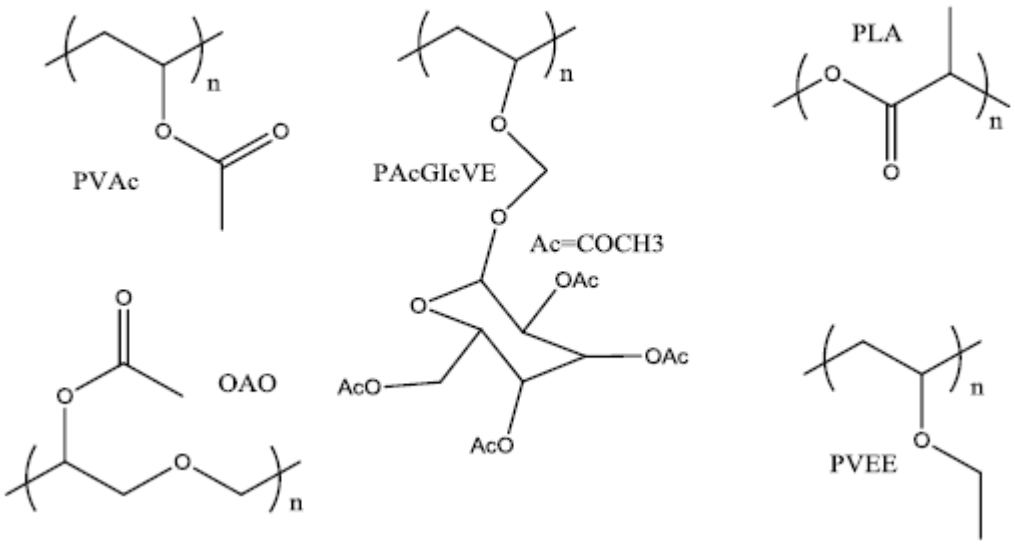

Fig. 2.13 Molecular structures of representative hydrocarbon CO_2-soluble thickener (Potluri et al. 2002)

However, these polymers have a feature in common: they all have low solubility in the dense CO_2. Moreover, the required pressure to dissolve them is exceptionally high (Shen et al, 2003; Tapriyal, 2009).The synthesis of polyBOVA lifted this issue to some extent, but still its behaviour is not encouraging (Tapriyal, 2009). To sum up, at the time of this review, an economic, viable and highly effective non-fluorous polymeric CO_2 thickener that enhances CO_2 viscosity in diluted concentrations at typical reservoir temperature and pressure is still not available.

2.2.6.2.2 Carbon Dioxide Thickener: Small Molecule Compound

The second category of the CO_2 thickeners includes the small molecule material that can associate and build macromolecular network for viscosity enhancement. Normally, the molecules of such material contain a CO_2-philic segment that facilitates the dissolution and CO_2- phobic segment that induces the intermolecular association (Heller and Kovarik, 1988). Based on the various associations of neighbouring molecules, small molecular CO_2 thickeners are mainly classified into the following groups:

- *Trialkyltin fluorides*: The tin atom exhibiting electropositive is attached to the fluoride atom exhibiting electronegative, thus a linear and transient structure is formed. In the meantime, the butyl atoms assist in maintaining the linear macromolecule. Heller et al. (1986) synthesized a series of trialkyltin fluorides thickeners, but just a few of them

possessed sufficient dissolution in the dense CO_2. Even the addition of a co-solvent could not considerably increase the solubility of such thickeners (Iezzi et al. 1989). Later on, it was found that fluorination of alkyl groups could improve CO_2 solubility, then tri (2-perfluorobutyl ethyl) tin fluoride, (F(CF2)4(CH2)2)3SnF was prepared and tested (Shi et al. 2001). Although its solubility in CO_2 was encouraging, its capability to thicken CO_2 was inadequate.

- *Fluorinated hydroxyaluminum disoaps*: The surfactant hydroxyaluminum bis (2-ethyl hexanoate) is renowned for its outstanding ability to thicken light alkanes and gasoline. In an analogous manner, researchers synthesized a train of hydroxyaluminum disoaps for CO_2 thickener application. The results showed a portion of them thickened propane and none of them were eligible as CO_2 thickeners due to their poor solubility (Enick, 1991).
- *Semi-fluorinated alkanes*: Early attempts to enhance CO_2 viscosity by using semi-fluorinated alkanes was made by Iezzi et al. (1989). They developed a linear compound and applied it as a thickener. Upon cooling, this semi-fluorinated alkane could form micro-fibrillar structure that gels the dense CO_2. However, the obtained gel was not applicable for EOR due to its thermodynamic behaviour which led to the retainment of this compound on the rock surface.
- *Hydroxystearic acid*: Gullipalli et al. (1995) proposed the use of a 12-hydroxystearic acid (HSA) that could thicken hydrocarbon and chlorinated solvents. However, the assessment results revealed that HSA was barely soluble in the dense CO_2 unless significant amount of ethanol is applied and that noticeable viscosity increase could be achieved at relative low temperature. Also, the presence of microfiber in the gel may be an impediment to flow through porous medium.
- *Fluorinated and non-fluorous bisureas*: Urea groups in these compounds can interact due to the existence of hydrogen bonding and form macromolecular network, which provides the possibility of identifying suitable CO_2 thickener from fluorinated and non-flurous bisureas (Shi et al. 1999). It has been shown that the bis-urea has a relatively high solubility in the dense CO_2 without being heated. Paik et al. (2007) proposed a new molecular structure with introducing the hydrocarbon and other CO_2-philic groups with the hope of obtaining a non-fluorous bis-ureas as outlined in Fig. 2.14. However, the homogenous and clear CO_2 solution turned into a dispersion with fibres coming out of the solution.

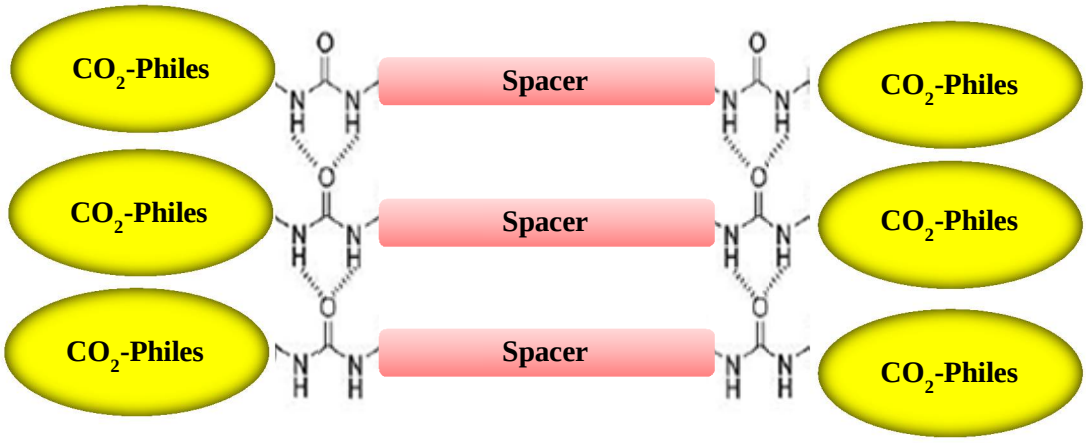

Fig. 2.14 The general molecular structure of a non-flurous bisures (modified after Paik et al. 2007)

- *Surfactants with divalent metal cations*: Based on the previous study on AOT-stabilized microemulsion, researchers developed one type of surfactant that dissolved in CO_2 and enhanced CO_2 viscosity as illustrated in Fig. 2.15. The surfactants dissolved in the dense CO_2 at room temperature and pressures higher than MMP. Unfortunately, these costly thickeners only induced modest rise in CO_2 viscosity at a relatively high concentration.

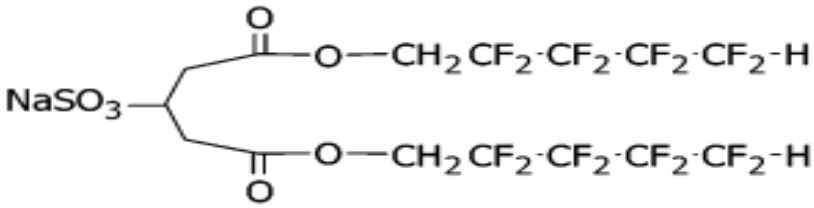

Fig. 2.15 Molecular structure of a fluorinated AOT surfactant as CO_2 thickener (Trickett, et al. 2010)

- *Hydrocarbon gelling agents*: A number of simple organic compounds contain the aromatic groups that can associate with other aromatic groups of neighbouring molecules via the π-π stacking mechanism (Clavier et al. 1999; Brotin et al. 1991).

These chemicals might be potential CO_2 thickeners taking into consideration the fact that they do not contain the functional groups that make the solubility in CO_2 poor, thus the formation of a viscosity-enhancing macromolecule structure could be possible. Placin et al. (2000) successfully obtained a dry, low-density, and fibre-like aerogel by mixing 2, 3-n-decyloxy anthracene (DDOA) with the dense CO_2. Although this study validated a favourable CO_2 solubility, its viscosifying performance was not included in their research. It is speculated that by tailoring the organogelator structure of these molecules, ideal CO_2 thickener that performs well over a broad reservoir conditions could be obtained.

In summary, a multitude of small molecule compounds have been identified as potential CO_2 thickeners. However, nearly all of them are fluorinated and cannot work properly at low concentration and typical condition of CO_2 flooding. As a consequence, the quest for a cost-effectiveness, high-performance and green CO_2 thickener is still continuing.

2.2.6.3 Carbon Dioxide Foams

2.2.6.3.1 Foam Generation and Decay in Porous Media

As mentioned before, the CO_2 foam flooding has been widely recognized as the most promising technology for the mobility control. It is noted that although the term “foam” is used generally in laboratory investigation and field operation, it is not thermodynamically stable. Instead, it is rather an unstable and multi-phase mixture (Liu et al. 2005). Although the foams used to modify the mobility ratio in the porous media share a number of characteristics with the household foams, there are also distinct differences between them (Heller, 1994). The flow of the foaming agent solution and high-pressure CO_2 in the tortuous pores channels of the porous formation rocks provides the indispensable shearing effect for the foam generation as shown in Fig. 2.16 (Radke and Gillis, 1990). Even if the foam is produced by the co-injection of the dense CO_2 and foaming agent at the wellhead, the foams would be re-created in the porous medium as they enter it. For the mobility control purpose, the CO_2 foam actually comprises of multitudes of lamellae rather than a collection of significantly tiny bubbles. An individual lamella is broken down and re-generated repeatedly during its transportation from injection well to the production well, and the rate of the generation is supposed to surpass the rate of collapse if the foam is to be used to control CO_2 mobility.

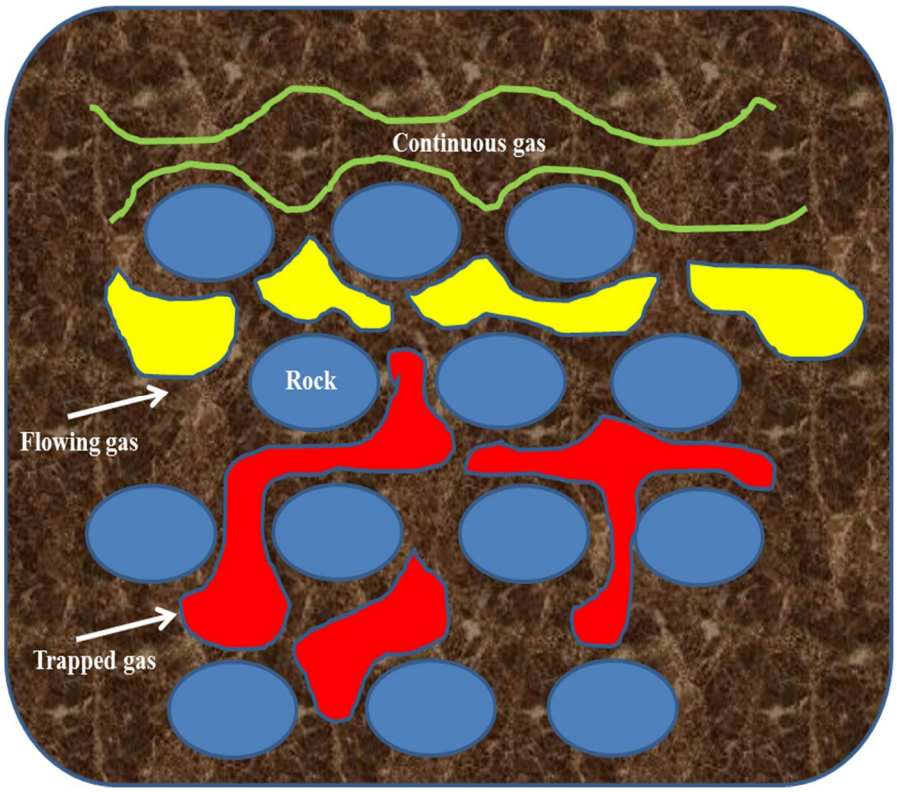

Fig. 2.16 Illustration of foams flowing in a porous medium (modified after Radke and Gillis, 1990)

There are mainly three mechanisms responsible for the foam generation namely leave-behind, lamella division and snap-off mechanisms (Chen et al, 2004; Nyuyen et al. 2000; Chambers and Radke, 1990). The illustrations of them are provided in Fig. 2.17. The 'leave-behind' refers to the stabilization of liquid films due to the entry of the gas into the porous medium. This effect leads to the creation of the lamella that is pointed parallel to the flow path of the invading gas. Foams produced by leave-behind are considered to be fairly feeble, however. When it comes to 'lamella division', this mechanism induces more evident mobility reduction because it is capable of squeezing bubbles through pore constrictions, thin liquid films perpendicular to the gas flow thereby the foam can be formed. The last mechanism of foam formation is the snap-off which is divided into several types. The "Pre-neck" is dominant in the case where the foaming agent solution is injected into the pores and pore throats, and a tiny bubble is pinched off from the initial big bubble by the pressure gradient. Likewise, foams are made by snap-off when the local capillary pressure drops to half of the entry

capillary pressure value. If the snap-off takes place in straight and long pores, it is named the “rectiliner snap-off” (Chambers and Radke, 1990).

The lamellae coalescence is also influenced by a few factors. First of all, low concentration or inappropriate surfactant can exacerbate the water drainage and decay of the lamellae. Next, the foam quality and flow rate can determine the extent of the two bubbles on each side of the lamella approaching each other which can cause the lamellae to breakdown. Last but not the least, the stability of the lamellae is affected by the presence of the oil and the rock wettability. Nevertheless, it is difficult modelling and predicting the foam decay, only some crucial parameters like foam quality, injection rate and surfactant type and concentration can be designed and optimized.

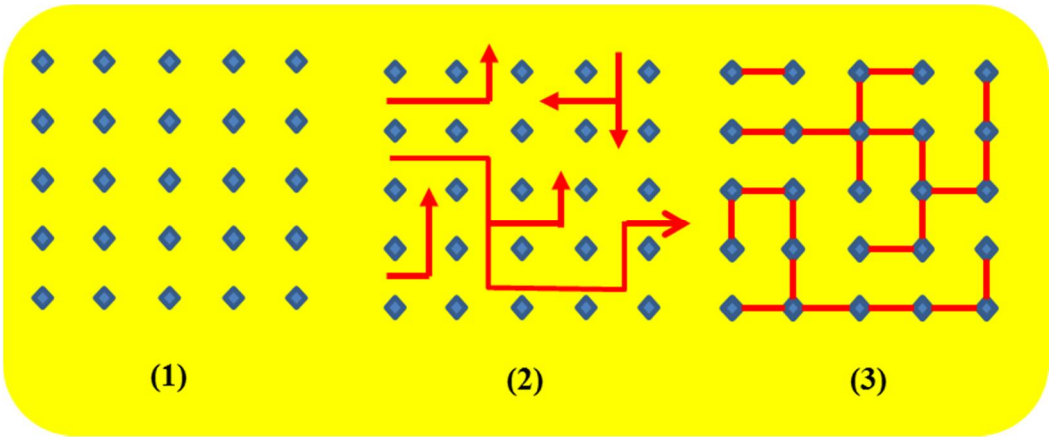

(a) Foam generation via leave-behind mechanism (blue diamond indicates the rock grains)

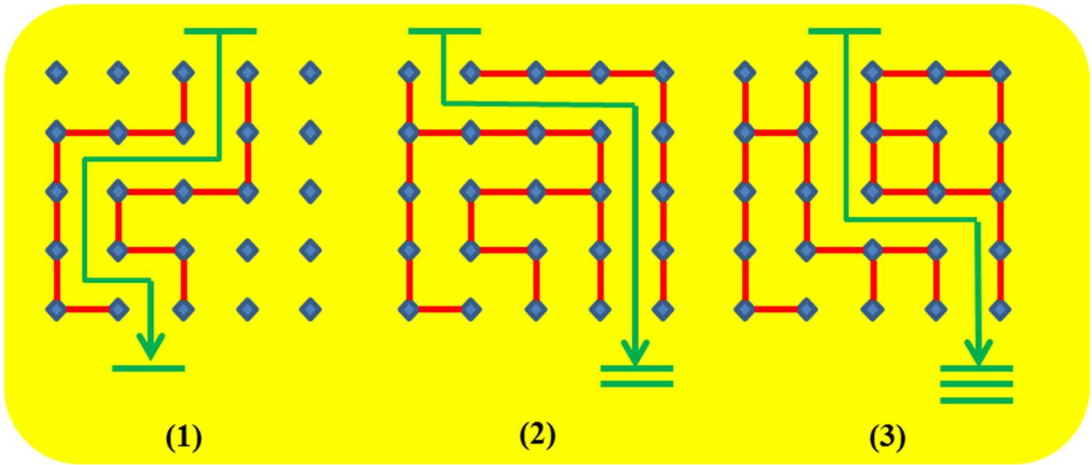

(b) Foam generation via lamella division mechanism (blue diamond indicates the rock grains)

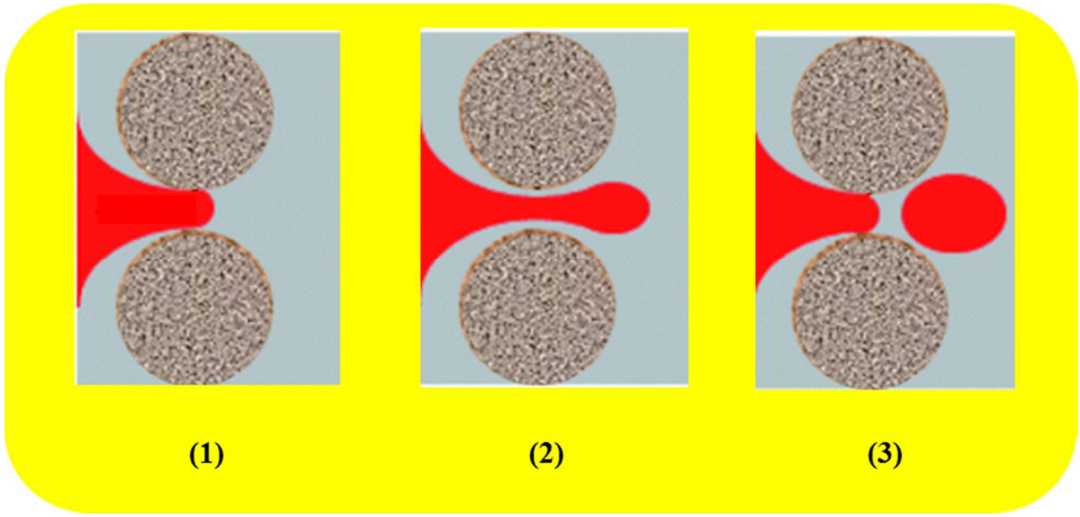

(c) Foam generation via snap-off mechanism

Fig. 2.17 Various mechanisms for foam generation (modified after Chen et al.2004)

2.2.6.3.2 Foaming Agents

As commonly known, the foam longevity would not be realized without the addition of a foaming agent. The most commonly applied agent is the water soluble surfactant with a great number of hydrophilic groups (Borchardt et al. 1988). For the application in a sandstone reservoir, anionic and non-ionic surfactants are effective. A cationic surfactant possesses positive charges and thus gets absorbed onto the sandstone surface that is normally negatively charged. However, a cationic surfactant exhibits better foaming performance in carbonate reservoir whose surface has positive charges, in this case thereby, anionic surfactant is not acceptable anymore.

Numerous commercial products have been experimentally approved to be viable for CO_2 foam generation. For example, the most renowned Chaser^{TM} CD 1045, developed by Chevron, has been investigated by many research groups and is identified as a remarkably promising foaming agent, although its chemical composition is still proprietary (Tsau and Heller, 1992; Yaghoobi and Heller, 1994; Bai et al. 2005). Other reported products include Alipas CD 128, Chaser CD 1040, Chaser CD 1050, NES-25, Shell Enordex X200, Sherex Varion CAS, Plurafoam NO-2N, Witcolate 1247-H, AOS (Kuhlman et al. 2000; Lee and Heller, 1990; Alkan et al. 1991; Casteel and Djabbara, 1988; Chang and Grigg, 1996), and a large quantity of water soluble surfactant assessed by Borchardt et al. (1985).

Besides water soluble surfactants, CO_2 soluble surfactants are also promising alternatives, which were first reported in the late 1960s (Bernard and Holm, 1967). Since then, the interest in designing and synthesizing viable and affordable CO_2 soluble surfactants has been growing steadily. For example, Scheievelbein (1991) suggested that the hydrocarbon-based surfactant might be used as a CO_2 soluble foaming agent. Others considered Tergitol TMN-6 to be a reliable surfactant that could dissolve in high-pressure CO_2 (Haruki et al. 2007; Ryoo et al. 2003). It is also discovered that surfactants incorporated with the functional group oligo (vinyl acetate), OVAC is the most likely to be CO_2-soluble (Fan et al. 2005). Recently, researchers developed a CO_2-soluble non-ionic surfactant that works at low concentration (0.1 wt%) and typical reservoir pressures (Sanders et al. 2010). In summary, these surfactants are hydrocarbon-based ethoxylates that are soluble in both water and CO_2. A few surfactants have either PEG or PPG segments. If the reservoir condition are suitable and the surfactant is soluble in CO_2, then the injection of brine can be reduced or even eliminated, since the CO_2-rich surfactant solution is capable of creating foams in-situ with the presence of the resident formation brine.

2.2.6.3.3 Main Mechanisms of Carbon Dioxide Foam Flooding

Foams can be employed for various purposes when injected as part of an EOR scheme. A CO_2 foam is intended to reduce the in-depth CO_2 mobility to the extent that it is comparable to the crude oil so that the fingering and channelling throughout the formation are alleviated or suppressed; the areal sweep efficiency thereby is improved considerably. For this reason, a modest and weak foam is expected to be generated for which a relatively dilute surfactant concentration is employed with the hope of avoiding the prohibitive pressure drop caused by extremely low foam mobility (Gauglitz et al. 2002).

On the other hand, a foam could be also designed for conformance control purposes which is referred to as the blocking foam. Typically, a relatively high surfactant concentration is applied to establish a short-term but strong foam that performs near the wellbore. Accordingly, displacing fluid is diverted to other lower permeability zone that is rich in residual oil. However, more often, foams are used for the both purposes of mobility control and conformance control during a foam flooding process rather than a single purpose (Mclendon et al. 2012).

In summary, the main mechanisms of CO_2 foam flooding include:

- *Improving the frontal stability*: Lawson and Reisberg (1980) pointed out the ability of the foams to stabilize the displacement front of a flood through decreasing the viscous instability. Two mechanisms were proposed for this effect to take place. The first one is closely related to the re-arrangement of the moving bubbles induced by the interfacial tension gradient, which inhibits the bubble motion and thus boosts the effective viscosity of the gaseous phase (Xu, 2003; Wassmuth, 1994). The second mechanism is associated with the fact that gas is firmly trapped in the foam by liquid lamellae (Llama, 2011). It has been found that the fraction of the trapped gas in the foam is controlled by numerous factors, like pressure gradient, foam texture and pore geometry (Nguyen et al. 2000). X-ray Computer Tomography (X-ray CT) scanning image of a CO_2 miscible flood clearly illustrates the influence of the foam on the displacement frontal stability as shown in Fig. 2.18 (Wellington and Vinegar, 1985). It can be seen that CO_2 injection alone leads to an evident gravity tongue while the occurrence of CO_2 foam noticeably suppresses the frontal instability. Perhaps the most unique quality of the foam flooding is the selective mobility reduction (SMR) which results in the preferential flow of foam into higher permeability zone (Tsau and Heller, 1992).

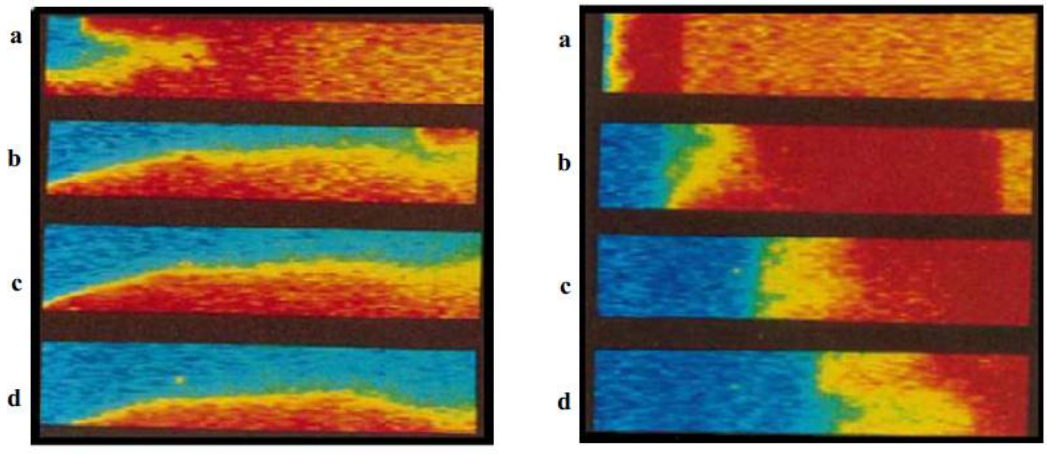

(a) **(b)**

Fig. 2.18 X-ray CT scan images of a miscible flood without (a) and with (b) foam **(**Wellington and Vinegar, 1985)

- *Reducing the capillary force*: The foam development and propagation is capable of improving the magnitude of viscous forces and reducing the interfacial tension, both

of which thereby affect the capillary number (Equation 2.3). It has been confirmed that the formation of oil emulsion during the foam flooding process contributes to the enhancement of oil recovery (Marsden, 1986). Moreover, Zhang et al. (2010) stressed that the detachment of crude oil from the porous rock required the decrease in capillary force via the emulsification mechanism. Due to the presence of the surfactant in the displacement slug, the oil/water interfacial tension is lowered, leading to the formation of an oil-in-water emulsion. As the surfactant slug propagates throughout the formation, more and more residual oil is mobilized and an oil bank appears at the displacement front, which has been validated by a recent study (Simjoo et al. 2012).

$$N_c = \frac{\mu.u}{\sigma} \tag{2.3}$$

Where: N_c: capillary Number, dimensionless,

μ: viscosity of the displacing fluid,

u: superficial displacement velocity,

σ: interfacial tension between the two fluids,

- *Altering the rock wettability*: The wetting state of a formation rock is an essential factor, because it has huge impact on the fluid flow and fluids distribution in the reservoir. Reed and Healy (1977) proposed another expression of capillary number (Equation 2.4). According to this expression the rise in capillary number can be realized by changing the contact angle and altering the rock wettability (Ayirala, 2002). Especially in an intermediate-wet reservoir, a large capillary number is yielded if the contact angle is close to 90° regardless of the IFT and rock permeability. An anionic surfactant is ideal for modifying the wettability in water-wet reservoirs. Wettability modification during a foam flooding process takes place when the surfactant in the slug is adsorbed onto the rock surface and thus alters the wetting preference of the reservoir rock. The magnitude of the surfactant adsorption is primarily influenced by the chemical composition of the rock, surfactant type and concentration, oil properties, brine pH and salinity, temperature and so forth (Schramm, 1994). Some researchers (Lescure and Claridge, 1986) investigated the correlation between the foam performance and the rock wettability and concluded an

oil-wet medium was more favourable for foam generation and propagation, while other groups have stated that foams performed better in water-wet formation (Farajzadeh, et al. 2012).

$$N_c = \frac{K\Delta P}{\sigma L cos\theta} \tag{2.4}$$

Where: N_c: capillary number, dimensionless,

ΔP: pressure drop along the porous medium,

K: absolute permeability of the porous medium,

σ: interfacial tension between the two fluids,

L: length of the porous medium,

θ: contact angle

- *Facilitating the interfacial mass transfer*: The existence of the foam greatly boosts the chance for CO_2 to interact with the oil and thus the interfacial mass transfer between CO_2 and oil. Generally, the foam significantly increases the CO_2 retention time in the porous medium and delays its breakthrough. Consequently, the CO_2-oil interaction is enhanced and in turn more residual oil is mobilized (Srivastava, 2010; Farajzadeh, et al. 2007).

2.2.6.3.4 Crucial Process Variables of Carbon Dioxide Foam Flooding

A great number of process variables are capable of impacting on the displacement performance of the CO_2 foam flooding directly or indirectly. The most significant ones are as follows:

- *Temperature*: It is widely recognised that more careful design and implementation are required when the investigated reservoir temperature is above 85°C. Elevated temperature lifts the surfactant adsorption onto the reservoir rock (Ziegler and Handy, 1979). It also reduces the surfactant solubility in the brine, exacerbates the thermal degradation of the foaming agent and intensifies the foam decay (Handy et al. 1982; Wang, 1984; Liu et al. 2005).

- *Brine composition*: Normally, increased hardness or salinity is a huge impediment to the foam longevity for a given surfactant, because as confirmed by previous studies (Alkan et al. 1991; Borchardt et al. 1988) and depicted in Fig. 2.19, the increased salinity negatively affects the foaming ability by compromising the electrostatic double layer and reducing the surfactant solubility in the brine. Nonetheless, for some excellent anionic surfactant like Chaser CD 1045, their foaming ability is hardly influenced by the total dissolved solid (TDS) value of the brine. Moreover, it has been discovered that the effect of the TDS on surfactant is more evident if the surfactant is CO_2-soluble (Torino et al. 2010).

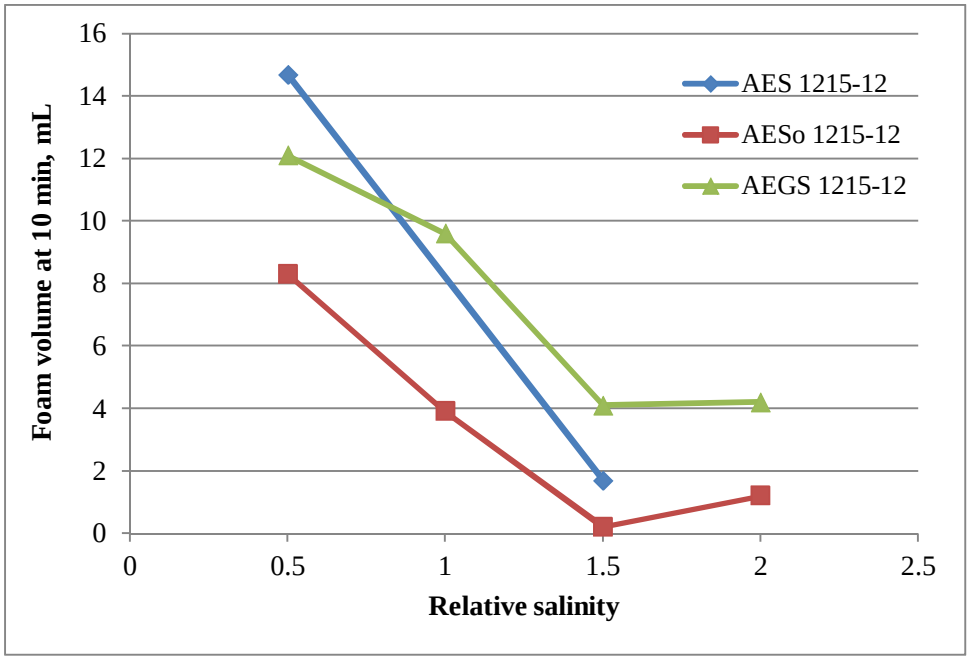

Fig. 2.19 Effect of relative salinity on foam volume (modified after Borchardt et al. 1988)

- *Oil composition*: The generated foam in a porous medium is desired to remain stable when it comes in contact with the residual oil. Assessments in low and high pressure have indicated that the presence of the crude oil decreases the foaming ability and foam stability of a surfactant considerably by damaging the lamella structure (Dellinger et al. 1984; Mannhardt et al. 2000). In an attempt to better understand the influence of oil on the dynamic foam behaviour in the porous media, X-Ray CT imaging of core floods during CO_2 foam displacement has been carried out by numerous research groups (Du et al. 2008; Andrianov et al, 2012; Wellington and Vinegar, 1985). Fig 2.20 is a typical X-ray CT image taken during CO_2 foam flooding.

Generally, it is believed that an oil saturation of greater than 20% is not suitable for CO_2 foam flooding (Schramm, 1994).

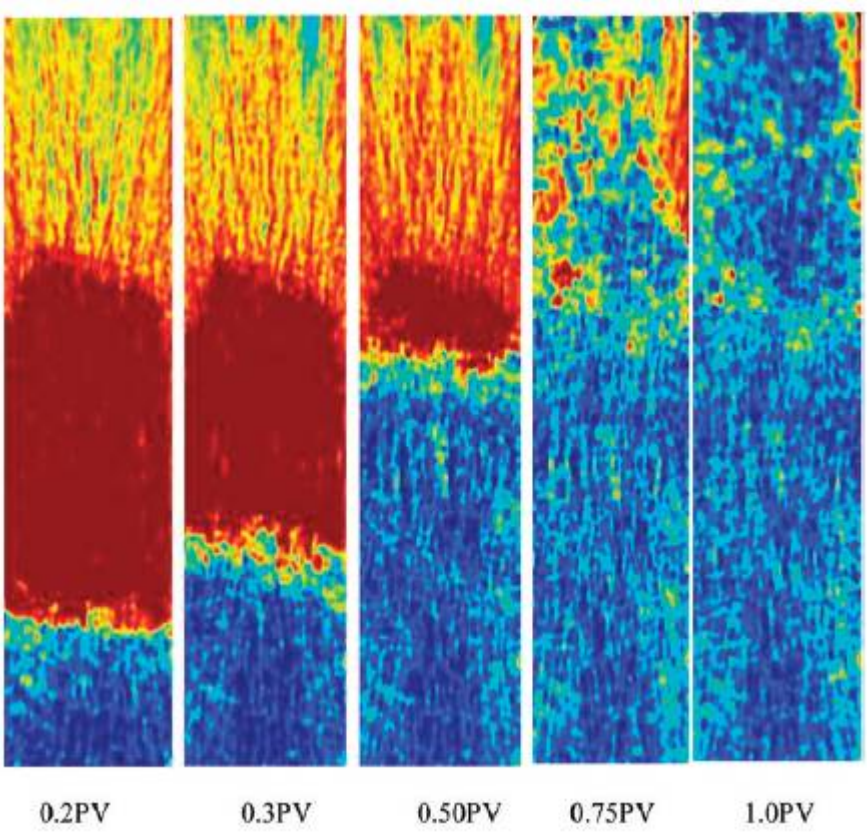

Fig. 2.20 X-Ray CT images showing the foam propagation in a porous medium during a core flooding experiment (Andrianov et al. 2012)

- *Surfactant adsorption*: By dissolving in the brine, a surfactant can stabilize the foams that otherwise would collapse in the reservoir as it flows through the rock. However, surfactant also migrates to the gas/liquid interface and then gets adsorbed onto the rock surface during the foam propagation process, which could significantly reduce the available surfactant amount responsible for generating the foam. In the case of sandstone reservoirs, cationic surfactants which have gained wide applicability in the carbonate reservoirs are seldom applied since the sandstone surface is normally negatively charged. Instead, anionic and non-ionic surfactants are dominant for foam flooding in sandstone reservoirs. It is worth noting that non-ionic surfactants have relatively very small degree of adsorptions due to the absence of charges within the molecules (Ren et al. 2011). If required, the extent of the surfactant adsorption can be

determined in the laboratory in two ways. The static test is conducted by immersing known amount of crushed rock powder into a surfactant solution with fixed original concentration and measuring the concentration variation as a function of time (Kuhlman et al. 1992). The dynamic test is conducted with the assistance of a core flooding experiment. The degree of the adsorption is determined by measuring the surfactant concentration in the effluent fluids and then it is compared with that of the original solution. In both cases, it is observed that the adsorption levels off when the surfactant concentration reaches critical micelle concentration (CMC) (Tabarabal et al. 1993; Grigg and Michalin. 2007).

- *Operational variables.* If the reservoir temperature and pressure, the composition of the crude oil and formation brine, the type and concentration of chemicals are all given, then the displacement performance of the foam flooding can be influenced to some extent by the operational factors such as the injection scheme and the gas/liquid ratio. Yin et al. (2014) attempted to perform foam flooding on a block in Daqing oil field and they conducted numerical simulation study that suggested gas-alternating-solution was an optimal injection scheme at the given condition; Hou et al. (2012) pointed out the direct foam injection might be the best injection strategy if the target reservoir was swept by polymers slug first; Fjelde et al. (2008) found co-injection of gas and solution was a suitable injection method for the investigated carbonated oil reservoir. When it comes to the determination of gas/liquid ratio during a foam flooding, the conclusions also vary from case to case based on the operational conditions (Pei et al. 2010; Lin and Yang 2006; Li et al. 2009). Consequently, operational variables should be well determined prior to any implementation of CO_2 foam flooding

2.2.6.3.5 Main Problems of Carbon Dioxide Foam Flooding

The foam effectiveness is a function of several factors like oil saturation, brine salinity and pH, oil composition, surfactant type and concentration, gas/liquid ratio, reservoir heterogeneity and so forth (Khatib et al. 1988; Zanganeh, 2011). As a consequence, it is vital to gain comprehensive and thorough understanding of the foam flow in the pore channels of the porous medium before the start-up of any CO_2 foam floods. This subsection describes least-understood aspects of foam flood and the challenges that should be given the most attention:

- *Foam stability*: It is considered that effective foam flooding is strongly dependent on the generation of a durable foam in a porous medium, as revealed by previously completed work (Maina and Ma, 1984; Zhu et al. 2004). However, lamellae destruction and foam coalescence tend to cause the creation of foams that can be prone to failure under reservoir condition. In the case where crude oil is present in small amount, for instance the water flooded zone, the oil has little effect on the liquid films that separate the gas bubbles, but the films still become thin due to the gravity drainage, which triggers the lamellae rupture. Capillary suction is proposed to be another mechanism of foam breakage (Radke, 1991). When the oil is present in significant amount, it may spread and then enter the foam lamellae, dramatically affecting the foam stability, which can be quantified by spreading and entering coefficient (Kuhlman, 1990; Ross and Becher, 1992); meanwhile, the foaming agent may be absorbed by some components in the crude oil, so the interface of gas-liquid would be depleted.
- *Using numerical simulations studies to assess viability*: In order to gain a detailed and thorough understanding of flowing properties of foams through porous media, a numerical simulation model incorporating various parameters should be developed for which the parameters are normally extracted from laboratory scale experimental measurements. Nevertheless, the flowing behaviour of a foam is extremely complex and is greatly influenced by issues associated with multiphase coexistence (gas, oil, water, micro-emulsion). Besides, lamellae-oil interactions, variables that influence foam stability (temperature, pH, salinity, oil composition, wettability) and up-scaling the parameters determined from laboratory scale experiments for field application impose extra complexities to any numerical simulation work (Falls et al. 1988; Kam et al. 2007).
- *Pilot test to full field operation*: At present, a successful pilot test of CO_2 foam flood rarely transitions to a feasible full field application. The most important challenges which impede this process include remote onshore environments, offshore supply limitation, separation and processing of the produced fluids, chemical transportation and storage and also HSE concerns (Janssen, 2012; Razali, 2012; Zain, 2012).

References

Alkan H, Goktekin A, Satman A, (1991). A laboratory study of CO_2-foam process for Bati. SPE Middle East Oil Show, held in Bahrain

Al-Shuraiqi HS, Muggeridge AH, Grattoni CA, (2003). Laboratory investigations of first contact miscible WAG displacement: The effects of WAG Ratio and flow rate. SPE International Improved Oil Recovery Conference in Asia Pacific. Kuala Lumpur, Malaysia

Al Wahaibi YM, Al Hadhrami AK, (2011). First-contact-miscible, vaporizing- and condensing-gas drive processes in a channeling heterogeneity system. SPE Middle East Oil and Gas Show and Conference, Manama, Bahrain

Andrianov A, Farajzadeh R, Mohmoodi M, Talanana M, Zitha PLJ, (2012). Immiscible foam for enhancing oil recovery: bulk and porous media experiments. Ind. Eng.Chem. Res. 51: 2214−2226

Asas HK, Okaygum H, Arshad A, (1989). An experimental investigation of first and multiple contact miscible displacement in Arabian Carbonate Cores. Middle East Oil Show, March, Bahrain

Attanucci V, Aslesen KS, Hejl KA, Wright CA, (1993). WAG process optimization in the Rangely CO_2 miscible flood. SPE Annual Technical Conference and Exhibition, Houston, TX, US

Ayirala SC, (2002). Surfactant-induced relative permeability modification for oil reservoir enhancement. M.S. thesis. Louisiana State University

Bae JH, Irani CA, (1990). A laboratory investigation of viscosified CO_2 process. SPE Advanced Technology Series, 1: 166–171.

Bai B, Grigg RB, Liu Y, Zeng Z, (2005). Adsorption kinetics of surfactant used in CO_2-foam flooding onto Berea sandstoneAnnual Technical Conference and Exhibition, Dallas, TX, US

Bernard G, Holm L, (1967). Method for recovering oil from subterranean formations. U.S. Patent 3,342,256.

Barrage T, (1987). A high pressure visual viscometer used in the evaluation of the direct viscosity enhancement of high pressure carbon dioxide. MS thesis, Department of Chemical and Petroleum Engineering, University of Pittsburgh, Pittsburgh, PA

Baviere M, (1980). Basic Concepts in Enhanced Oil Recovery Processes. Data from US Department of Energy, Target reservoirs for CO_2 miscible flooding. DOE/MC/08341

Bayraktar Z, Kiran E, (2000). The miscibility and phase behaviour of polyethylene with carbon dioxide. J. Appl. Polym Sci, 75:1397–1403.

Bennion B, Bachu S, (2005). Relative permeability characteristics for supercritical CO_2 displacing water in a variety of potential sequestration zones in the Western Canada Sedimentary Basin. SPE Annual Technical Conference and Exhibition, Dallas, TX, US

Birarda GS, Dilger CW, McIntosh I, (1990). Re-evaluation of the miscible WAG flood in the Caroline Field, Alberta. SPE Reser. Eng. 5(04): 453-8.

Borchardt JK, Bright DB, Dickson MK, Wellington SL, (1985). Surfactants for CO_2 foam flooding. 60th SPE Annual Technical Conference and Exhibition, Las Vegas, NV, US

Borchardt JK, Bright DB, Dickson MK, Wellington SL, (1988). Surfactants for carbon dioxide foam flooding: Effects of surfactant chemical structure on one-atmosphere foaming properties. Ch. 8 of Surfactant-Based Mobility Control – Progress in Miscible Flood Enhanced Oil Recovery, edited by Duane Smith, ACS Symposium Series 373, ACS, Washington DC: 163–180

Braun E, Holland R, (1995). Relative permeability hysteresis: laboratory measurements and a conceptual model. SPE Reser. Eng. 10(03): 222-228.

Brotin T, Utermohlen R, Fages F, Bouas-Laurent H, Desvergne JP, (1991). A novel small molecular luminescent gelling agent for alcohols. J. Chem. Soc., Chem. Commun.: 416–418.

Brownlee MH, Sugg LA (1987). East Vacuum Grayburg-San Andres Unit CO_2 injection project: development and results to date. SPE Annual Technical Conference and Exhibition, Dallas, TX, US

Carroll SA, Knauss KG, (2005). Dependence of labradorite dissolution kinetics on CO_2 (aq), Al (aq) and temperature. Chem. Geol. 217(3-4): 213-225.

Casteel JF, Djabbarah NF, (1988). Sweep improvement in CO_2 flooding by use of foaming agents. SPE Reser. Eng.: 1186–1192

Chambers KT, Radke CJ, (1990). Micromodel foam flow study. Prepared for U.S. Department of Energy, University of California, Chemical Engineering Department

Chang SH, Grigg RB, (1996). Foam displacement modelling in CO_2 flooding processes. SPE/DOE Tenth Symposium of Improved Oil Recovery, Tulsa, OK, US

Chen M, Yortsos YC, Rossen WR, (2004). A pore-network study of the mechanisms of foam generation. SPE Annual Technical Conference and Exhibition, Houston, TX, US

Christensen JR, Stenby EH, Skauge A, (2001). Review of WAG field experience. SPE Reserv. Eng. 4(02): 97-106

Claridge EL, (1972). Prediction of recovery in unstable miscible recovery. SPE J 12(02): 143–155.

Clavier G, Mistry M, Fages F, Pozzo JL, (1999). Remarkably simple small organogelators: di-n-alkoxy-benzene derivatives. Tetrahedron Letters, (40): 9021–9024.

Craig F, (1957). A laboratory study of gravity segregation in frontal drives," Trans. AIME 210: 275–282.

Craig F, (1971). The reservoir engineering aspects of water flooding, Monograph Series, Dallas, Tx.

Dandge DK, Heller JP, (1987). Polymers for mobility control in CO_2 floods. SPE International Symposium on Oilfield Chemistry. San Antonio TX, US

Deberry DW, Clark WS, (1979). Corrosion due to use of CO_2 for Enhanced Oil Recovery. US Department of Energy, Report DOE/MC/08442-1

Dellinger SE, Patton JT, Holbrook ST, (1984). CO_2 Mobility Control. SPE J: 191–196.

Eastone J, Fragneto G, Robinson BH, Towey TF, heenan Rk, Leng FJ, (1992). Variation of surfactant counterion and effect on the structure and properties of Aerodol-OT-based water-in-oil microemulsions. J. Chem. Soc. Faraday Trans. 88: 461

Eastoe J, Paul A, Nave S, Steytler DC, Robinson BH, Rumsey E, Thorpe M, Heenan RK, (2001). Micellization of hydrocarbon surfactants in supercritical carbon dioxide. J. Am. Chem. Soc. 123 (05): 988–989.

Element D, Masters J, Sargent N, Jayasekera A, Goodyear S, (2003). Assessment of three-phase relative permeability models using laboratory hysteresis data. SPE International Improved Oil Recovery Conference in Asia Pacific. Kuala Lumpur, Malaysia

Enick R, (1991).The effect of hydroxyl aluminium disoaps on the viscosity of light alkanes and carbon dioxide. SPE International Symposium on Oilfield Chemistry, Anaheim CA, US

Enick RM, (1998). A literature review of attempts to increase the viscosity of dense carbon dioxide. www.netl.doe.gov/publications/others/techrpts/co2thick.pdf

Enick R, Karanikas C, Bane S, Potluri V, Hamilton A, (2003). The high CO_2 solubility of per-acetylated α-, β- and γ cyclodextrin. Fluid Phase Equilibr. 211(02): 211–217.

Enick R, Hong L, Thies M, (2005). CO_2 + β-D-Maltose octaacetate system exhibits a global phase behaviour of CO_2-philic solids that melt in dense, CO_2-Rich fluids" J. Supercritical Fluids 34 (01): 11–16.

Falls AH, Hirasaki GJ, Patzek TW, Gauglitz DA, Miller DD, Ratulowski T, (1988). Development of a mechanistic foam simulator: the population balance and generation by snap-off. SPE Res. Eng. 3(3): 884-892

Fan X, Potluri V, McLeod M, Wang Y, Liu J, Enick RM, Hamilton A, Roberts C, Johnson J, Beckman E, (2005). Oxygenated hydrocarbon ionic surfactants exhibit CO_2 solubility. J. Am. Chem. Soc. 127 (33): 11754–11762.

Farajzadeh R, Salimi H, Zitha PLJ, Bruining J, (2007). Numerical simulation of density-driven natural convection in porous media with application for CO2 injection projects. SPE-EUROPEC/ EAGE Conference, London, UK

Farajzadeh R, Andrianov A, Zitha PLJ, (2009). Foam assisted enhanced oil recovery at miscible and immiscible conditions. SPE Kuwait International Petroleum Conference and Exhibition, held in Kuwait City, Kuwait

Farajzadeh R, Andrianow A, Krastev R, Hirasaki GJ, Rossen WR, (2012). Foam-oil interaction in porous media: implication for foam assisted enhanced oil recovery. SPE- EOR Conference at Oil and Gas West Asia, Muscat, Oman

Fjelde I, Zuta J, Duyilemi OV, (2008). Oil recovery from matrix during CO_2-foam flooding of fractured carbonate oil reservoir. Europec/EAGE Conference and Exhibition, Rome, Italy

FTH Chung, (1988). Recovery of viscous oil under high pressure by CO_2 displacement: A laboratory study. International Meeting on Petroleum Engineering, Tianjin China

Fullbright GD, Hild GP, Korf TA, Myers JP, O'Toole FS, Wackowski RK, Smith ME, (1991). Evolution of conformance improvement efforts in a major CO_2 WAG injection project. SPE/DOE Improved Oil Recovery Symposium, Tulsa, Oklahoma, US

Gauglitz PA, Friedmann F, Kam SI, Rossen WR, (2002). Foam generation in homogeneous porous media.Chem.Eng.Sci.57: 4037-4052.

Gaus I, (2010). Role and impact of CO_2-rock interaction during CO_2 storage in sedimentary rocks. Int. J. Greenhouse Gas Control, 4(1): 73-89.

Genrich JF, Choi GN, Haldorsen HH (1986). Profile control of Prudhoe Bay WAG miscible floods. Reservoir Engineering Technology Exchange Conference, Scottsdale, Arizona, US

Ghani Z, (2013). Improved oil recovery using CO_2 as an injection medium: a detailed analysis. Master thesis, Australian Maritime College, University of Tasmania

Ghedan, S, (2009). Global laboratory experience of CO_2-EOR flooding. SPE/EAGE Reservoir Characterization and Simulation Conference, Abu Dhabi, United Arab Emirates

Goodrich JH, (1980). Review and analysis of past and ongoing carbon dioxide injection field tests. SPE/DOE Symposium on Improved Oil Recovery, Tulsa, Oklahoma, US

Graham BD, Bowen JF, (1980). Design and implementation of a Levelland Unit CO_2 Tertiary pilot. SPE/DOE Symposium on Enhanced Oil Recovery, Tulsa, Oklahoma, US

Graue DJ, Zana ET, (1981).Study of a possible CO_2 flood in Rangely Field. J. Petrol. Technol. 33(7): 1312-1318

Grigg RB, Mikhalin AA, (2007). Effects of flow conditions and surfactant availability on adsorption. SPE International Symposium on Oilfield Chemistry, Houston, TX, US

Grigg RB, Schechter DS, (1997). State of industry in CO_2 floods. SPE Annual Technical Conference and Exhibition, San Antonio, Texas, US

Gullapalli P, Tsau JS, Heller JP, (1995). Gelling Behaviour of 12-hydroxystearic acid in organic fluids and dense CO_2. SPE International Symposium on Oilfield Chemistry, held in San Antonio, TX, US

Habermann B, (1960). The Efficiency of Miscible Displacement as a Function of Mobility Ratio. Trans AIME 219: 264–272.

Hadlow RE, (1992). Update of industry experience with CO_2 injection. SPE Annual Technical Conference and Exhibition, Washington, DC, US

Hakiki F, Maharsi DA, Marhaendrajana T, (2016). Surfactant-Polymer coreflood simulation and uncertainty analysis derived from laboratory study. Journal of Engineering and Technological Sciences. 47(6): 706-724

Handy LL, Amaefule JO, Ziegler VM, Ershaghi I, (1982). Thermal stability of surfactants for reservoir application. SPE Journal: 722–730.

Hangx SJT, Spiers CJ, (2010). Reaction of plafioclase feldspars with CO_2 under hydrothermal conditions. Chem. Geol. 265 (1-2): 88-98.

Harris TV, Irani CA, Pretzer WR, (1990). Enhanced oil recovery using CO_2 flooding. U.S. Patent 4,913,235

Haruki M, Yawata H. Nishimoto M, Tanto M, Kihara SI, Takishima S, (2007). Study on phase behaviours of supercritical CO_2 including surfactant and water. Fluid Phase Equilibria 261: 92–98.

Heller JP, Dandge DK, Card RJ, Donaruma LG, (1985). Direct thickeners for mobility control of CO_2 floods. SPE J: 679-685

Heller JP, (1994). CO_2 foams in enhanced oil recovery. Advances in Chemistry Series 242: 201-234

Heller JP, Kovarik FS, (1988). Improvement of CO_2 flood performance. Fourth annual report for the period of Oct. 1, 1987–Sept. 30, 1988, Contract no.FC21-84MC21136, New Mexico Petroleum Recovery Research Centre, Socorro, NM, DOE/MC/21136-24.

Heller JP, (1986). Mobility control for CO_2 injection. Final report, Contract No. AC21-81MC16426, New Mexico Petroleum Recovery Research Center, New Mexico Institute for Mining and Technology, Socorro, NM, DOE/MC/16426-19.

Heller J, (1994). CO_2 foams in enhanced oil recovery. Ch. 5 in Foams: Fundamentals and Applications in the Petroleum Industry, ACS Advances in Chemistry Series 242, ACS, Washington DC, 201–234.LJ Mohammed-Singh, AK Singhal, (2005). Lessons from Trinidad's CO_2 immiscible pilot projects. SPE Reserv. Eval. Eng. 8(05): 397-403.

Høier L, Whitson CH, (1998). Miscibility variation in compositionally grading reservoirs. Annual Technology Conference and Exhibition of Society Petroleum Engineers, New Orleans, US

Holloway HD, Fitch RA, (1964). Performance of a miscible flood with alternate gas-water displacement. J Pet Technol. 16(04): 372

Holm LW, (1959). Carbon dioxide solvent flooding for increased oil recovery processes. Pet. Trans. 216: 225–231.

Holm LW, (1972). Propane-gas-water miscible floods in watered-out areas of the Adena Field. J Pet Technol. 24 (10): 1264-1270

Holm LW, Josendal VA, (1974). Mechanism of oil displacement by carbon dioxide. J of Pet Technol, Trans A, 257: 1427–1438.

Hou Q, Zhu Y, Luo Y, Weng R, (2012). Studies on foam flooding EOR technique for Daqing Reservoirs after polymer flooding. SPE Improved Oil Recovery Symposium, Tulsa, Oklahoma, US

Hsie JC, Moore JS, (1986). The Quarantine Bay 4RC CO_2-WAG pilot project: A post-flood evaluation. SPE Annual Technical Conference and Exhibition, New Orleans, US

Huang ETS and Holm LW, (1988). Effect of WAG injection and rock wettability on oil recovery during CO_2 Flooding. SPE Reserv. Eng. 3(01): 119-129

Huang Z, Shi C, Xu J, Kilic S, Enick RM, Beckman E, (2000). Enhancement of the viscosity of carbon dioxide using styrene/fluoroacrylate copolymers. Macromolecules, 33 (15): 5437–5442.

Iezzi A, Enick R, Brady J, (1989). The direct viscosity enhancement of carbon dioxide. Supercritical Fluid Science and Technology, ACS Symposium Series 406: 122–139.

Iezzi, A.; Bendale, P.; Enick, R.; Turberg, M.; Brady, J. (1989). Gel Formation in Carbon Dioxide-Semifluorinated Alkane Mixtures and Phase Equilibria of a Carbon Dioxide-Perfluorinated Alkane Mixture, Fluid Phase Equilibria, 52: 307–317.

Janssen A, (2012). Enhanced fluid separation for chemical floods. SPE Chemical Flooding-EOR workshop. Penang, Malaysia Jarrell PM, Fox CE, Stein MH, Webb SL. Practical aspects of CO_2 flooding: Richardson, Tex., Society of Petroleum Engineers Monograph Series, 22: 220

Jensen J, Nesteby H, Slotte PA, (1996). Brage WAG Pilot. RUTH 1992-1995, Norwegian Petroleum Directorate, Stavanger.

Kam SI, Nquyen QP, Li Q, Rossen WR, (2007). Dynamic simulation with an improved model for foam generation. SPE J 12(01): 35-48

Kaszuba JP, Janecky DR, Snow WG, (2003). Carbon dioxide reaction processes in a model brine aquifer at 200°C and 200 bar: implication for geologic sequestration of carbon. Appl. Geochem. 18 (7): 1065-1080.

Khatib ZI, Hirasaki GJ, Falls AH, (1988). Effects of capillary pressure on coalescence and phase mobility in foams flowing through porous media. SPE Reserv. Eng. 3: 919-926

Klauda JB, Sandler SI, (2000). A fugacity model for gas hydrate phase equilibria. Ind. Eng. Chem. Res. 39 (9): 3377–3386

Kralik J, Manak L, Jerauld G, Spence A, (2000). Effect of trapped gas on relative permeability and residual oil saturation in an oil-wet sandstone. SPE Annual Technical Conference and Exhibition. Dallas, Texas, US

Kuhlman MI, (1990). Visualizing the effect of light oil on CO_2 foams. J. Petrol. Technol. 07(42): 902-908.

Kuhlman MI, Falls AH, Hara SK, Monger-McClure TG, Borchardt JK, (1992). CO_2 foam with surfactants used below their critical micelle concentrations. SPE Reser. Eng.: 445–452.

Kuhlman MI, Lau HC, Falls AH, (2000). Surfactant criteria for successful carbon dioxide foam in sandstone reservoirs. SPE Reser. Eval. Eng. 3(01): 35–41.

Larsen J, Skauge A, (1998). Methodology for numerical simulation with cycle dependent relative permeabilities. SPE J 3(02): 163-173.

Lasater JA, (1958). Bubble point pressure correlation. J of Pet Technol, Trans A. 10(05): 379–381.

Lawson JB, Reisberg J, (1980). Alternate slugs of gas and dilute surfactant for mobility control during chemical flooding. SPE/DOE Enhanced Oil Recovery Symposium. Tulsa, OK, US

Lee HO, Heller JP, (1990). Laboratory measurements of CO_2-foam mobility. SPE Reser. Eng.: 193–197.

Leontraritis KJ, Ali Mansoori G, (1988). Asphaltene deposition: A survey of field experiences and research approaches. J. Pet. Sci. Eng. 229-239

Lewis E, Dao EK, Mohanty KK, (2008). Sweep efficiency of miscible floods in a high-pressure quarter-five-spot pattern. SPE J 13(04): 432–439.

Lescure BM, Claridge EL, (1986). CO_2 foam flooding performance vs. rock wettability. SPE Annual Technical Conference and Exhibition, New Orleans, LA

Li Z, Song X, Wang Q, (2009). Enhanced foam flooding pilot test in Chengdong of Shengli oilfield: Laboratory experiment and field performance. International Petroleum Technology Conference, Doha, Qatar.

Lin Y, Yang G, (2006). A successful pilot application for N2 foam flooding in Liaohe Oilfield. SPE Asia Pacific Oil and Gas Conference and Exhibition, Adelaide, Australia.

Liu Y, Grigg R, Bai B, (2005). Salinity, pH, and surfactant concentration effects of CO_2-foam. SPE International Symposium on Oilfield Chemistry, Houston, TX, US

Liu Y, Grigg RB, Svec RK, (2005). CO_2 foam behaviour: influence of temperature, pressure, and concentration of surfactant. SPE Production and Operations Symposium, Oklahoma City, OK, US

Llama OG, (2011). Mobility control of chemical EOR fluids using foam in highly fractured reservoirs. M.S. thesis. Faculty of the Graduate School, The University of Texas at Austin

Llave FM, Chung FTH, Burchfield TE, (1990). Use of entrainers in improving mobility ratio of supercritical CO_2. SPE Reser. Eng.: 47-51

Ma TD, Youngren GK, (1994). Performance of immiscible Water-Alternating-Gas (IWAG) injection at Kuparuk River Unit, North Slope, Alaska. SPE Annual Technical Conference and Exhibition, New Orleans, US

Ma TD, Rugen JA, Stoisits RF, (1995). Simultaneous water and gas injection pilot at the Kuparuk River Field, Reservoir Impact. SPE Annual Technical Conference and Exhibition, Dallas, TX, US

Macintyre KJ, (1986). Design consideration for carbon dioxide injection facilities. J Can Petr. Techn. 25 (02): 90-95.

Maina BB, Ma V, (1984). Relationship between foam stability measured in static tests and flow behaviour of foams in porous media. SPE 59th Annual Technical Conference and Exhibition, Houston, Texas, US

Mannhardt K, Novosad JJ, Schramm LL, (2000). Comparative evaluation of foam stability to oil. SPE Res. Eval. Eng. 3 (1): 23–34.

Mardsen SS, (1986). Foams in porous media. US Department of Energy, National Petroleum Technology Office, Tulsa, OK

Martin FD, Heller JP, Weiss WW, Stevens J, Harpole K, Siemers T, Gerard, M., Sugg L, Hidajat I, Moradi-Aragh A, Zomes D, Grigg R, Chang E, Tsau JS, Ouenes A, Sultan J, Killough J, Kuehne D, (1991). Field verification of CO_2-Foam. Final report, Contract No. DE-FG21-89MC26031, New Mexico Institute of Mining and Technology, Socorro, NM, DOE/MC/26031-32.

Masoner LO, Abidi HR, Hild GP, (1996). Diagnosing CO_2 flood performance using actual performance data. SPE/DOE Symposium on Improved Oil Recovery, Tulsa, Oklahoma, US

McClain JB, Betts DE, Canelas DA, Samulski ET, DeSimone JM, Landona JD, Wignall GD, (1996). Characterization of polymers and amphiphiles in supercritical CO_2 using small angle neutron scattering and viscometry. Proceeding of spring meeting of the ACS, Division of Polymeric Materials, New Orleans, LA: Science and Engineering, 74: 234–235.

Mclendon WJ, Koronaios P, Mcnulty S, Enick RM, Biesmans G, (2012). Assessment of CO2-soluble surfactant for mobility control reduction using mobility measurement and CT imaging. SPE Improved Oil recovery Symposium. Tulsa, OK, US

Merchant DH, (2010). Life beyond 80—A look at conventional WAG recovery beyond 80 % HCPV injection in CO_2 tertiary flood. SPE International Conference on CO_2 Capture, Storage, and Utilization, New Orleans, LA, USA

Mizenko GJ, (1992). North Cross Unit CO_2 flood, status report. 8th SPE/DOE Symposium on EOR, Tulsa, US

Monger TG, Trujillo DE, (1991). Organic deposition during CO_2 and rich-gas flooding. SPE Reser. Eng. 6(01): 17-24

Moritis G, (2002). Special report: enhanced oil recovery-2002 worldwide EOR survey. Oil Gas J 100:43–47

Nguyen QP, Alexandrov AV, Zitha PL, Currie PK, (2000). Experimental and modelling studies on foam in porous media: A review. SPE International Symposium on Formation Damage Control, held in Lafayette, Louisiana, US

Odd MM, (2003). CO_2 as injection gas for enhanced oil recovery and estimation of the potential on the Norwegian Continental Shelf. Department of Petroleum Engineering and Applied Geophysics, Norwegian University of Science and Technology

Okwen RT, (2006). Formation damage by CO_2- induced asphaltene precipitation. SPE International Symposium and Exhibition on Formation Damage, Lafayette LA, US

Orr FM, Jr, Yu AD, Lien CL, (1981). Phase behaviour of CO_2 and crude oil in low temperature reservoirs. Soc. Pet. Eng. J. 21: 480-492.

Orr, FM, Jr, Silva MK, Lien CL, (1982). Laboratory experiments to evaluate field prospects for CO_2 flooding. Pet. Tech. J 34

Paik IH, Tapriyal D, Enick R, Hamilton A, (2007). Fiber formation by highly CO_2-soluble bis-ureas based on peracetylated carbohydrate groups. Angewandte Chemie International Edition 46(18): 3284–3287.

Pei H, Zhang G, Wang J, Ding B, Liu X, (2010). Investigation of polymer-enhanced foam flooding with low gas/liquid ratio for improving heavy oil recovery. Canadian Unconventional Resources & International Petroleum Conference, Calgary, Alberta, Canada.

Placin F, Desvergne J, Cansell F, (2000). Organic low molecular weight aerogel formed in supercritical fluids. J. Mater. Chem. (10): 2147–2149.

Potluri V, Xu J, Enick R, Beckman E, Hamilton A, (2002). Per-Acetylated sugar derivatives show high solubility in liquid and supercritical carbon dioxide. Organic letters, 4: 2333-2335.

Prieditis J, Wolle CR, Notz PK, (1991). A laboratory and field injectivity study: CO_2 WAG in the San Andres Formation of West Texas. SPE Annual Technical Conference and Exhibition, Dallas, TX, US

Radke CJ, (1991). Emulsion, Foams and Suspensions: Fundamentals and Applications. In Interfacial Phenomena in Petroleum Recovery, Morrow, N. R., Ed., Marcel Dekker: New York, Chapter 6, pp 191-255.

Radke C, Gillis J, (1990). “A dual gas tracer technique for determining trapped gas saturation during steady foam flow in porous media. 65th Annual Technical Conference and Exhibition of the SPE, New Orleans, LA, US

Razali HM, (2012). General requirement of chemical EOR from HSE perspective. SPE Chemical Flooding-EOR workshop. Penang, Malaysia.

Reed RL, Healy RN, (1997). Some physio-chemical aspects of microemulsion flooding. D.O. Shah, R.S. Schechter (Eds.), Improved Oil Recovery by Surfactant and Polymer Flooding, Academic Press, London

Reinbold EW, Bokhari SW, Enger SR, Ma TD, Renke SM, (1992). Early performance and evaluation of the Kuparuk hydrocarbon miscible flood. SPE Annual Technical Conference and Exhibition. Washington, D.C., US

Ren G, Zhang H, Nguyen Q, (2011). Effect of surfactant partitioning between CO_2 and Water on CO_2 mobility control in hydrocarbon reservoirs. SPE Enhanced Oil Recovery Conference, Kuala Lumpur, Malaysia

Ring JN, Smith DJ, (1995). An overview of the North Ward Estes CO_2 flood. SPE Annual Technical Conference and Exhibition, Dallas, US

Robin M, (2001). Interfacial phenomena: Reservoir wettability in oil recovery. Oil Gas Sci. Technol. 56(1): 55-62

Robie DR Jr, Roedell JW, Wackowski RK, (1995). Field trial of simultaneous injection of CO_2 and water, Rangely Weber Sand Unit, Colorado. SPE Production Operations Symposium, Oklahoma City, Oklahoma, US

Rogers JD, Grigg RB, (2000). A literature analysis of the WAG injectivity abnormalities in the CO_2 process. SPE/DOE Improved Oil Recovery Symposium, Tulsa, Oklahoma, US

Ross S, Becher P, (1992). The history of the spreading coefficient, J. Colloid Interface Sci. 149(2), 575-579.

Ryoo W, Webber S, Johnston K, (2003). Water in carbon dioxide microemulsions with methylated branched hydrocarbon surfactants. Ind. Eng. Chem. Res. 42: 6348–6358

Saeedi, A., (2012). Experimental Study of Multiphase Flow in Porous Media during CO_2 Geo-Sequestration Processes. Sprinegr Thesis. Springer Publishing, Heidelberg, Germany.

Salem S, Moawad T, (2013). Economic study of miscible CO_2 flooding in a mature waterflooded oil reservoir. SPE Saudi Arabia Section Technical Symposium and Exhibition. Al-Khobar, Saudi Arabia

Sanders A, Jones R, Mann T, Patton L, Linroth M, Nguyen Q, (2010). Successful implementation of CO_2-foam for conformance control. 2010 CO_2 Conference, Midland Texas, US

Sankur V, (1986). A laboratory study of Wilmington Tar Zone CO_2 injection project. J SPE Reser. Eng. 1(1):95-104

Schievelbein V, (1991). Method of decreasing mobility of dense carbon dioxide in subterranean formations. U.S. Patent 5,033,547

Schlumberger, (1998). Oil field glossary. http://www.glossary.oilfield.slb.com/en/Terms/d/

Schneider F, Owens W, (1976). Relative permeability studies of gas-water flow following solvent injection in carbonate rocks. Soc. Petrol. Eng. J 16(01), 23-30.

Schramm LL, (1994). Foam sensitivity to crude oil in porous medium. Foams: fundamentals and application in petroleum industry. American Chemistry Society, Washington DC, Chapter 4: 165-197

Shao H, Ray JR, Jun YS, (2010). Dissolution and precipitation of clay minerals under geological CO_2 sequestration condition: CO_2-brine-phlogopite interaction. Environ. Sci. Technol. 44: 5999-6005

Shen Z, McHugh MA, Xu J, Belardi J, Kilic S, Mesiano A, Bane S, Karnikas C, Beckman EJ, Enick RM, (2003). CO_2-solubility of oligomers and polymers that contain the carbonyl group. Polymer 44: 1491–1498.

Shi C, Huang Z, Kilic S, Xu J, Enick RM, Beckman EJ, Carr AJ, Melendaz RE, Hamilton AD, (1999). A sustainable route to the creation of microcellular materials. Science 286: 1540-1543

Shi C, Huang Z, Beckman E, Enick R, Sun-Young K, Curran DP, (2001). Semifluorinated trialktyltin fluorides and fluoroether telechelic ionomers as viscosity enhancing agents for carbon dioxide. Ind. Eng. Chem. Res. 40 (03): 908–913.

Shuler JP, Freitas EA, Bowker KA, (1991). Selection and application of $BaSO_4$ scale inhibitors for a CO_2 flood, Rangely Weber Sand. SPE Production Engineering. 6(03): 259-264

Simjoo M, Dong Y. Andrianov A, Talanana M, Zitha PJL, (2012). A CT scan study of immiscible foam flow in porous media for EOR. SPE-EOR Conference at Oil and Gas West Asia, Muscat, Oman

Skauge A, Aarra M (1993). Effect of wettability on the oil recovery by WAG. 7th European Symposium on Improved Oil Recovery, Moscow, Russia

Skauge A, Larsen JA, (1994). New approach to model the WAG process. 15th Intl. Energy Agency Collaborative Project on Enhanced Oil Recovery, Workshop and Symposium, Bergen, Norway

Skauge A, Larsen JA, (1994). Three-phase relative permeabilitites and trapped gas measurements related to WAG processes. International Symposium of the Society of Core Analysists. Stavanger, Norway

Skauge A, Berg E, (1997). Immiscible WAG injection in the Fensfjord Formation of the Brage Oil Field. 1997 European Symposium on Improved Oil Recovery, Hague, Norway

Srivastava M, (2010). Foam assisted low interfacial tension enhanced oil recovery. Ph. D. thesis, The University of Texas Austin

S Sahin. Bate Raman Field immiscible CO_2 application--status quo and future plans. SPE Reserv. Eval. Eng. 11 (04): 778-791

Stalkup, FI Jr, (1982). Status of miscible displacement. International Petroleum Exhibition and Symposium, Beijing, China

Stalkup FI, Jr, (1983). Miscible Displacement. Monograph Series, Society Petroleum Engineers.

Stalkup FI, Jr, (1983) Status of miscible displacement. J. Pet. Technol. 35(04): 815–826.

Stalkup FI, (1987). Carbon dioxide miscible flooding: past, present, and outlook for the future. J Pet Tech 30: 1102-1112.

Stein MH, Frey DD, Walker RD, Pariani GJ, (1992). Slaughter Estate Unit CO_2 Flood: Comparison between pilot and field-scale performance. J Pet. Technol. 44(09): 1026-1032

Sweatman RE, Parker ME, Crookshank SL, (2009). Industry experience with CO_2-enhanced oil recovery technology. SPE International Conference on CO_2 Capture, Storage and Utilization. San Diego, California, US

Tabatabal A, Gonzalez MV, Harwell JH, Scamehorn JF, (1993). Reducing surfactant adsorption in carbonate reservoirs, SPE Reserv. Eng.: 117–122.

Tapriyal D, Enick R, (2008). Poly (vinyl acetate), poly ((1-O-(vinyloxy) ethyl-2, 3, 4, 6-tetra-O-acetyl-β-D-glucopyranoside) and amorphous poly (lactic acid) are the most CO_2-soluble Oxygenated Hydrocarbon-Based Polymers. J. Supercritical Fluids, 46: 252–257.

Tapriyal D, (2009). Design of non-fluorous CO_2-soluble compounds. PhD dissertation University of Pittsburgh, Department of Chemical and Petroleum Engineering, Pittsburgh, PA, 2009.

Terry RE, Zaid A, Angelos C Whitman DL, (1987). Polymerization in supercritical CO_2 to improve CO_2/oil mobility ratios. SPE International Symposium on Oilfield Chemistry. San Antonio TX, US

Torino E, Reverchon E, Johnston KP, (2010) Carbon dioxide/water, water/carbon dioxide emulsions and double emulsions stabilized with a nonionic biocompatible surfactant. J. Colloid Interface Science, 348: 469–478.

Trickett K, Xing D, Enick R, Eastoe J, Hollamby MJ, Mutch KJ, Rogers SE, Heenan RK, Steytler DC, (2010). Rod-like micelles thicken CO_2. Langmuir, 26 (01): 83–88.

Tsau JS, Heller JP, (1992). Evaluation of furfactants for CO_2-foam mobility control. SPE Permian Basin Oil and Gas Recovery Conference, held in Midland, TX, US

Van Poollen HK, (1980). Fundamentals of Enhanced Oil Recovery. PennWell Books, Tulsa, Oklahoma, US

Verma MK, (2015). Fundamentals of Carbon Dioxide-Enhanced Oil Recovery (CO_2-EOR) — A supporting document of the assessment methodology for hydrocarbon recovery using CO_2-EOR associated with carbon sequestration. US Department of the Interior and Geological Survey.

Wang GC, (1984). A laboratory study of CO_2 foam properties and displacement mechanism. SPE/DOE Fourth Symposium on Enhanced Oil Recovery, held in Tulsa, OK, US

Wang Y, Hong L, Kim IC, Paik IH, Crosthwaite JM, Hamilton AD, Thies M, Beckman EJ, Enick RM, Johnson K, Tapriyal D, (2009). Design and evaluation of non-fluorous CO_2-soluble polymers. J. Phys. Chem. B 113(45): 14971–14980.

Wassmuth F, (1994). Foams: basic principles. In: Schramm LL (Ed.), Foams: fundamentals and application in the petroleum. Vol. 242, American Chemistry Society: 3-45 (Chapter 1).

Wellington SL, Vinegar HJ, (1985). CT studies of surfactant-induced CO_2 mobility control. SPE-ATC. Las Vegas NV, US

White CM, Strazisar BR, Granite EJ, Hoffman JS, Pennline HW. Separation and capture of CO_2 from large stationary sources and sequestration in geological formations-coalbeds and deep saline aquifers. J. Air Waste Manage. Assoc. 53, 645-715.

Wiebe and Gady, (1939). Solubility of CO_2 in water. 61: 316.

Williams LL, Rubin JB, Edwards HW, (2004). Calculation of hansen solubility values for a range of pressure and temperature conditions, including the Supercritical Region. Ind Eng Chem Res, 43 (16): 4967 – 4972

Xu J, Wlaschin A, Enick RM, (2003). Thickening carbon dioxide with the fluoroacrylate-styrene copolymer. SPE J: 85-91

Xu Q, (2003). Theoretical and experimental study of foam for enhanced oil recovery and acid diversion. Ph. D thesis. The University of Texas Austin.

Xu T, Apps JA, Pruess K, (2005). Mineral sequestration of carbon dioxide in a sandstone-shale system. Chem. Geol. 217(3-4 SPEC. ISS.): 295-318.

Yaghoobi H, Heller JP, (1994). Laboratory investigation of parameters affecting CO_2-foam mobility in sandstone at reservoir conditions. Eastern Regional Conference and Exhibition, held in Charleston, WV, US

Yang D, Tontiwachwuthikul P, Gu Y, (2005). Interfacial interactions between reservoir brine and CO_2 at high pressures and elevated temperatures. Energy Fuels, 19(1): 216-223.

Yin H, Liu C, Wang M, (2014). Injection scheme optimization of foam profile control on Block S103. Eng. 6, 7-11

Yuan M, Mosley J, Hyer N, (2001) Mineral scale control in a CO_2 flooded oilfield. SPE International Symposium on Oilfield Chemistry, Huston, US

Zain TFM, (2012). Storage, logistic and chemical transferring in offshore environment. SPE Chemical Flooding-EOR workshop. Penang, Malaysia.

Zanganeh MN, (2011). Simulation and optimization of foam EOR processes. Ph. D. thesis. Faculty of Civil Engineering and Geoscience, Delft University of Technology

Zhang Y, Luo P, Sam Huang, (2010). Improved heavy oil recovery by CO_2 injection augmented with chemicals. SPE International Oil and Gas Conference, Beijing, China

Zhu T, Ogbe DO, Khataniar S, (2004). Improving the foam performance for mobility control and improved sweep efficiency in gas flooding. Ind. Eng. Chem. Res. 43 (15): 4413–4421.

Ziegler VM, Handy LL, (1979). The effect of temperature on surfactant adsorption in porous media. 54th Annual Fall Technical Conference and Exhibition of the SPE of AIME, Las Vegas, NV, US

Chapter 3 Material, Experimental Setup and Methodology

3.1 Introduction

This chapter presents in details the materials, apparatuses and procedures employed during the course of development of this experimental research. To be able to develop a novel foaming formulation, which is a primary objective of this work, a variety of chemicals including surfactants, polymers and additives are needed. Therefore, the first section of this chapter describes the properties and the composition of the chemicals as well as the synthetic formation water, crude oil and the rock samples used. The following section presents the details of the experimental setup and a number of laboratory based methodologies that were applied for the purpose of evaluation and optimization of the techniques and formulations developed in this study.

3.2 Materials

3.2.1 Surfactant

The rock samples applied in this research are sandstones which, as indicated in the previous chapter, are negatively charged on their grain surfaces. Consequently, cationic surfactants are excluded by default for the study to avoid adsorption loss. Instead, the other three remaining categories of commercial surfactants (anionic, non-ionic and amphoteric) are employed and assessed in terms of their foaming ability and foam durability. Some information about each of these surfactant products are shown in Table 3.1.

Table 3.1 Basic information about the applied surfactant products

Surfactant	Product Name	Category	Supplier
Sodium alpha-olefin Sulfonate	AOS	Anionic	Stepan Company
Alcohol ethoxysulfates	AES	Anionic	Solvay Chemicals
Sodium dodecyl sulfate	SDS	Anionic	Sigma-Aldrich
Disodium monolauryl sulfosuccinate	DLS	Anionic	Usolf Chemicals
Polyethylene glycol tert-octylphenyl ether	Triton X-100	Non-ionic	Sigma-Aldrich
Trimethylnonylpolyethylene glycol	TMN-6	Non-ionic	Sigma-Aldrich
Alkyl polyglycoside	APGs	Non-ionic	Sigma-Aldrich
Cocoamidopropyl betaine	CAB-35	Amphoteric	Xuejie Chemicals
Lauramidopropyl betaine	LAB-35	Amphoteric	Xuejie Chemicals

3.2.2 Polymers and Additives

In general, polymers are used to boost the apparent viscosity of the bulk solution and additives are normally added to strengthen the liquid membrane in the foam system. For this research, two high-performance and economical polymer alternatives are evaluated. One is the commonly used hydrolyzed polyacrylamide (HPAM) with the molecular weight of 25 × 10^6 g/mol and the degree of hydrolysis of 25%. This product is supplied by Beijing Hengju Chemical Co. Ltd. (China). The other polymer is named as AVS, a ter-polymer of acrylamide (AM), 2-Acrylamido-2-methylpropane sulfonic acid (AMPS) and one synthesized functional monomer. This product was donated to this research by the Research Institute of Petroleum Exploration & Development (RIPED, China). The molecular structures of HPAM and AVS are given in Figure 3.1. The analysis results of the Fourier transform infrared spectroscopy (FTIR) of the AVS polymer is also shown in Fig. 3.2. Besides, three effective chemicals are chosen as the additives namely triethanolamine, coconut diethanolamide (CDEA) and N70K-T. The first two products are purchased from Sigma-Aldrich and the last one is provided by Solvay Chemicals without a charge.

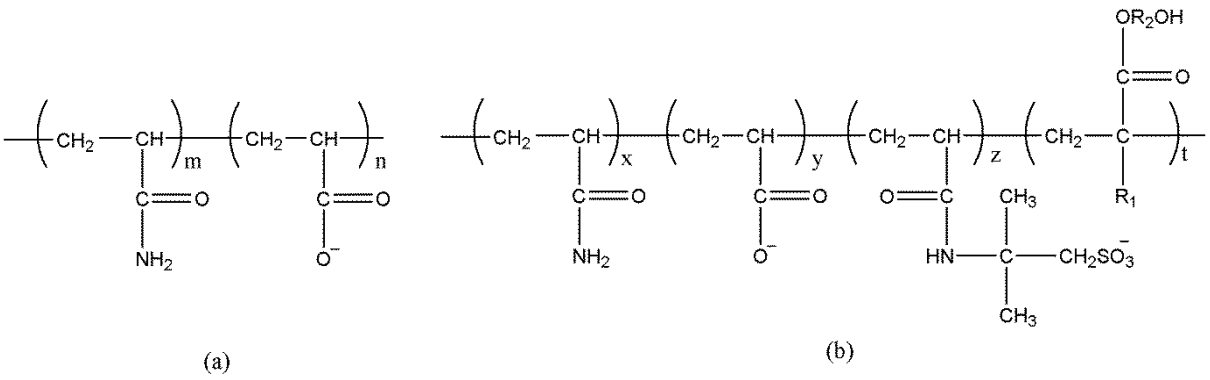

Fig 3.1 Schematic of of the molecular structures of HPAM (a) and AVS (b)

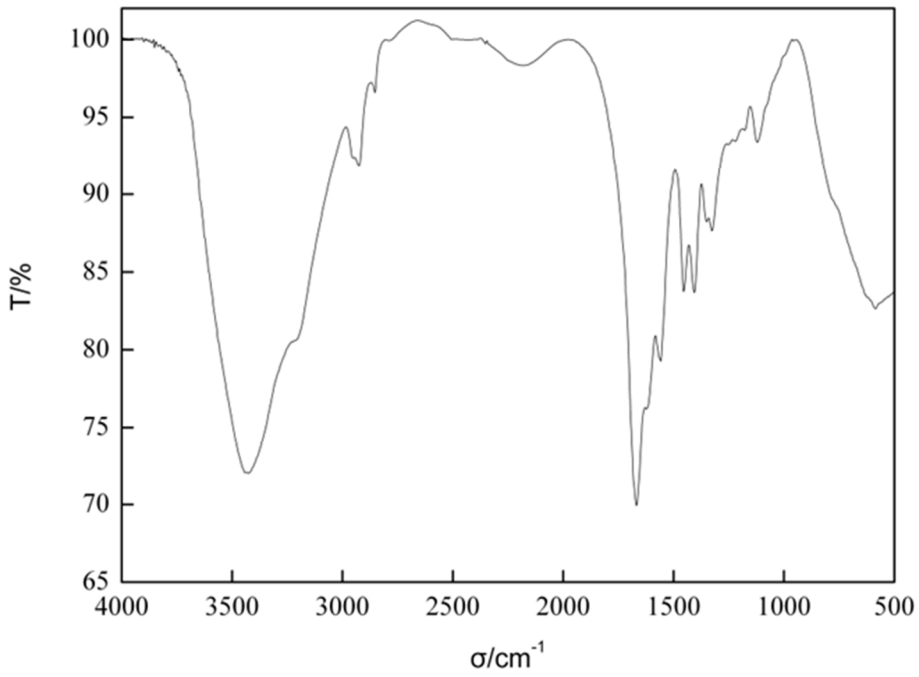

Fig. 3.2 Results of the FTIR analysis of the AVS molecule (σ and T are wave members and transmittance respectively)

3.2.3 Crude Oil

In order to mimic the multiphase flow properties of a real oil field and obtain representative and convincing outcomes, actual crude oil rather than a hydraulic oil or synthetic oil is used. The oil sample is provided from an offshore oil reservoir in Western Australia and is filtered before any use to remove any small solid particles from the oil. The main properties of the oil sample are presented in Table 3.2.

Table 3.2 Properties of the oil sample

Test	Unit	Result
Density @ 15°C	Kg/L	0.9428
API gravity	°API	18.5
Asphaltenes	%mass	0.14
Kinematic Viscosity @40°C	cSt	37.26
Sulphur-Total	%mass	0.14
Total Acid Number	mg KOH/g	0.50

3.2.4 Rock Sample

Berea samples with lengths around 6.9 cm and diameters of 3.8 cm are cut from quarried sandstone blocks (Ohio, USA). The samples are all fairly homogeneous with very similar expected petrophysical properties. The porosity and permeability of the core plugs are measured using an Automated Porosi-Permeameter (Coretest Systems, Inc., U.S.A.) and will be presented in the next chapter. Their chemical compositions are determined by the X-ray diffraction (XRD) technique conducted on an offcut of one of the plugs. This data is shown in Table 3.3 and Fig. 3.3. Scanning electron microscope (SEM) image of the sample powder is given in Fig. 3.4.

Table 3.3 XRD analysis results revealing the mineral composition of the core plugs

Mineral	Quartz	Albite	Kaolin	Muscovite	Feldspar	Anothite	Illite	Dolomite	Ankerite
Weight%	74.9	0.8	0.8	0.6	8.9	3.0	1.0	5.1	4.9

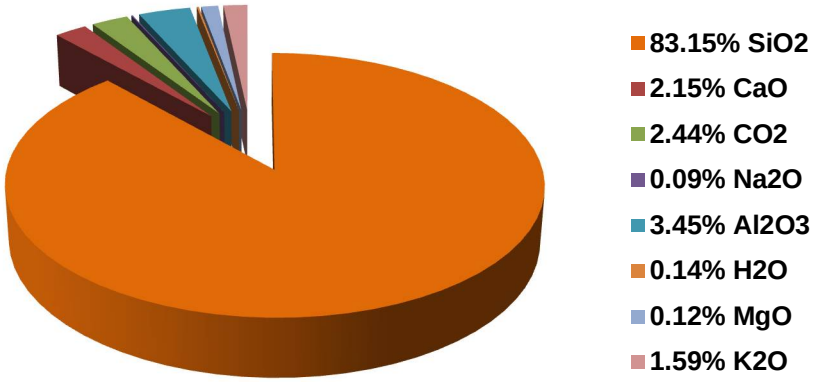

Fig 3.3 XRD analysis of oxides composition of the core plug

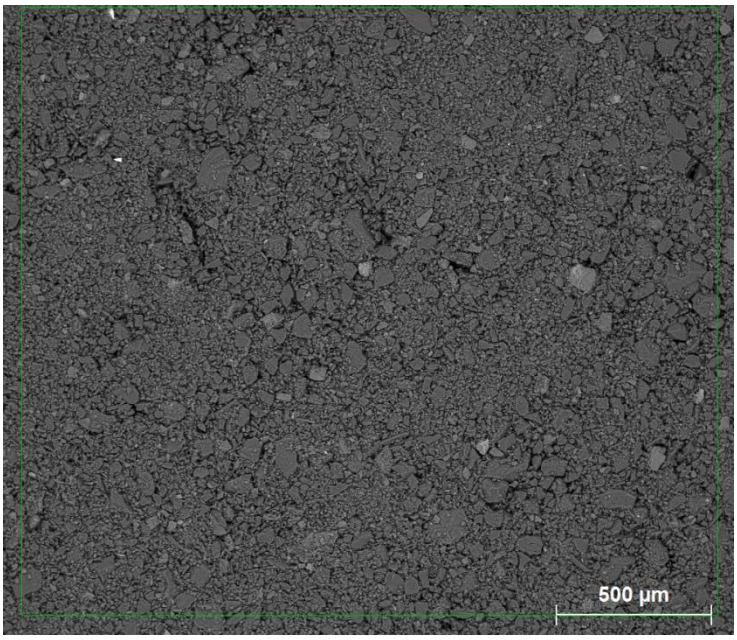

Fig. 3.4 SEM image of the rock powder used for the XRD analysis

3.2.5 Other Materials

Calcium chloride ($CaCl_2$) and sodium chloride (NaCl) supplied by Sigma-Aldrich are used to prepare the foaming solution and synthetic formation brine that are applied during the core flooding process. CO_2 gas with a purity of 99.99% is obtained from BOC (Australia) and applied in the static and dynamic evaluation of foam performance. Distilled water is used in this research for the preparation of all aqueous solutions.

3.3 Experimental Setup and Methodology

3.3.1 Foaming Ability and Foam Stability Evaluation

Both Ross-Miles pour test method (Rosen and Solash, 1969) and Waring blender method (Duan et al. 2004) are widely recognized and applied in academia and industry to initially screen of suitable candidates for foam flooding. As a result of its simplicity and reliability, Waring blender method is selected in this work to investigate the foamability and foam stability of the foaming solution in determining whether a reliable and robust foam can be generated. These two parameters thereby can predict the EOR capacity of the foam during the subsequent CO_2 foam flooding process. The experimental setup used for the evaluation is illustrated in Fig. 3.5.

Synthetic formation water containing 20,000 ppm NaCl and 100 ppm $CaCl_2$ is employed to prepare foaming solution in the assessment of foaming ability and foam stability. A given amount of (100 mL) foaming solution (containing the surfactant alone or a surfactant/polymer or surfactant/polymer/additive mixture) with varying concentrations is added into a blender and agitated with the rotation speed of 2000 rpm for 60 seconds with continuous low pressure CO_2 gas directed into the blender using a nylon 1/4" tubing, as depicted in Fig. 3.5. For the health and safety related reasons, this whole process is carried out under a fume cupboard. The produced foam is then quickly transferred to a graduated cylinder which is standing in a water bath whose temperature is controlled by a digital thermal couple. The initial volume (V_0) of the generated foam is measured as the foamability indicator and the time period ($t_{1/2}$) for half of the liquid to dropout (i.e. the liquid drainage volume reached 50 mL) is recorded as the foam stability indicator under various test conditions. To test the reliability and reproducibility of this method, all the tests are conducted at 50°C. To ensure a relatively safe conclusion and also examine the reproducibility of the results, all the tests are repeated three times under the same experimental conditions. If the results of the three trials are similar, an average value is taken as the final result to be reported.

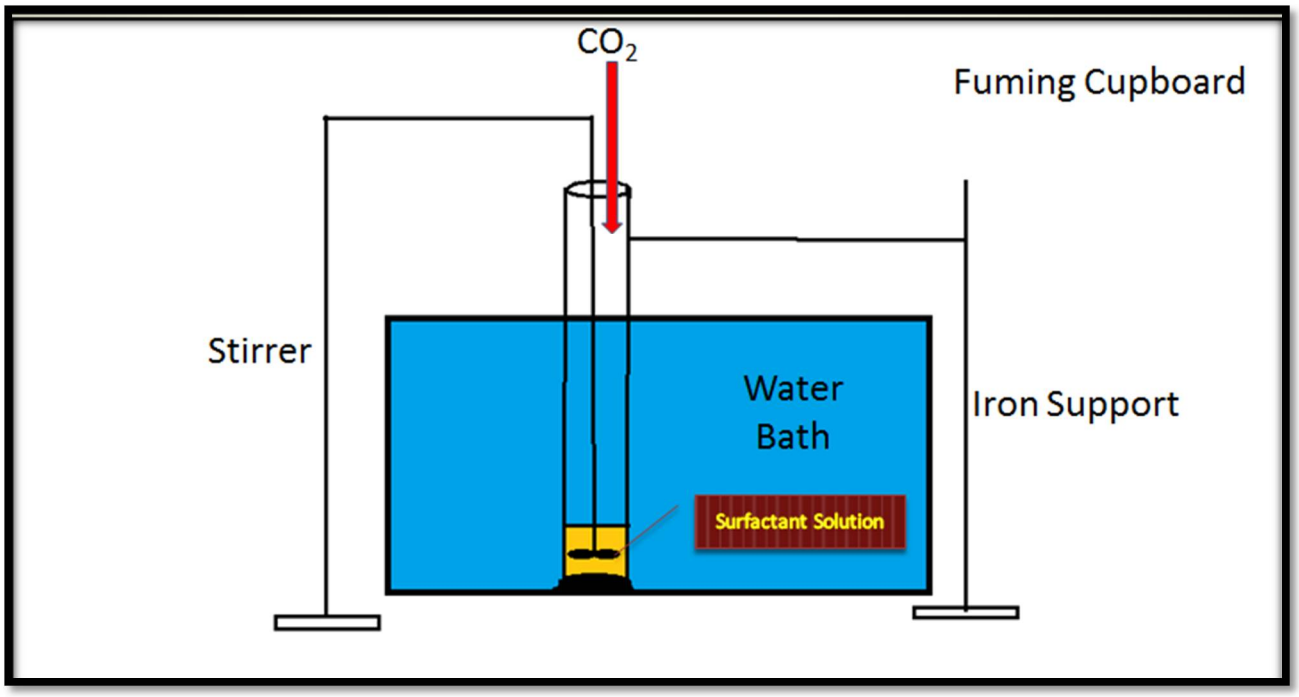

Fig. 3.5 Illustration of the experimental setup for static foam behavior evaluation

3.3.2 Foam Apparent Viscosity

Foam effectiveness is a strong function of the foam apparent viscosity which can be seen as the pressure gradient normalized with respect to the permeability and the total flux of surfactant solution and gas (Ma et al. 2013), although another form of the foam apparent viscosity has been proposed elsewhere (Holm, 1970). If foaming solution and CO_2 are injected through a core plug, on the basis of the single-phase Darcy Law, the apparent foam viscosity can be expressed as:

$$\mu_{foam,app} = \frac{\mathrm{kA\Delta p}}{(q_g + q_l)L} \tag{3.1}$$

Where k is the effective permeability of the core plug, A is the cross sectional area available to the foam flow, q_g and q_l are the volumetric flow rate of CO_2 gas and foaming solution, respectively, and $\Delta p/L$ is the pressure gradient across the full length of the core plug.

The experimental setup used to conduct the apparent viscosity measurements is illustrated in Fig. 3.6. As shown, the setup consists of two displacement pumps (HPLC pump), a high-pressure syringe pump, a foam generator whose internal configuration is further illustrated in Fig. 3.7, two fluid accumulators, a core holder, a pair of pressure transmitters, data

acquisition system, back pressure regulator, plug valves and stainless flow lines, etc. The whole setup is heated up using a digital temperature controller (regulation accuracy±0.5℃) providing power to heating tapes wrapped around all the components of the setup. The HPLC pumps (LC-20AD, Shimadzu Co.) feed various fluids into the core holder via the two accumulators and are set to operate at constant flow rate mode. The foam generator (Haian Oil Scientific Research Apparatus Co., Ltd., China) is made from hastelloy and can resist extreme chemical corrosion. The dense CO_2 and foaming solution are mixed sufficiently by the porous medium integrated into the foam generator and the produced foam is discharged from its outlet. Further details about the internal configuration of the core holder (Corelab Inc., U.S.A.) that is capable of working at 68.95 MPa and 150 °C is illustrated in Fig. 3.8. The core holder is placed horizontally while allowing fluids to flow in and out under elevated temperature and pressure. The differential pressure is continuously monitored and recorded during an experiment by a pair of high accuracy (0.01 % FS) pressure transmitters (KELLER, Switzerland) which are mounted at the inflow and outflow ends of the core holder. The temperature and pressure history during core flooding process can be recorded and stored by the data acquisition system (Control Center Series 30). A sample snapshot of its interface is shown in Fig 3.9.

The experimental procedure employed in conducting the foam apparent viscosity measurements is as follows. After vacuuming the apparatus for prolonged period of time, the foaming solution (5.0 PV) is fed into the core plug to satisfy the surfactant adsorption before the injection of the CO_2 foam with a specific gas/liquid ratio. The differential pressure during an experiment is monitored and recorded continuously using the pressure transducers mounted at the inflow and outflow ends of the core holder. The experiment is not terminated until steady state flow is achieved which is indicated by negligible fluctuation (less than 5 psi) of pressure drop across the core sample. Then the apparent foam viscosity is computed according to Darcy's Law. Upon completion of the first experiment, further experiments are conducted using varying gas/liquid ratios but following the exact same procedure as the first experiment. Throughout the entire process, the temperature of the flow-lines and all the components containing the test fluids was controlled by heating tapes wrapped around them and pressure controlled using a back pressure regulator (BPR). The temperature and pore pressure applied during the experiments were 50°C and 10.34MPa, respectively.

It is worth noting that in order to protect the conventional Viton sleeve used to confine the core plugs against the highly diffusive CO_2, the Viton sleeve was lined on the inside with

other more CO_2 resistant sleeve material as depicted in Fig. 3.8. Further information about this combination sleeve can be found elsewhere (Saeedi et al, 2011).

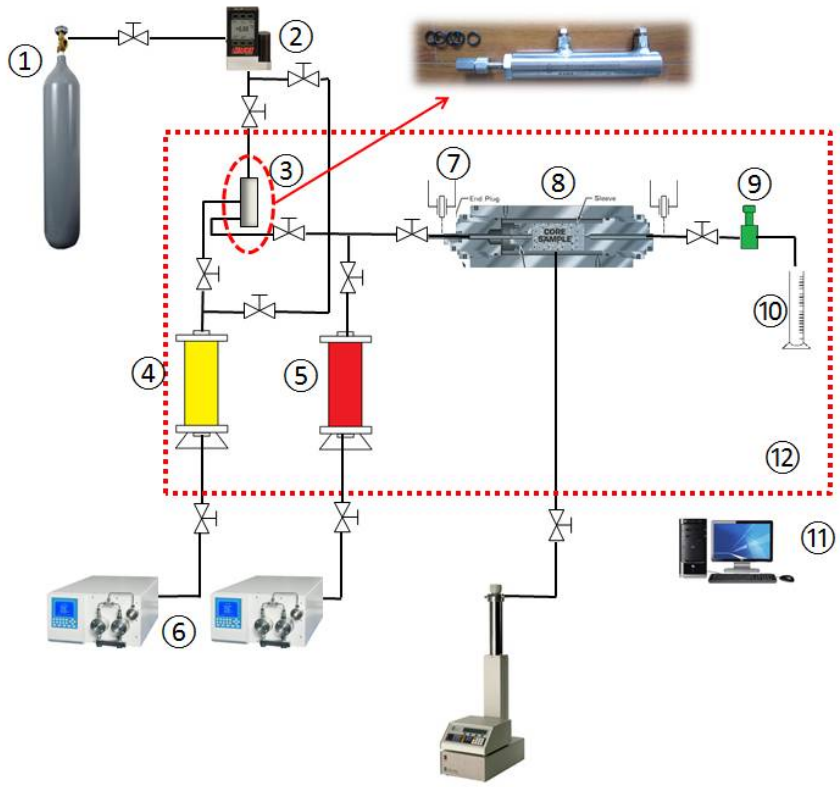

Fig. 3.6 Illustration of the setup of the core flooding apparatus.

(1- CO_2 tank 2- Gas mass flow control system 3- Foam generator 4- Foaming solution 5- Formation water 6- Injection pump 7- Pressure transducer 8- Core holder 9- Back pressure regulator 10- Graduated cylinder 11- Data acquisition system 12- Heating system)

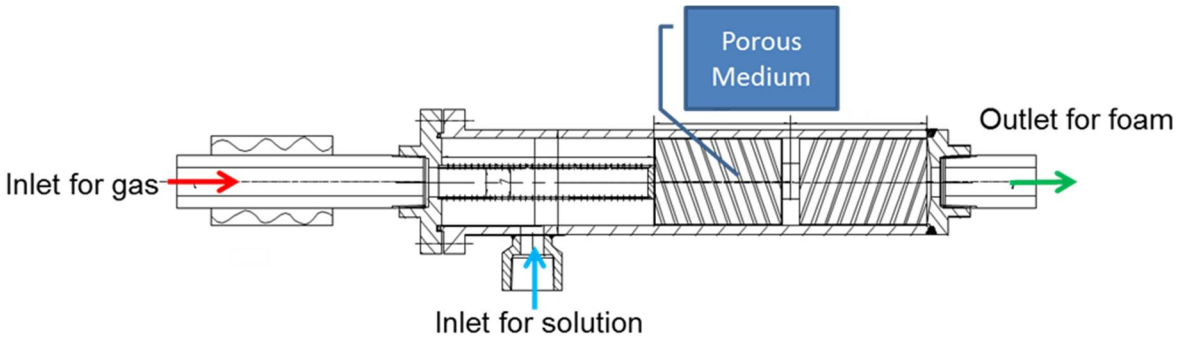

Fig 3.7 Illustration of the internal configuration of the foam generator.

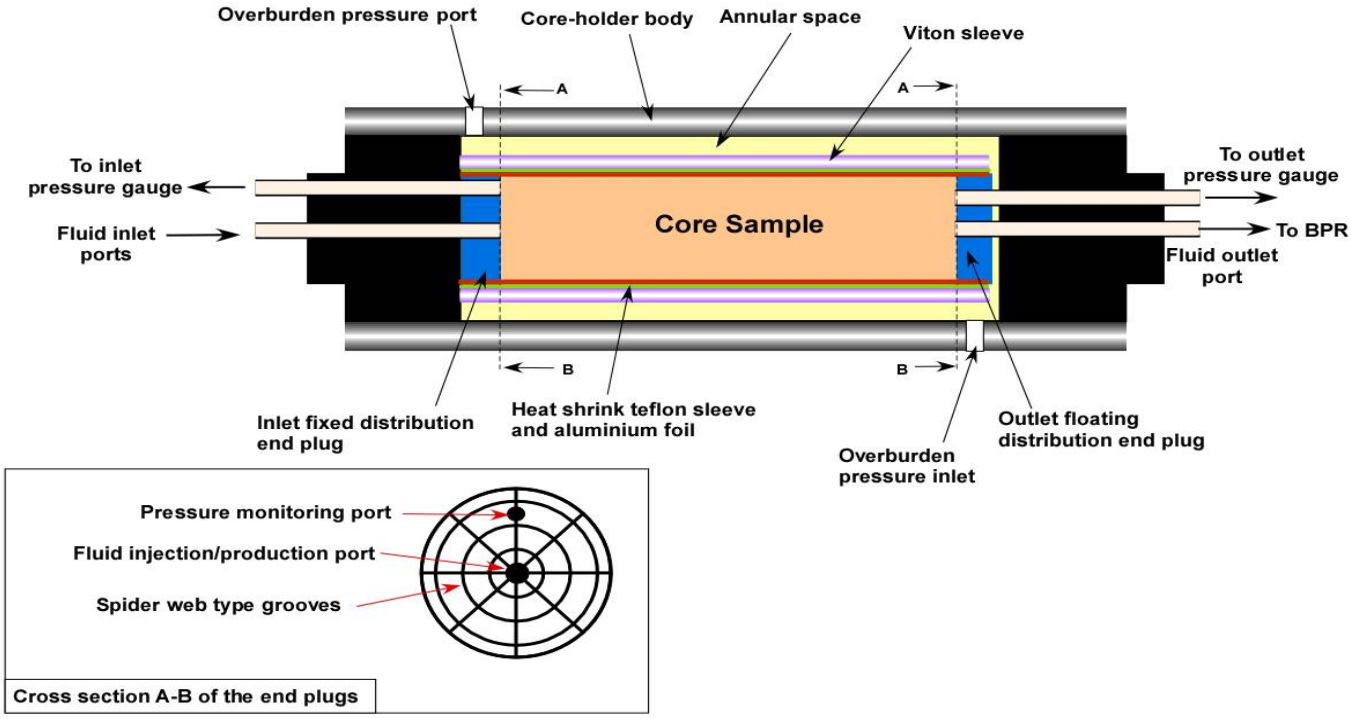

Fig 3.8 Schematic of the core holder used for the core-flood experiments.

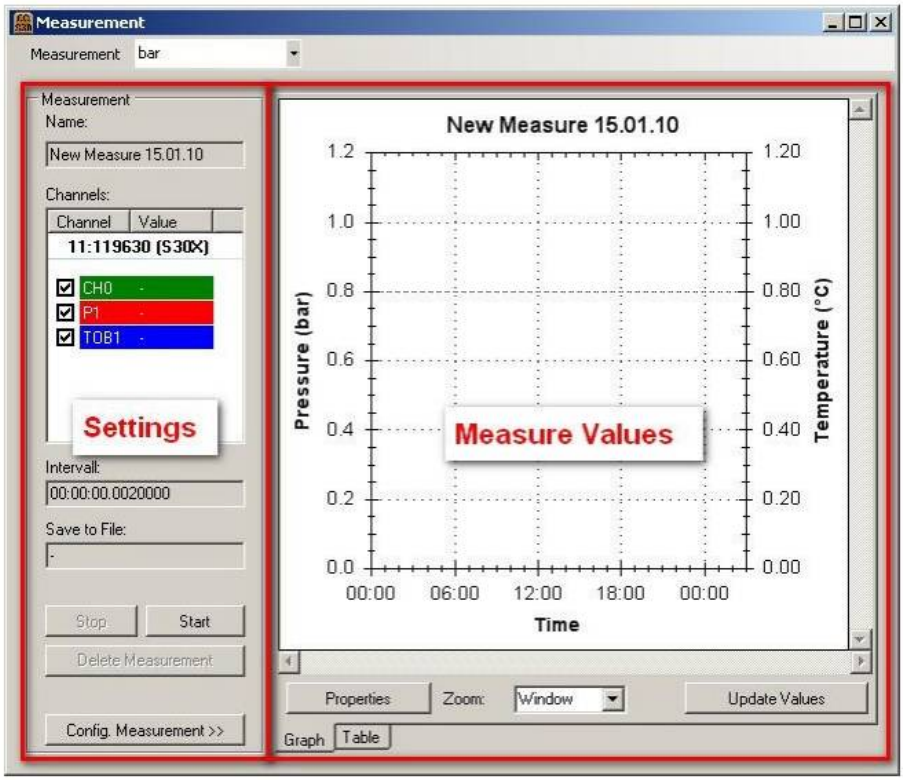

Fig 3.9 A snapshot of the interface of the CCS30 software used for data acquisition

3.3.3 Resistance Factor (RF) and Residual Resistance Factor (RRF)

Resistance factor (RF) indicates the ability of a foam to modify the mobility ratio and is defined as follow (Schneider and Owens, 1982):

$$RF = \frac{\lambda_w}{\lambda_p} = \frac{K_w}{\mu_w} / \frac{K_p}{\mu_p} \tag{3.2}$$

Where λ_w, K_w and μ_w are the mobility, effective permeability and viscosity of synthetic formation water/brine, respectively; λ_p, K_p and μ_p are the mobility, effective permeability and viscosity of the generated CO_2 foam, respectively.

If both formation water/brine and foam flow in the same core sample at the same flow rate, based on the Darcy's Law (Equation 3.1), the definition of RF can be simplified as:

$$RF = \frac{\lambda_w}{\lambda_p} = \frac{\Delta p_2}{\Delta p_1} \tag{3.3}$$

Where $\Delta p_1 and\ \Delta p_2$ are the pressure drops of the brine phase and foam phase, respectively.

Residual resistance factor (RRF), which is the ratio of the brine effective permeability before and after the foam flooding, shows the ability of the foam to reduce effective permeability to brine in a porous medium. Therefore, if the flowrate of the brine for both pre- and post-foam flooding remains the same, RRF can be calculated using the following equation (Schneider and Owens, 1982):

$$RRF = \frac{K_w}{K_f} = \frac{\Delta P_3}{\Delta P_1} \quad (3.4)$$

Where K_w is the effective permeability to the brine before foam flooding and K_f is the effective permeability to the brine after foam flooding; $\Delta P_1 and\ \Delta P_3$ are the pressure drops of the brine flow before and after foam flooding, respectively.

The experimental setup used for RF and RRF evaluations is the same as that illustrated in Fig. 3.6. Prior to the measurements, the apparatus is put under vacuum for long enough time before sufficient amount of the foaming solution (5.0 PV) is fed into the core plug to meet the demand of surfactant adsorption. Then, the synthetic formation water (NaCl 20,000 ppm and $CaCl_2$ 100 ppm) is then injected at 1.0 mL/min until steady ΔP_1 was reached. Next, both CO_2 and foaming solution are injected into the sample with flow rate of 0.75mL/min and 0.25 mL/min, respectively (foam quality is fixed at 75%). The injection is shifted to single brine again flowing at 1.0 mL/min after steady Δp_2 is obtained, and then brine flow continued until ΔP_3 could be measured. All the experiments are conducted at 50°C and 10.34 MPa. It is noted that CO_2 foam could be created through different injection modes: with the assistance of the foam generator (direct injection of foam) or without the foam generator (simultaneous injection of gas and solution and solution-alternating-gas injection).

3.3.4 Mobility Reduction Factor (MRF) Assessment

As discussed in details in Chapter 2, most CO_2 floods encounter the issue of early breakthrough which is very often due to the relatively high CO_2 mobility compared to that of reservoir fluids. Numerous investigations have demonstrated that the application of foam could be an effective technique to modify the flow mechanisms at the pore level by decreasing the CO_2 mobility. The mobility reduction factor (MRF) is an indication widely used for the assessment of the magnitude of such mobility modification. The MRF is usually defined as the mobility of CO_2/synthetic formation water divided by that of CO_2 / foaming solution, though there are other forms of MRF as outlined in the literature (Svorstol et al.

1996; Simjoo et al. 2013). According to the Darcy's Law, the mobility of a fluid (gas, brine or the foaming agent) in a porous medium can be expressed as:

$$\lambda = \frac{k}{\mu} = \frac{QL}{A\Delta P} \tag{3.5}$$

Where k is the permeability of the porous medium, μ is the apparent viscosity of the fluid, Q is the total flow rate of the fluid, A is the cross-sectional area available to flow, Δp is the total pressure drop across the core plug and L is the length of the core plug over which the pressure drop takes place.

Thereby, if the total flow rate of CO_2/brine and CO_2/foaming agent are identical, since other variables included in Equation 3.5 remain the same (the same core sample is used for both floods), MRF can be determined by the following equation:

$$MRF = \frac{\Delta P_{gas-foaming\ agent}}{\Delta P_{gas-brine}} \tag{3.6}$$

Once again, the MRF assessment experiments are performed using the setup shown in Fig 3.6. The gas and liquid (i.e. brine or foaming solution) are injected simultaneously with a fixed gas/liquid ratio (3:1) regardless of whether the foaming agent is applied or not. Either gas or liquid flow rate would be varying to investigate the dependence of MRF on the gas or liquid flow rate. Differential pressures are monitored and recorded to verify the attainment of steady-state conditions in both scenarios (with and without the foaming agent). Accordingly, MRF with differing gas or liquid flow rates can be calculated using Equation 3.6. Once again, all the MRF assessment experiments are carried out at 50°C and 10.34MPa throughout the whole process.

3.3.5 Viscosity Measurement

A base polymer solution with a concentration of 5000 ppm is prepared by adding a given polymer into synthetic brine (20000 ppm NaCl) and mixing them with an overhead stirrer (VELP Scientifica, Australia) at a speed of 400 rpm for 2 hours to ensure that a homogenous polymer solution is obtained. Afterward the base solution is diluted to solutions with other desired concentrations. It is worth noting that the diluted polymer solution is always aged for 24 hours in order to completely dissolve the polymer particle before any viscosity measurements that are all conducted using a Brookfield DV-II + Pro viscometer (Brookfield

Engineering Laboratories, Inc., USA). The shear rate is fixed at 7.34 S^{-1} for all the viscosity measurement experiments.

3.3.6 Surface Tension Measurement

Surface tension measurements are performed using a JZHY-180 Tensiometer (Jinan Presision Testing Equipment Co. Ltd., China), as illustrated in Fig. 3.10. It works based on the Du Nouy Ring method. Prior to any tests, the tensiometer is carefully calibrated by adjusting the screw nuts mounted on the lever arm to maximize the measurement accuracy. Then 20 mL of the solution under investigation is poured into a glass cup sitting on a metal stand whose height would be set to enable the platinum ring with a radius of 9.55 mm to slightly touch solution, followed by increasing the torque applied on the platinum ring until the liquid membrane between the ring and gas/liquid surface collapses. At this moment, the corresponding surface tension is displayed on the large dial attached to the equipment. Each sample solution is tested five times and the average value is taken. All measurements are carried out at the room temperature.

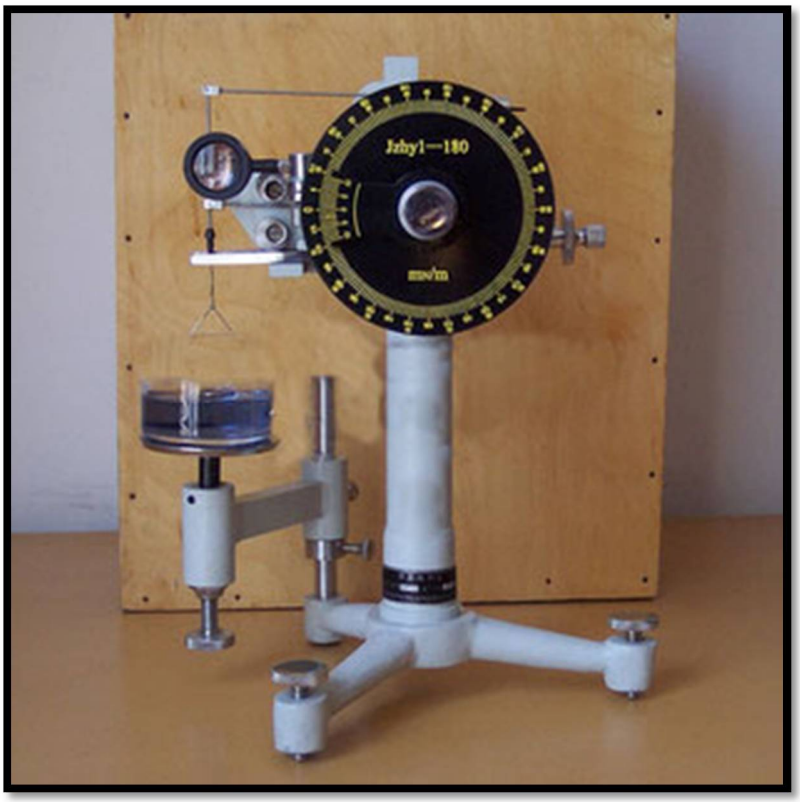

Fig. 3.10 Illustration of the JZHY-180 Tensiometer

3.3.7 Core Flooding Experiment

A number of core flooding experiments have been carried out in this research to evaluate the EOR capacity of various foaming formulations at varying injection schemes. The experimental procedure for a typical experiment is as follows:

1. The initial core plug is dried out at 65°C for four days and its porosity and gas permeability are determined using AP-608 Automated Permeameter-Porodimeter (Coretest Systems, Inc., U.S.A.) before it is loaded horizontally into the core holder. Then a confining pressure of 27.58 MPa is applied to the core plug before putting the system under vacuum for at least 12 hours.

2. The core plug is fully saturated with the synthetic brine (20,000 Nacl and 100 ppm $CaCl_2$) until steady-state flow is achived. Then its liquid permeablity can be obtained by applying single-phase Darcy's Law.

3. Crude oil is pumped into the core holder at 0.3 ml/min until the water cut reaches 1% to attain the residual water saturation; afterwards, the core plug is aged for 24 hours.

4. Water floods with synthetic brine (20,000 Nacl and 100 ppm $CaCl_2$) at 0.5 ml/min is conducted to allow the residual oil saturation to be established, which is indicated by the 99% water cut.

5. Given amounts of supercritical CO_2 and chemicals are injected into the core plug under varying experimental condition (injection scheme, injection rate, gas/liquid ratio and so forth), which is followed by the chase waterfloods at 0.5 ml/min until 99% water cut is reached.

The system temperature is kept at 50°C throughout the experiments.

References

Duan M, Hu X, Ren D, Guo H, (2004) Studies on foam stability by the actions of hydrophobically modified polyacrylamides. Colloid Polym. Sci. 282: 1292-1296.

Holm LM, (1970) Foam injection test in the Siggins Field, Illinois. J. Petrol. Technol. 22(12): 1499-1506.

Ma K.; Lopez-Salinas JL, Puerto MC, Miller CA, Biswal SL, Hirasaki GJ, (2013) Estimation of parameters for the simulation of foam flow through porous media. Part 1: The Dry-Out Effect. Energy Fuels, 27: 2363-2375.

Rosen M J, Solash J, (1969) Factors affecting initial foam height in the ross-miles foam test. J. Am. Chem. Soc. 46(8): 399-402.

Saeedi, A., Rezaee, R., Evans, B. and Clennell, B., 2011. Multiphase flow behaviour during CO2 geo-sequestration: Emphasis on the effect of cyclic CO_2-brine flooding. J Pet. Sci. Eng. 79(3-4): 65-85.

Schneider FN, Owens WW, (1982). Steady-state measurements of relatively permeability for polymer/oil system. Socie. Petrol. Eng. J 22(01): 79-86

Simjoo M, Dong Y, Andrianov A, Talanana M, Zitha PLJ, (2013) Novel sight into the foam mobility control. SPE J 18(03): 416-427.

Svorstol I, Vassenden F, Mannhardt K, (1996) Laboratory studies for design of a foam pilot in the Snorre Field. SPE/DOE Improved Oil Recovery Symposium, Tulsa, Oklahoma, US

Chapter 4 Experimental Results and Discussion

4.1 Introduction

In an attempt to realize the objectives of this research, a variety of investigations are conducted. The previous chapter presented in details the experimental approaches followed in completing the planned investigations. This chapter in turn provides the results of the experimental work conducted along with the detailed discussion and interpretation of those results. The contents of this chapter are organised around two main components: firstly, the discovery of a novel foaming formulation that brings together a surfactant with polymer and additives for the use of CO_2 foam flooding; secondly, the evaluation and optimization of a new EOR technique named chemicals-alternating-foam (CAF) flooding that utilises the above proposed new formulation.

4.2 Development of a Novel Foaming Formula

4.2.1 Selection of the Foaming Agent

The static foam behaviour is strongly related to the type and concentration of the foaming agent or the surfactant used, which can be verified by the results shown in Figs. 4.1-4.9. It is worth noting that the indicated concentrations are based on the active substance of these surfactant products. In general, the non-ionic surfactants (Triton X-100, APG and TMN-6) generate much less foam than their anionic (AOS, SDS, AES and ABS) and the amphoteric (CAB-35 and LAB-35) counterparts irrespective of their concentration, but the non-ionic products do relatively well in stabilizing the foam.

Among the non-ionic surfactants, the foamablity of Triton X-100 fluctuates with the maximum value being only 380 mL which hardly satisfies the foaming requirement. Its foam stability varied between 84s and 123s, peaking at the concentration of 0.4 wt%. The scenario of APG, a highly attractive “green surfactant” due to its remarkable biodegradability, is quite different: the foamability rises smoothly as surfactant concentration increases and the growth rate is nearly constant throughout the test; yet APG is not attractive for foaming purposes under the test condition if its relatively insufficient foam creation is taken into consideration as it provides a maximum of just above 400mL of foam at the relatively high concentration of 0.7 wt%. Interestingly, though sufficient amount of foam cannot be obtained, the foam generated by APG is remarkably robust and stable mostly owning to its extraordinary bulk

viscosity. The foam is capable of lasting up to 300s at the optimal surfactant concentration. The foam that is generated by TMN-6 possesses a comparable foaming ability to the APG foam, though its foamability is not positively correlated with its concentration similar to that of APG. The foam stability of TMN-6, however, is far lower than the APG foam. To summarise, APG can be considered as the best candidates among these non-ionic foaming agents in terms of the foam stability, but poor foamability is expected to hamper its possible application for CO_2 foam flooding.

With regards to the two amphoteric surfactants evaluated, the effect of the CAB-35 concentration on its foamability and foam stability is illustrated in Fig. 4.4. It is found that, compared to the non-ionic surfactants evaluated earlier; its foamability is significantly higher. The amount of the generated foam increases with the surfactant concentration until the concentration of 0.6 wt% is reached. Within the investigated range of surfactant concentrations, the maximum volume of the foam generated is approximately 625 mL which is considered to be superior. On the other side, there is an apparently positive correlation between the CAB- 35 foam longevity and its concentration, indicating that the foam is able to last longer at higher surfactant concentrations. LAB-35 is the other amphoteric surfactant evaluated in this study. Similar to CAB-35, the foamability of LAB-35 greatly surpasses that of its non-ionic counterparts and displays the optimal value at the concentration of 0.5 wt%. Despite the similarity in terms of foamability with CAB-35, the LAB-35 foam exhibits a noticeable difference with CAB-35 in terms of its stability. As can be observed, its longevity does not increase steadily with the surfactant concentration. Instead, the maximum stability is achieved when the concentration reaches 0.5 wt%, suggesting that both the foamability and stability attain their optimal values at this specific concentration. In comparison with CAB-35, the capability of LAB-35 in terms of the foam stability is slightly less, however.

As may be expected, anionic foaming agents exhibit an exceptional foaming ability. As seen in Fig. 4.6, the foamability of AOS increases rapidly at low concentration before reaching a plateau (around 620 mL) after which its foamability starts to decrease slightly. Its foam stability, although is not comparable with that of APG, seems to be the most distinguishing among the anionic surfactants evaluated. In contrast to AOS, foamability of SDS increases with its concentration during the course of the experiment and is slightly higher than that of AOS under the same concentrations. However, with regard to its foam stability, the scenario is completely opposite: AOS performs far better than SDS within the whole range of investigated concentrations and this tendency becomes more noticeable as the concentration

rises. In the case of AES and ABS, the tendencies of the foamability and foam durability variations are identical: increasing surfactant concentration leads to an improvement in both foamability and foam stability within the tested surfactant concentration ranges. However, the increase in foamability is marginal after 0.6 wt %. Moreover, the foaming capability of AES is generally better than ABS, while ABS is more attractive than ABS in terms of stabilizing the foam.

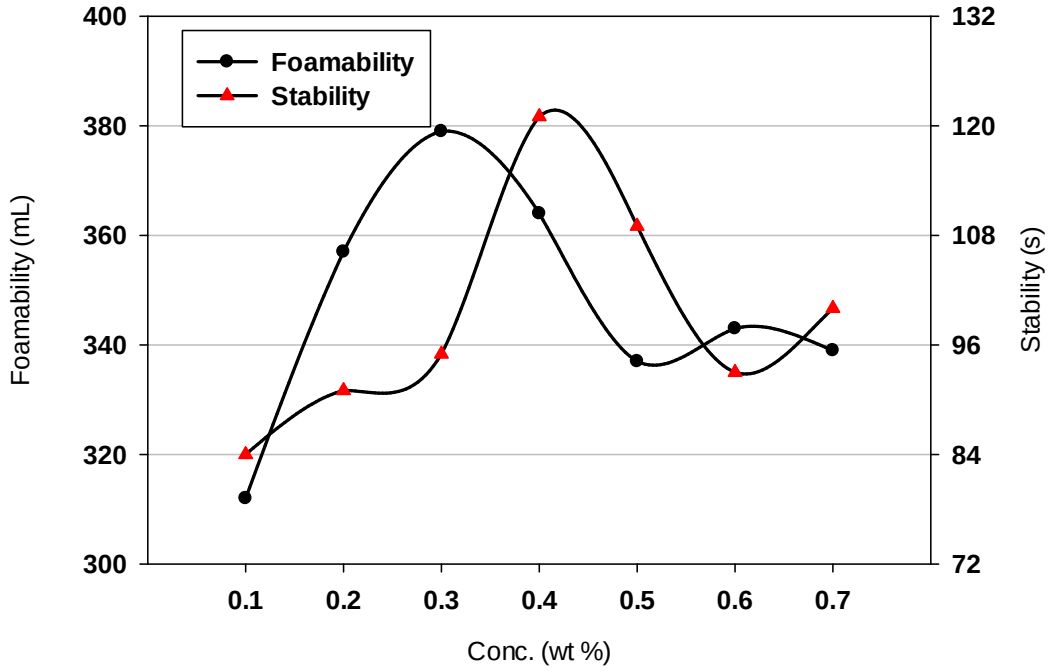

Fig. 4.1 Dependence of foamability and foam stability on Triton X-100 concentration

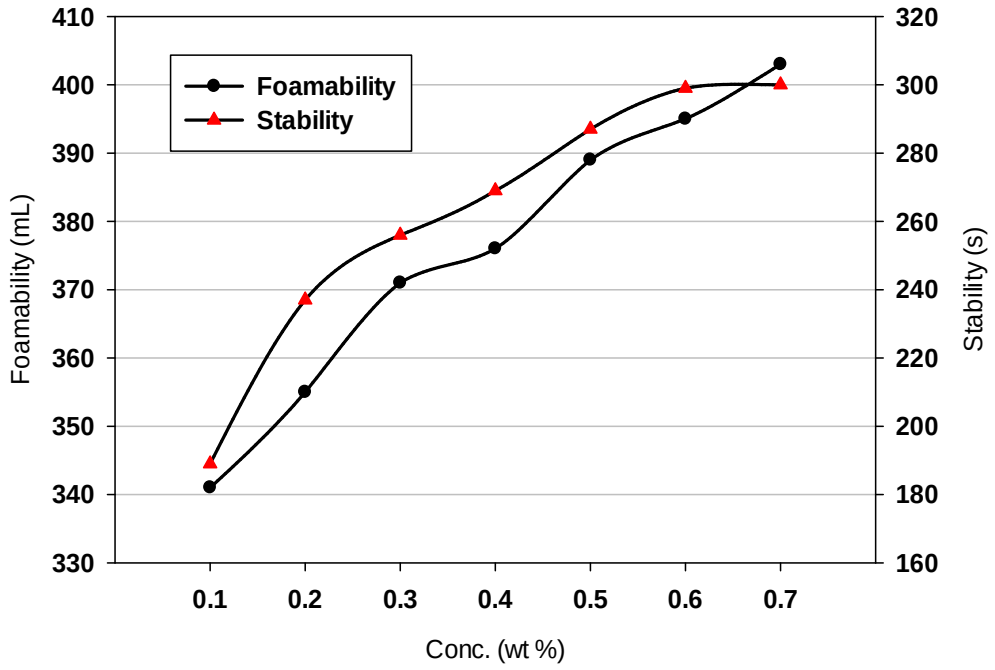

Fig. 4.2 Dependence of foamability and foam stability on APG concentration

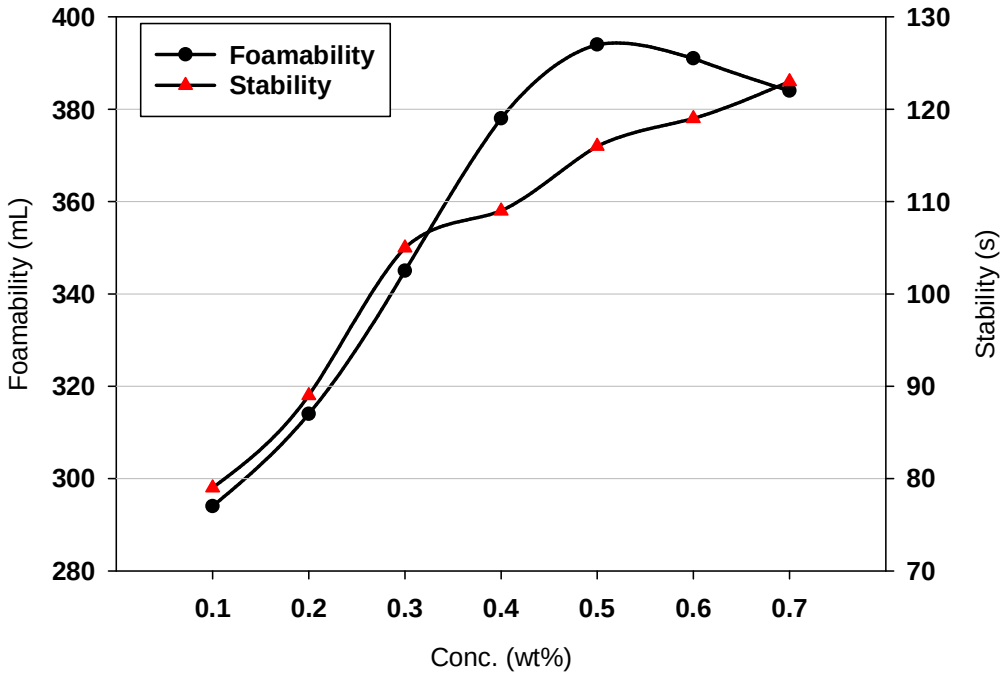

Fig. 4.3 Dependence of foamability and foam stability on TMN-6 concentration

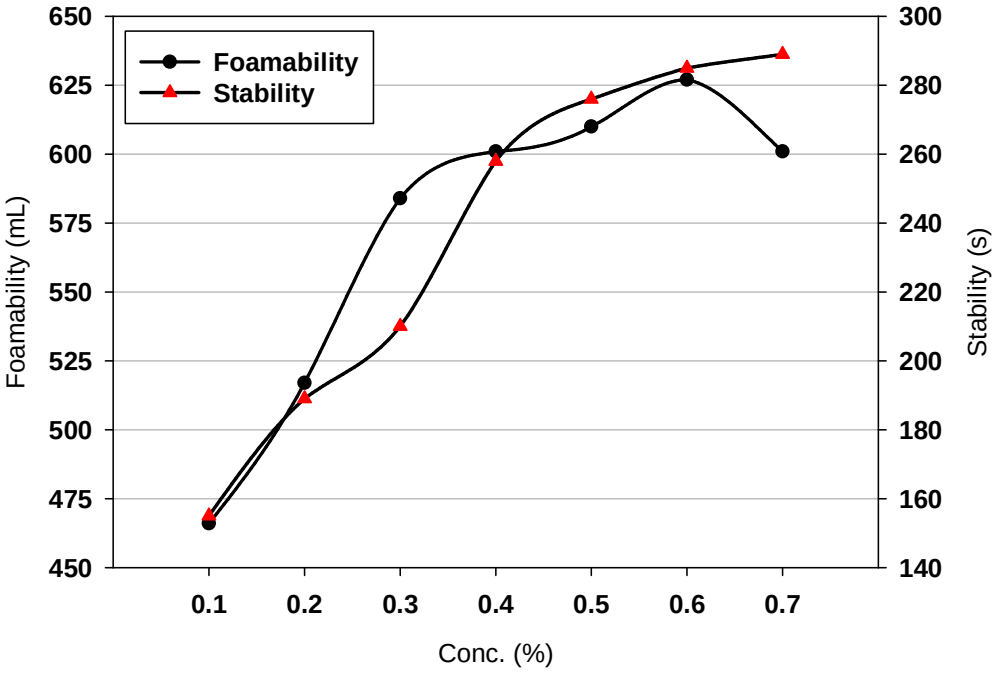

Fig. 4.4 Dependence of foamability and foam stability on CAB-35 concentration

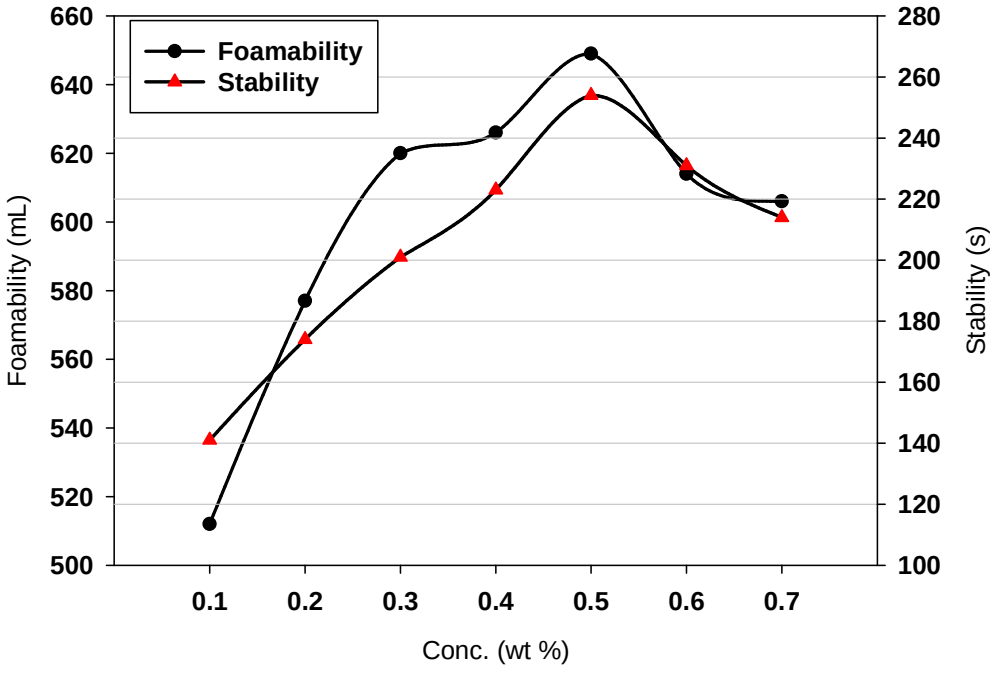

Fig. 4.5 Dependence of foamability and foam stability on LAB-35 concentration

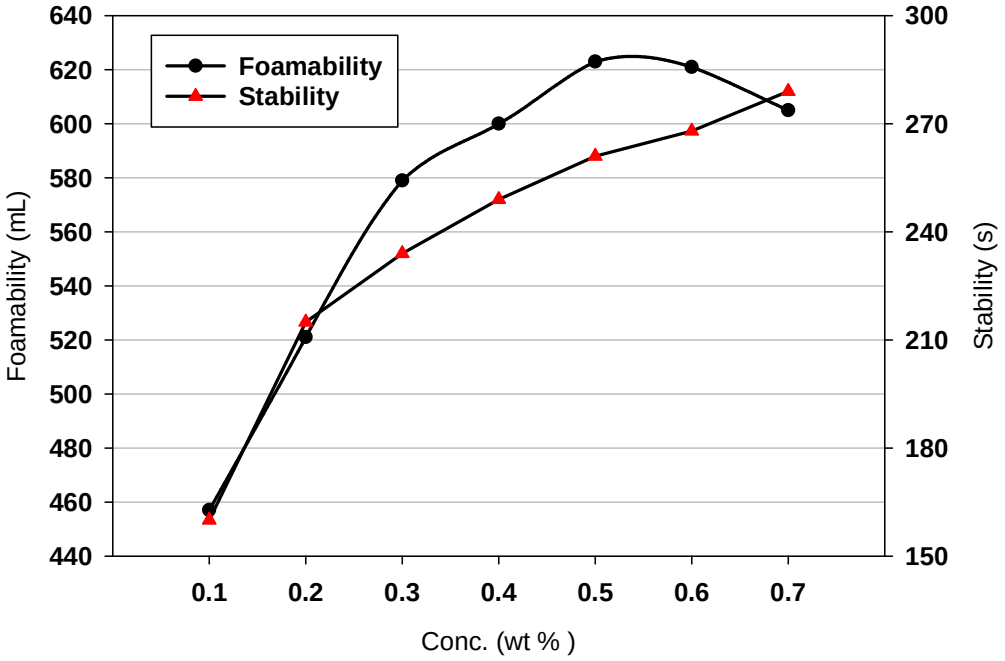

Fig. 4.6 Dependence of foamability and foam stability on AOS concentration

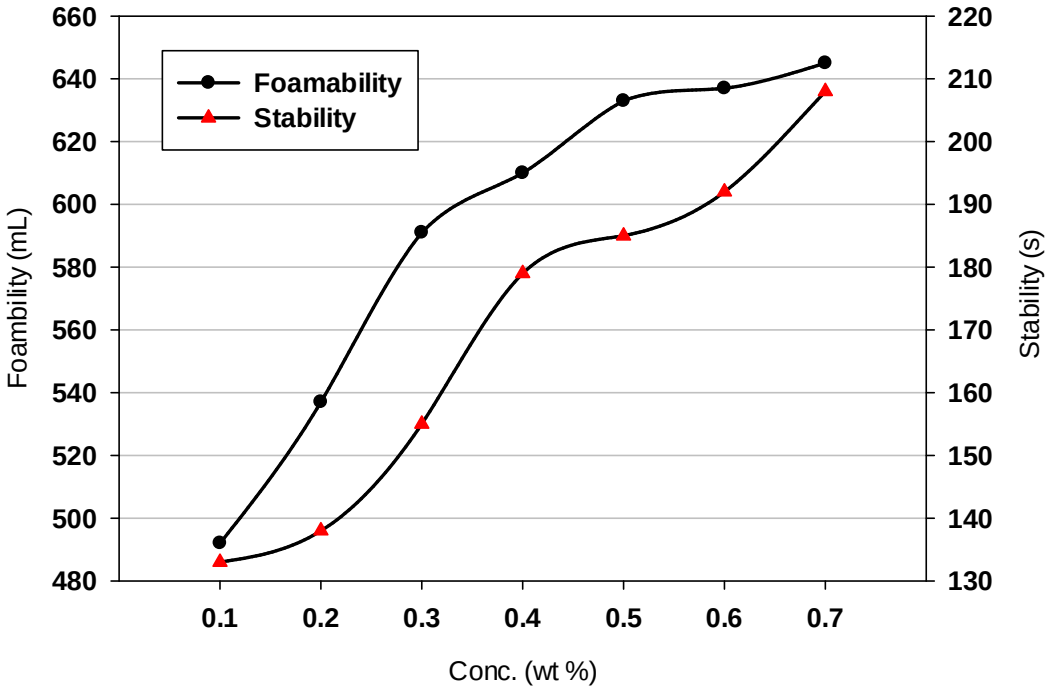

Fig. 4.7 Dependence of foamability and foam stability on SDS concentration

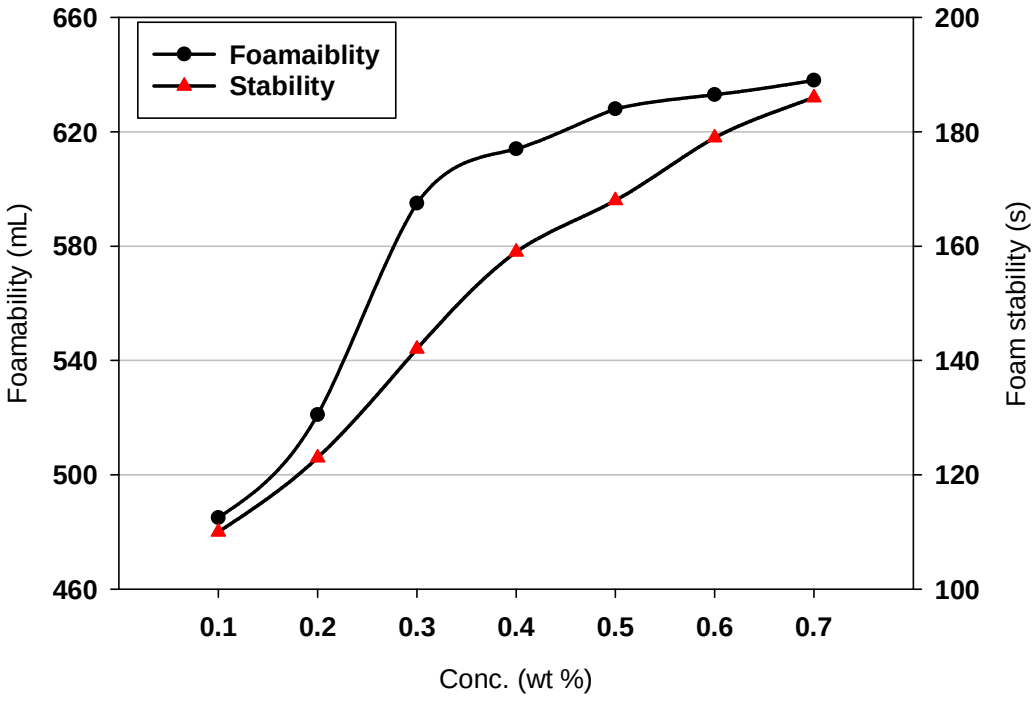

Fig. 4.8 Dependence of foamability and foam stability on AES concentration

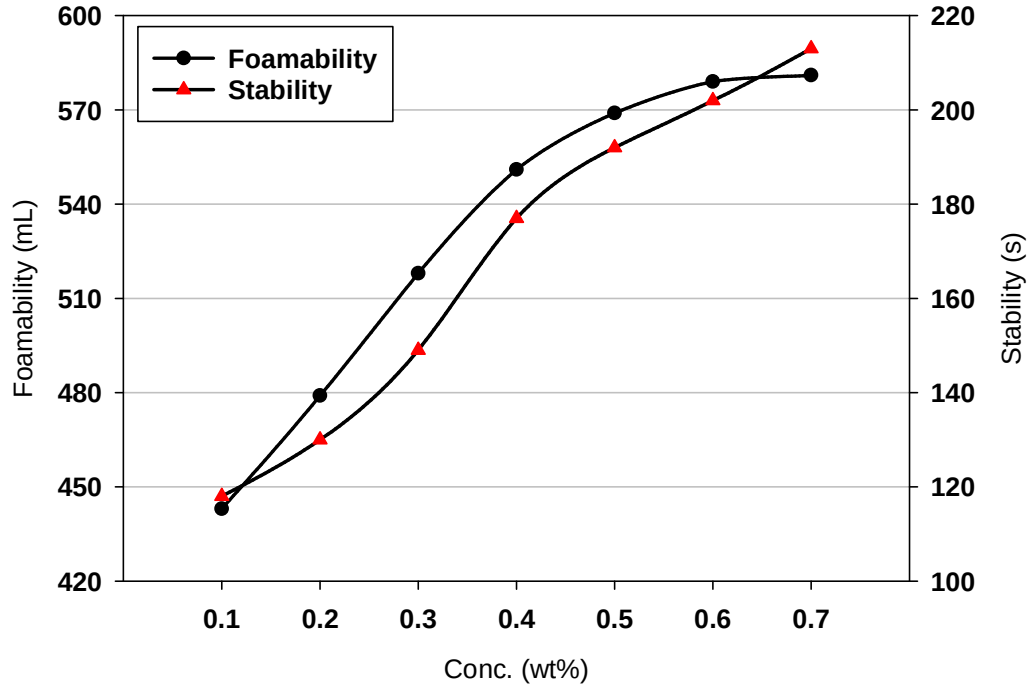

Fig. 4.9 Dependence of foamability and foam stability on ABS concentration

Foamability and foam stability are the two most critical parameters determining the EOR potential of the CO_2 foam flooding. Obviously, robust foam flooding requires both

foamability and stability to be fairly high; therefore, foaming factor or foaming indices is introduced as a comprehensive index to readily evaluate the overall foam behaviour (Zhao et al. 2014):

$$F = 0.75 \times F_V \times F_T \quad (4.1)$$

Where F is the foaming index, and F_V and F_T are the foamability and foam stability, respectively.

The influence of the surfactant type and concentration on the foaming index is illustrated in Fig. 4.10. Clearly, the non-ionic surfactants Triton X-100 and TMN-6 possess the lowest foaming index among these investigated products, suggesting both of them are relatively poor candidates for CO_2 foam flooding. Three anionic surfactants, AES, ABS and AOS, exhibit extremely encouraging foaming indices that range from 40 to 90 with the increasing surfactant concentration. Furthermore, AOS has the highest foaming index among them overall. It is noted that although APG is a non-ionic product, its foaming index is as good as some of the anionic surfactants if not better. This is primarily attributed to its considerable capability to stabilize its foam. AOS, LAB-35 and CAB-35 display the best foaming index among all of the nine surfactants tested. Balanced foamability and foam stability results in their excellent comprehensive foaming behaviours. Nevertheless, LAB-35 and CAB-35 are amphoteric surfactants and relatively costly. They are thereby not applicable for large-scale application in a real field operation. In summary, AOS and SDS are selected as the most attractive foaming agents in terms of their foaming performance and cost effectiveness.

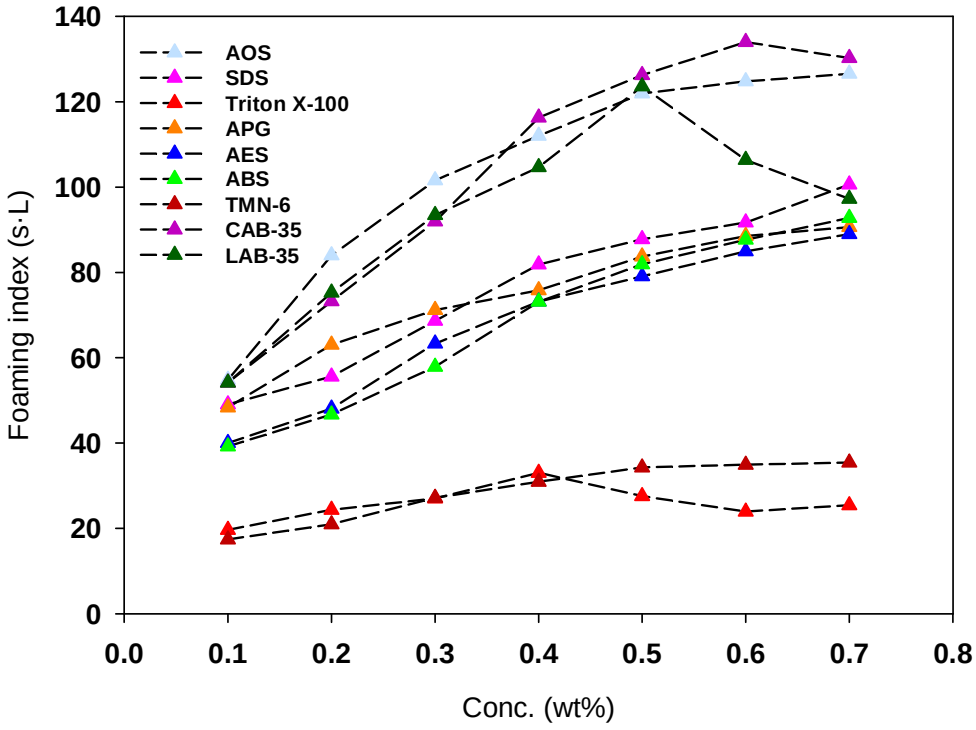

Fig 4.10 Effect of surfactant concentration on foaming index

As mentioned earlier, AOS and SDS exhibited comparable foaming abilities. The variation in their foaming index therefore is due to their foam stability difference. This disparity can mostly be explained by the noticeable difference in the bubble size distribution between these two candidates. Figs. 4.11-4.14 are captured using a digital camera (lenka, Germany) and can visually demonstrate the bubble size distribution of foams generated using AOS and SDS (0.5 wt.%) over a 600s time interval. The corresponding bubble size distributions are measured and calculated using the image analysis software (Nano Measurer 1.2, Fudan University) and the results are quantitatively shown in Figs. 4.15-4.16. A conclusion made by Monsalve and Schechter (1984) is that longer foam lifetime is associated with narrower bubble size distribution; that is, smaller variances favoured the foam stability. In the experiments conducted here, it is observed that the initial bubble diameter of foams produced by these two foaming agents are highly uniform, which indicated both bubble size distributions to be narrow right after the generation of foam with the average bubble diameters of AOS foam and SDS foam to be 45 μm and 80 μm, respectively. Although it could be expected that the size distribution would be varying over time, the distributions of AOS foam and SDS foam changed in different manners after the 600s time window: the bubble size of the former is still distributed relatively narrowly with around 70% of its bubbles sitting in the range of 125μm

and 180 μm, while the bubble size distribution of the latter becomes much wider than before, which could be validated by the image included in Fig. 4.14 where bubbles with various diameters stacked together. Furthermore, on the basis of Laplace's equation, smaller bubbles tend to coalesce into larger ones owing to the capillary pressure difference, leading to a dramatic foam stability reduction.

Consequently, it can be concluded that AOS is the best foaming agent among the candidates evaluated under the test condition applied. Considering the foamability and stability equally, 0.5 wt. % is chosen as the foaming agent concentration unless specified otherwise.

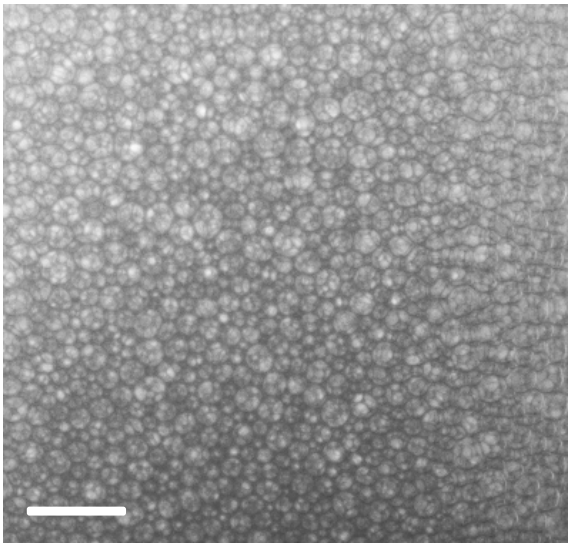

Fig. 4.11 Microscopic image for AOS bulk foam right after the agitation (t=0)

(Scale bar = 200 μm)

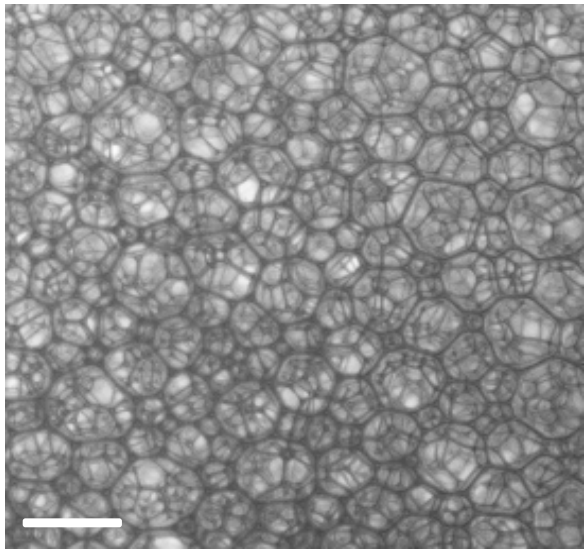

Fig.4.12 Microscopic image for AOS bulk foam over 600 s

(Scale bar = 200 µm)

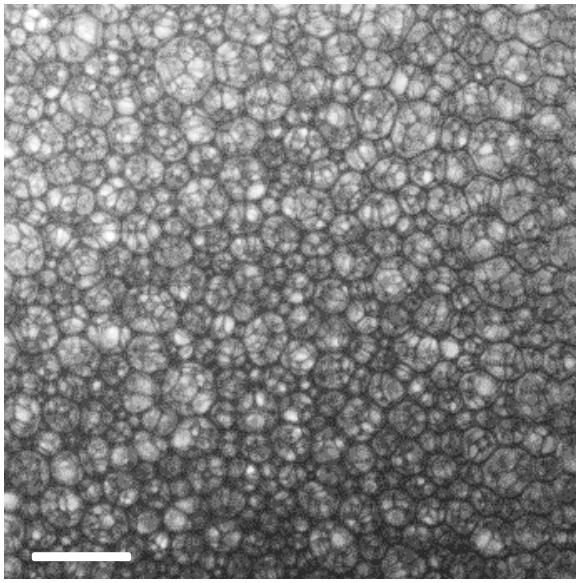

Fig. 4.13 Microscopic image for SDS bulk foam right after the agitation (t=0)

(Scale bar = 200 µm)

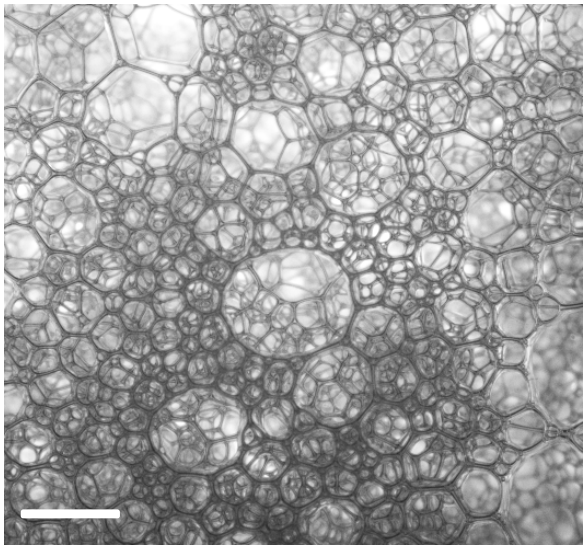

Fig. 4.14 Microscopic image for SDS bulk foam over 600 s

(Scale bar = 200 µm)

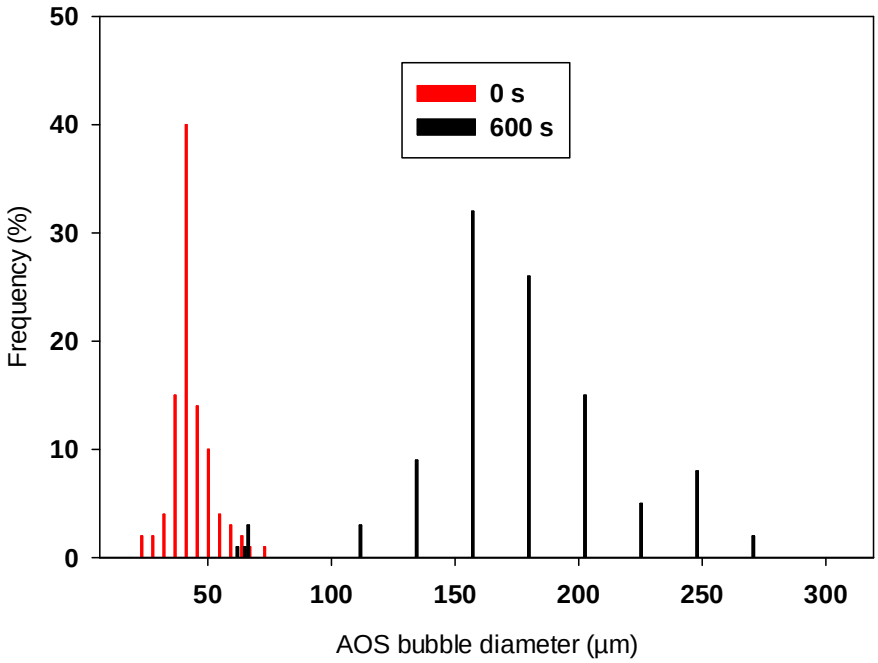

Fig. 4.15 AOS bulk foam size distribution at t=0 and 600 s

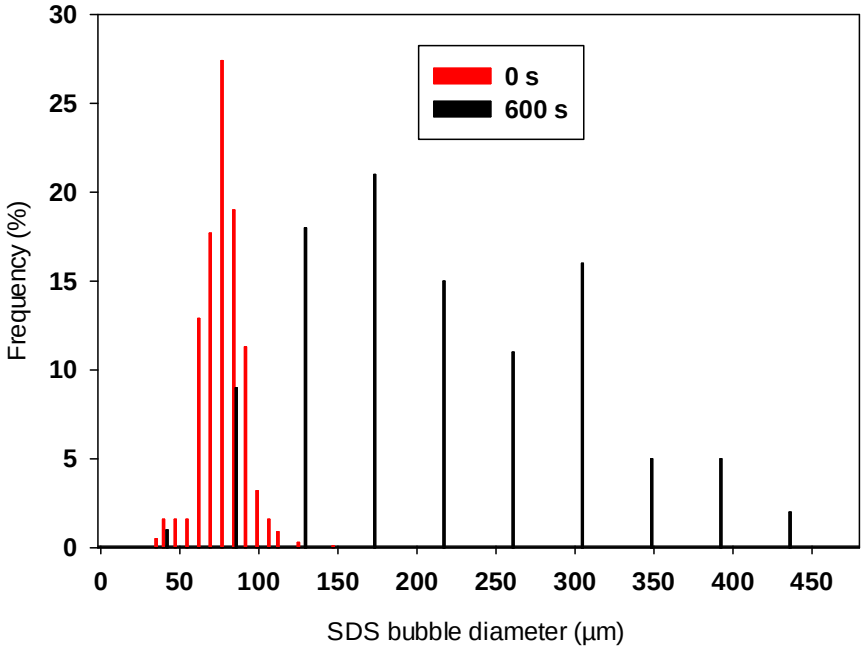

Fig. 4.16 SDS bulk foam size distribution at t=0 and 600 s

4.2.2 Selection of Polymer

Despite its outstanding foaming ability, AOS alone is not able to secure adequate foam stability which is critical for successful application of foam flooding. Very often, a polymer is applied to assist in the improvement of the foam stability. HPAM, the widely used thickener, and AVS, a novel amphiphilic ter-polymer with surface activity are selected to investigate the influence of polymer type and concentration on the foam behaviour.

4.2.2.1 Viscosity of Polymer Solution

The destruction of lamellae in a foam system can be considerably hindered through the addition of a polymer, which is capable of boosting the strength of the liquid membranes in the foam which encase the gas bobbles. The effect of the polymer concentration on the solution viscosity is shown in Fig. 4.17 for both polymers investigated. Below the concentration of 750 ppm, there are no significant viscosity differences between HPAM and AVS. However, when the concentration goes above 750 ppm, viscosities of the AVS solutions are roughly twice those of the HPAM solutions with the same concentration, which is an indication of the outstanding thickening performance of AVS.

It is widely accepted that the temperature can greatly influence the viscosity of a polymer solution. From Fig. 4.18, it is noticeable that the viscosity of both HPAM and AVS drop with increasing temperature. This is because the intermolecular forces are weaker relatively at higher temperatures due to increased kinetic energy. Nevertheless, AVS contains hydrophobic groups (functional monomer) which lead to hydrophobic association; therefore, the molecules are bonded strongly in a 3D network and the impact of temperature on polymer viscosity is therefore mitigated. Furthermore, the high temperature is in favour of boosting the hydrophobic association through reducing the solution polarity, which enables AVS to resist high temperature and yield higher viscosity than the counterpart HPAM.

The effect of solution salinity on the polymer viscosity is illustrated in Fig. 4.19. It can be observed that the viscosity decreases with increase in salinity. It is known that the charge repulsion can induce the molecular coil swelling; yet, with the presence of salt, the swelling effect would be negatively affected by the charge screening. Accordingly, solution viscosity drops significantly, as depicted in Fig. 4.19. However, the large and rigid side groups such as methylpropane sulfonic acid group in AVS molecules can improve the rigidity of molecular chain. Meanwhile the ionic forces are weakened in high salinity solutions while the hydrophobic interactions are favoured. Therefore, AVS exhibits excellent capacity of salt tolerance, which could be verified by the relatively high viscosity of the AVS solution under high salinity (Fig. 4.19).

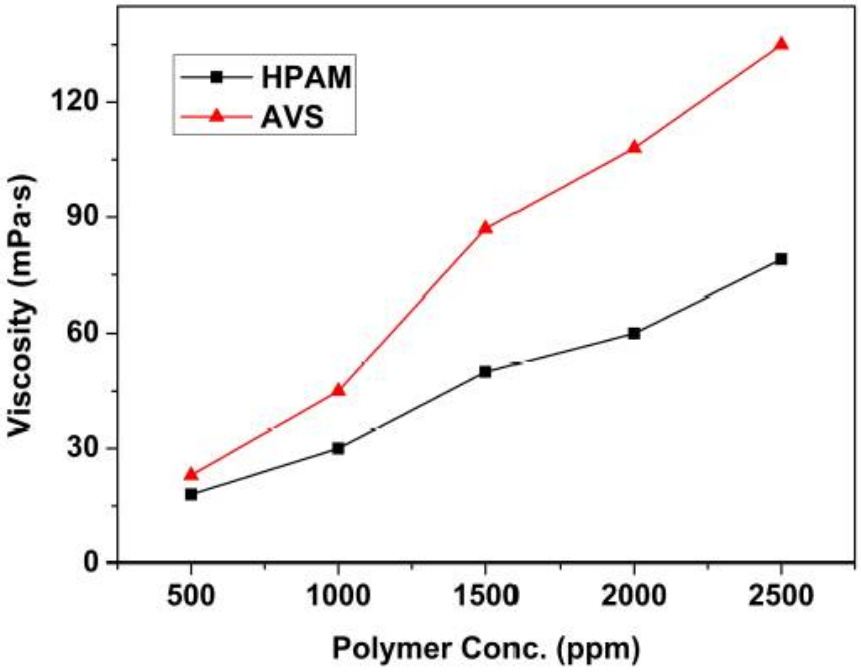

Fig. 4.17 Effect of polymer concentration on solution viscosity

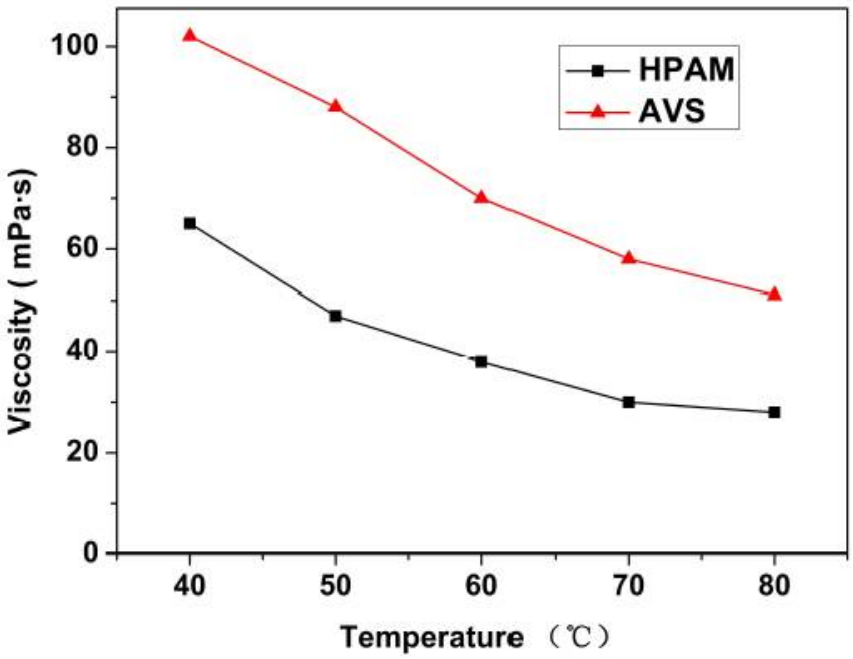

Fig. 4.18 Effect of temperature on solution viscosity

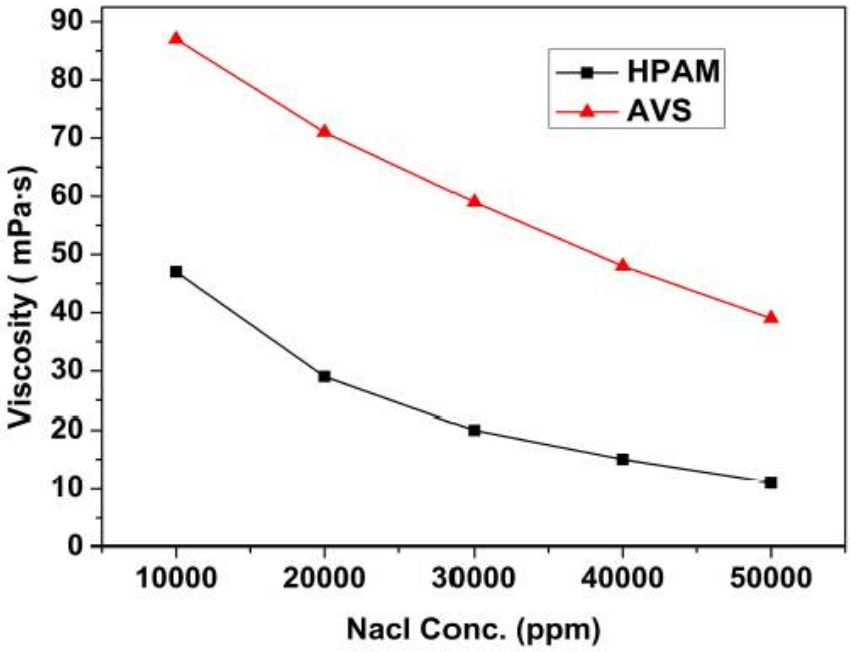

Fig 4.19 Effect of salinity on solution viscosity

4.2.2.2 Surface Tension

The surface tension of the HPAM and AVS solutions with different concentrations are summarized in Table 4.1. as evident from the data include in the table, it is found that the surface tension of the AVS solution declines with increasing concentration and can reach as low as 45.8 mN/m. AVS is an amphiphilic ter-polymer which contains hydrophilic as well as hydrophobic groups in its molecular chain, so its molecules are capable of being adsorbed at the interface between the gas and liquid phases just like an ordinary surfactant. With increase in the AVS concentration, more AVS molecules can gather at the interface until reaching a point where it cannot accommodate any more molecules. That is why, as shown in Table 4.1, after the concentration of 1500ppm, the surface tension remains relatively stable and higher concentrations only lead to the formation of a thicker solution rather any other favourable surface activity. As expected, due to the molecular structure limitation, HPAM molecules exist mainly in the bulk solution, so it is not able to lower the surface tension and can make limited contribution to the foamability.

To further understand the dependence of the foamability on the surface tension, foaming agent/polymer solutions (AOS concentration 0.5 wt %) instead of polymers alone are utilized in a new set of measurements. The assessment results are listed in Table 4.2. Interestingly,

unlike the scenario of polymer solutions alone, the surface tension of both of the AOS/AVS and AOS/HPAM solutions appear to be concentration-independent and the surface tension differences between them are quite small. This may be because the foaming agent AOS endowed with a lot better surface activity than the counterpart AVS or HPAM; therefore, the polymers' surface activity would be overshadowed by the existence of the foaming agent. The investigation results agree with the widely accepted conclusion that the foamability can be barely correlated with the gas/solution surface tension. Consequently, the superior foaming ability of the AOS/AVS solution, most likely, can be attributed to the surface activity of the AVS polymer, although the exact mechanism of how it assists in the foamability is not very clear yet.

Table 4.1 Influence of concentration of polymer on the surface tension

Concentration (ppm)	**Surface tension ($mN \cdot m^{-1}$)**	
	AVS	HPAM
500	51.7	68.9
750	50.4	68.8
1 000	48.0	68.9
1 250	46.6	69.5
1 500	46.2	69.8
1 750	45.9	70.1
2 000	45.8	70.9

Table 4.2 The dependence of surface tension on foaming formula

Concentration (ppm)	**Surface tension ($mN \cdot m^{-1}$)**	
	AOS/AVS	AOS/HPAM
500	29.5	30.4
750	29.6	31.2
1 000	28.8	31.5
1 250	29.3	31.0
1 500	28.9	31.3
1 750	28.6	31.1
2 000	29.0	31.5

4.2.2.3 Foamability and Foam Stability

The results of the foamability and foam stability tests on AOS in the presence of the two polymers are presented in figures 4.20 and 4.21. Clearly, both of the foamability and foam stability are closely related to the polymer concentration. In general, foamability drops with the increase in the polymer concentration. Due to the high bulk solution viscosity, AOS molecules would encounter considerable resistance when migrating from the bulk solution to the gas/liquid interface, which can detrimentally affect the foaming ability. However, AVS polymer displays a degree of surface activity just like ordinary surfactants, therefore, the foamability loss of the AOS/AVS foaming solution is less noticeable than that of the AOS/HPAM foaming solution due to the introduction of the surface active groups that would favour the generation of the foam. It is also found that the AOS/AVS solution exhibits a greater stability compared to the AOS/HPAM solution under the same polymer concentration. This can be mainly attributed to the viscosity differences between AVS and HPAM. Accordingly, the AOS/AVS solution is more viscous and has more capacity to reduce the chance of lamellae in the foaming system to collapse and cause foam decay and thus better foam stability can be achieved with AVS in solution. With the purpose of balancing the foamability and stability, taking into account the data presented in figures 4.20 and 4.21, 0.15 wt.% (1500 ppm) AVS is determined to be used in the main foaming formulation to be applied during the flooding tests.

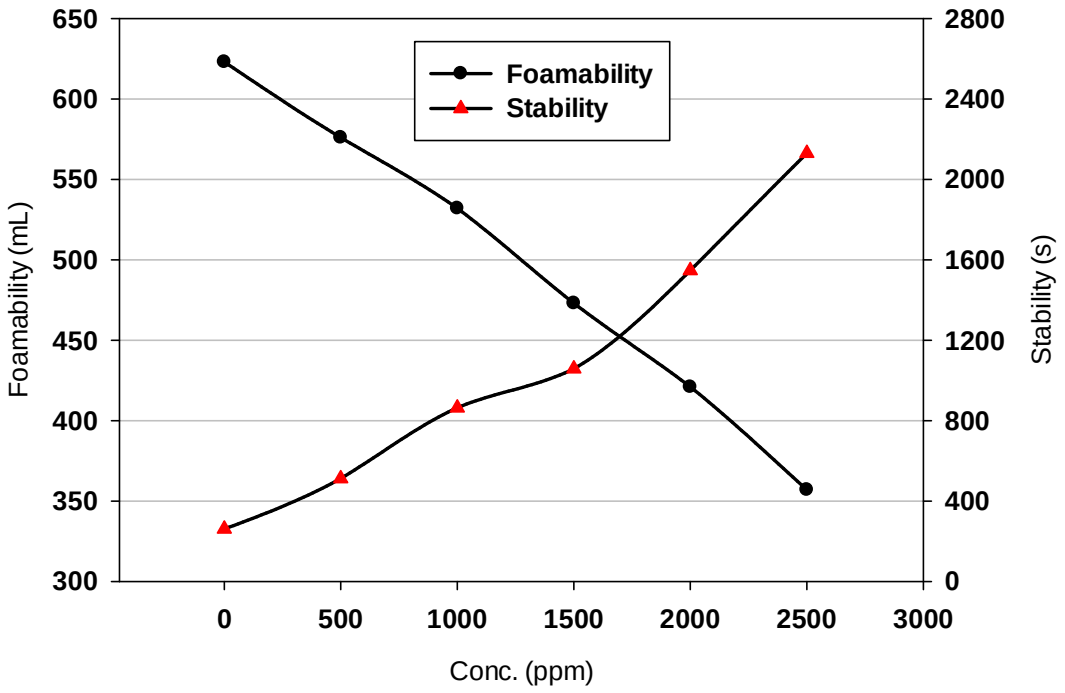

Fig. 4.20 The dependence of foamability and foam stability on HPAM concentration

(AOS 0.5 wt%)

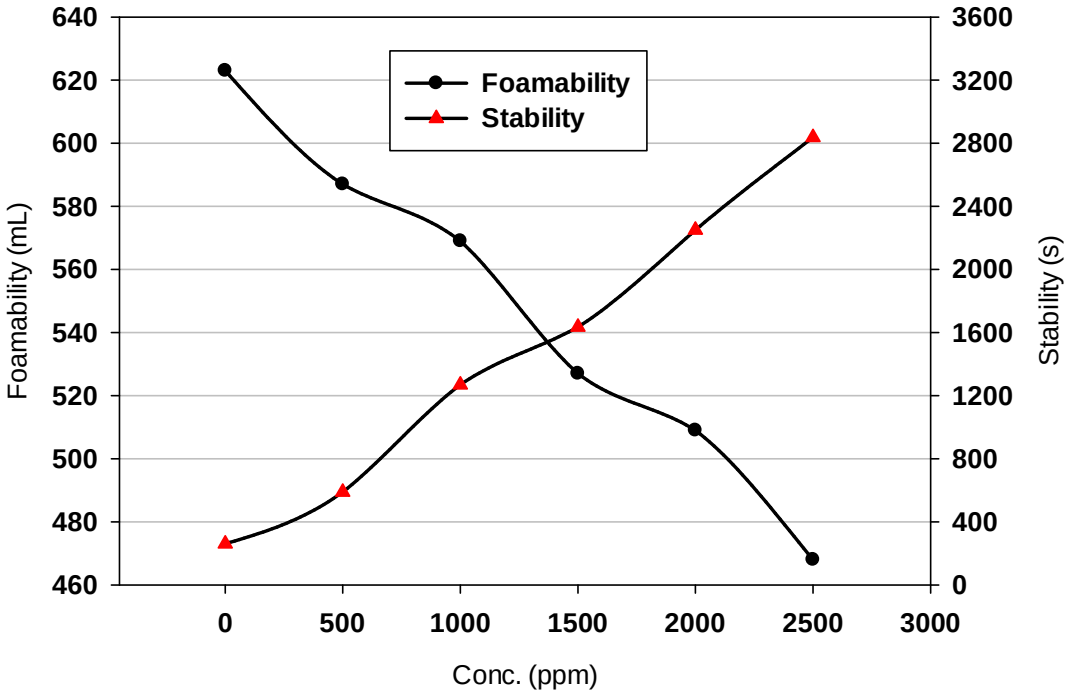

Fig. 4.21 The dependence of foamability and foam stability on AVS concentration

(AOS 0.5 wt%)

4.2.2.4 Core Flooding Experiments

Two sets of core flooding experiments are carried out at temperature and pore pressure of 50°C and 13.79 MPa, respectively, to compare the EOR potential of the AOS/AVS foaming system to that of AOS/HPAM with the direct foam injection and a gas/liquid ratio of 3:1. Some information about the core flood experiments and their key end results are tabulated in Table 4.3. The pressure drop histories during the secondary recovery (brine injection) and tertiary recovery (foam flooding and chase water-floods) floods are plotted in Figs. 4.22 and 4.23 as functions of the overall injected pore volumes (PVs). It is clear that, regardless of the rock permeability and the foaming formulation, the pressure drop across the core plug increases dramatically right after the introduction of the polymer enhanced foams, which indicates the outstanding blocking ability of the foams. Nevertheless, compared to the

AOS/HPAM foam, the counterpart AOS/AVS foam is endowed with a better blocking performance verified by its higher differential pressure over a longer period of time. This can be attributed to its remarkable foam stability associated with the surface activity and thickening ability of the AVS polymer. Another intriguing fact is that the steady pressure drop of the AOS/AVS foam flooding in chase water-floods are greater than that of the AOS/HPAM foam, suggesting the brine relative permeability after foam flooding is better modified; that is, more areas in the core plug can be swept more efficiently due to the greater brine permeability reduction, which explains the higher tertiary oil recovery of CO_2 foam flooding enhanced by the AVS polymer.

In the lower permeability range samples, the tertiary recovery of the CO_2 foam flooding enhanced by AVS is 3.7% higher than that of the foam flooding enhanced by HPAM. This difference can be attributed to the excellent foamability, stability and blockage of the AOS/AVS foaming system under the test conditions, which have already been discussed in the earlier sections of this chapter. Furthermore, when the enhanced foam collapses in the pores, the polymer can still work as a thickener to displace the residual oil. As the thickening ability of AVS was found to be much better, it may be expected to contribute more to the tertiary recovery. When it comes to the higher permeability range samples, both foam formulations result in the enhanced recoveries, while, compared with the lower permeability range, the recovery difference between them increases from 3.7% to 6.7%, which may suggest that the higher permeability is more favourable to the polymer enhanced foam flooding. It should be noted, however, that irrespective of the rock permeability range, the oil recovery differences between the two foaming formulations are not quite remarkable. This can be attributed to the limitations imposed on the experiments, such as the relatively short core plugs, etc. Overall, it can be concluded that compared to HPAM, AVS is able to enhance the foam stability without significantly affecting the foamability during a CO_2 foam flooding process.

Table 4.3 Effect of chemical formulation and permeability on oil recovery **(**50°C and 13.79 MPa**)**

Run No.	1	2	3	4
Formulation	0.5%AOS +1500ppm HPAM	0.5%AOS +1500ppm AVS	0.5%AOS +1500ppm HPAM	0.5%AOS +1500ppm AVS
Porosity (%)	14.7	15.1	17.3	17.5
Permeability (mD)	155.36	149.83	395.48	399.78
Gas/liquid ratio	3:1	3:1	3:1	3:1
Injection scheme	direct injection	direct injection	direct injection	direct injection
Slug size (PV)	1.0	1.0	1.0	1.0
Initial oil saturation (%)	60.6	62.1	69.2	67.5
Waterflood recovery (%IOIP)	32.5	33.0	39.1	38.8
Tertiary recovery (%IOIP)	20.4	24.1	22.2	28.8
Ultimate recovery (%IOIP)	52.9	57.1	61.3	67.6

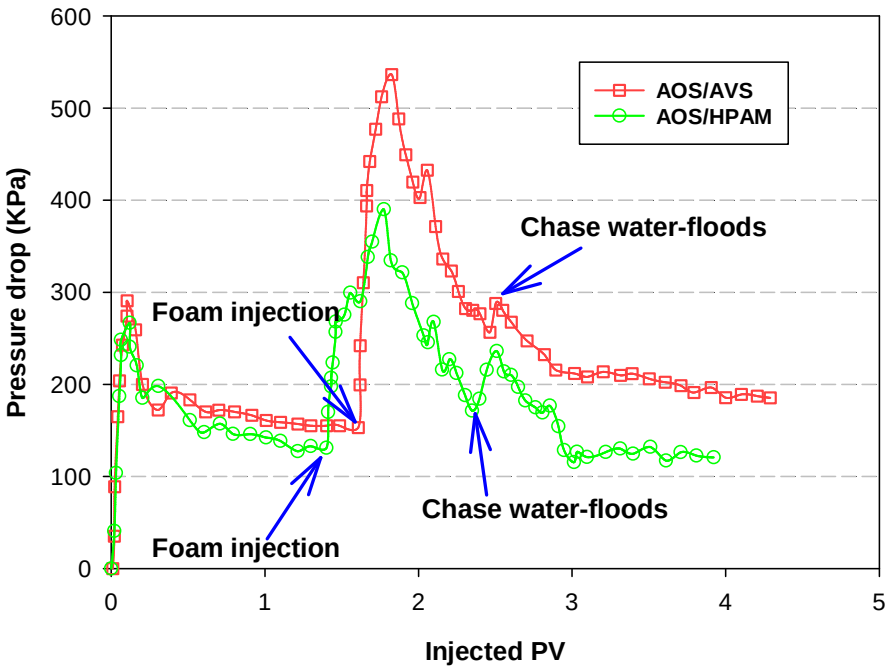

Fig. 4.22 Pressure drop during core flooding process in Run #1 (AOS/HPAM and k=155.36 mD) and #2 (AOS/AVS and k=149.83 mD)

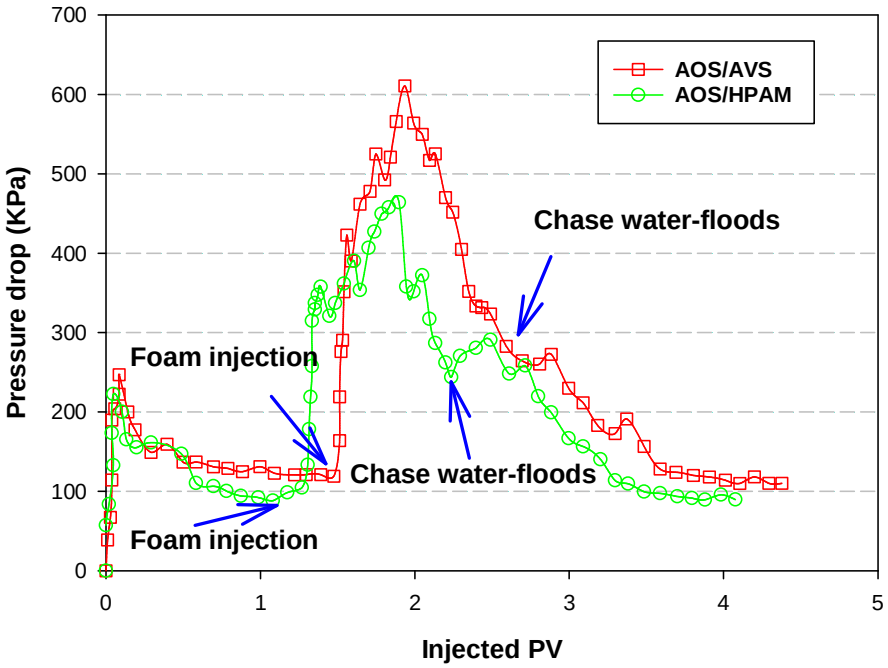

Fig 4.23 Pressure drop during core flooding process in Run #3 (AOS/HPAM and k=395.48 mD) and # 4 (AOS/AVS and k=399.78 mD)

4.2.3 Selection of the Additive

4.2.3.1 Foamability and Foam Stability

As mentioned in the early sections, the addition of a polymer into the foaming system significantly facilitates the enhancement of foam stability through improving the bulk solution viscosity and preventing the bubbles from coalescence and breakdown. However, the lamella strength which governors the thinning and rupture of the liquid films separating gas bubble would not be improved by the polymer. In this subsection, the results of the evaluations performed on the effect of additives or the so called lamella strength boosters on the static foam behavior are presented. Triethanolamine, also known as TEA which is a viscous compound, coconut diethanolamide (CDEA) and N70K-T, a mixture of nonionic surfactant and alcohol are selected to be applied as lamella strength boosters.

As shown in Fig. 4.24, below the concentration of 0.6 w.t.%, the life span of the foam generated by the AOS/AVS/triethanolamine foaming solution increases rapidly as the additive concentration rises until a plateau is reached, while its foaming ability drops steadily

with more boosters added. Triethanolamine is a viscous compound with a strong polarity and thus it can readily adsorb onto the gas/liquid interface and interact with the existing amphiphilic AVS. Such an interaction leads to the formation of regional micro-network on the liquid membrane whose rigidity, thereby, can be enhanced substantially. On the other hand, a number of the AOS molecules would be expelled from the interface as a result of the invasion and spatial occupation of the triethanolamine molecules, causing considerable loss of the foaming ability. In other words, the tremendous boost in the foam stability comes largely at the cost of loss of its foamability in this case.

The CDEA affects the static behavior of the CO_2 foam in a similar manner in comparison with the TEA, but the extent is fairly different as demonstrated in Fig. 4.25. With the increasing CDEA concentration, its foaming capability declines more dramatically than that of TEA. For instance, only 237 mL of CO_2 foam is produced when 0.6 wt% CDEA is added into the AOS/AVS solution, while, as seen previously (Fig. 4.24), 311 mL of CO_2 foam could be generated if the same amount of TEA was applied. Moreover, this foamability variation becomes more pronounced in higher additive concentration. On the other hand, the AOS/AVS/CDEA foam is endowed with an extraordinarily attractive life span. Above the concentration of 0.8 wt%, the generated foam is able to last for 3000 seconds without any significant breakdown, but only limited foams are created. Consequently, CDEA is not recommended as a promising additive under the experimental condition applied here.

The dependence of the foam behavior on the concentration of the next booster (N70K-T) is illustrated in Fig. 4.26. Interestingly, a peak appears on the foamability plot, indicating that the optimal foaming performance can be attained under the additive concentration of 0.4 wt.%. As mentioned earlier, N70K-T is a blend of a nonionic surfactant and alcohol and both of which are added at a given concentrations. Sett et al. (2014) reported that the foamability of a nonionic/anionic surfactant solution can be greater than the foamability of either of them on their own. These researchers also pointed out that the primary cause of the foamability enhancement may be the higher disjoining pressure which generates thinner but more stable lamellae; thereby, in the experiment conducted here, a larger volume of the foam would be created from the solution below the additive concentration of 0.4 wt.%. Still, the foamability declines dramatically beyond the peak and reaches down to 470 ml. This may arise from the accumulated alcohol in the solution hampering the association between AOS and nonionic surfactant contained in N70K-T. As for the foam stability, it increases with the N70K-T

concentration and is enhanced mainly via two mechanisms: 1) the adsorption of nonionic surfactant molecules onto the gas/liquid interface can rearrange the ionic distribution on the liquid membrane, which triggers stronger repulsion between the bubbles; 2) the interaction between the polar alcohol and amphiphilic AVS forms a rigid structure on the liquid membrane. Based on the results obtained, 0.5 wt.% N70K-T would be employed to meet the criteria set for both foamability and stability. In conclusion, the optimal foaming formulation in this study is determined to be 0.5 wt.% AOS + 0.15 wt.% AVS + 0.5 wt.% N70K-T.

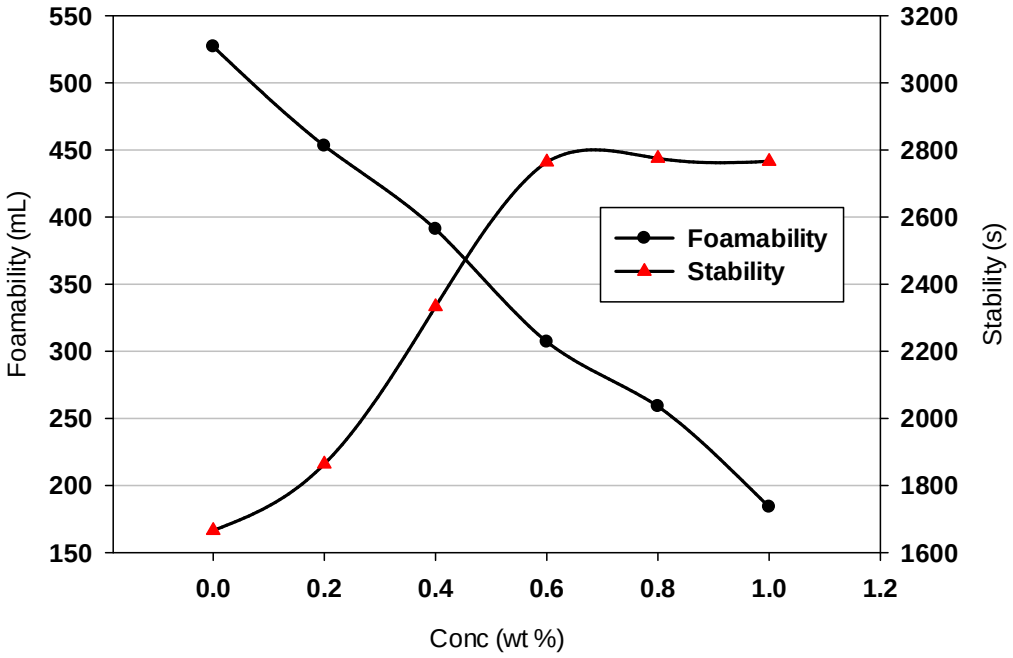

Fig. 4.24 The dependence of foamability and foam stability on TEA concentration (AOS 0.5 wt% and AVS 0.15 wt %)

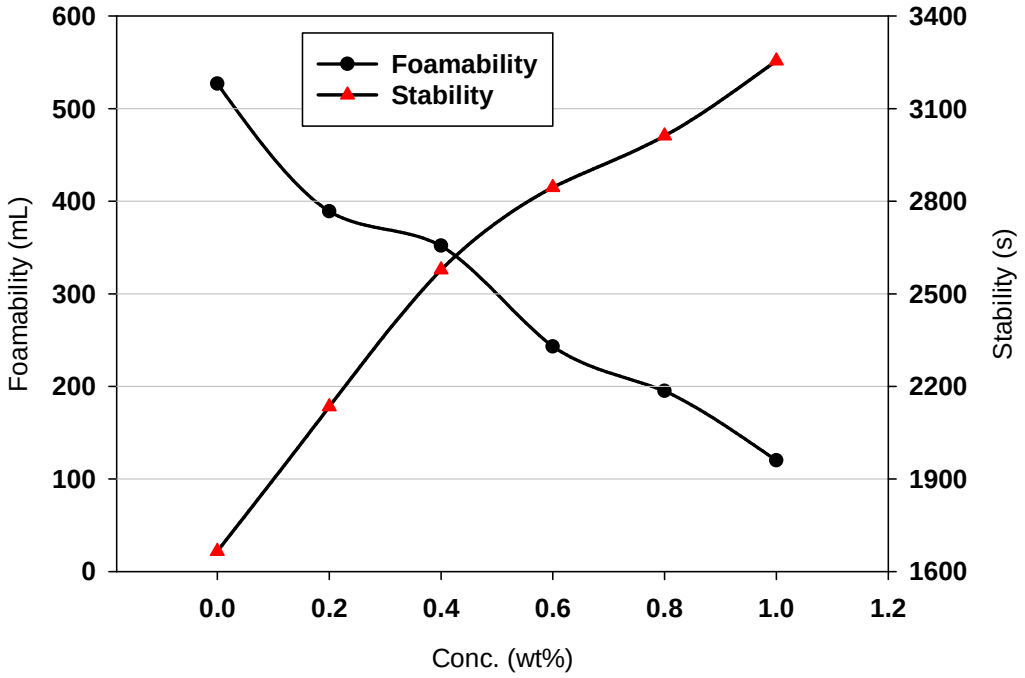

Fig. 4.25 The dependence of foamability and foam stability on CDEA concentration (AOS 0.5 wt% and AVS 0.15 wt %)

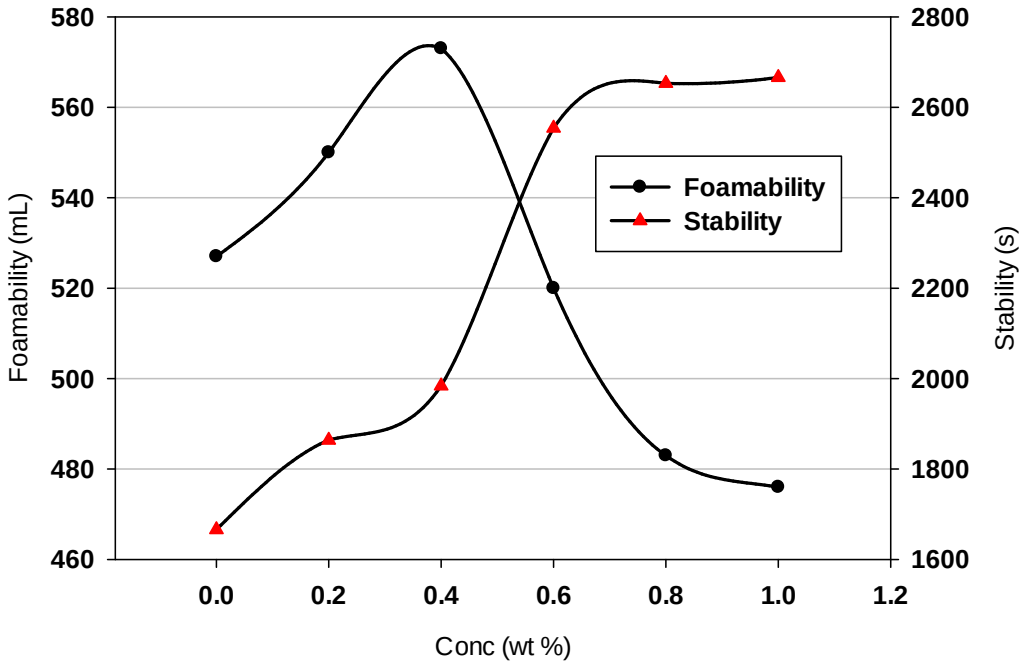

Fig. 4.26 The dependence of foamability and foam stability on N70K-T concentration (AOS 0.5 wt% and AVS 0.15 wt %)

4.2.3.2 Apparent Foam Viscosity

As stated before, treating the foam as a single phase would allow the application of the Darcy's Law and calculation of the foam apparent viscosity. In fact, the consideration of the foam as a single phase is reasonable as confirmed by the constant differential pressure profiles observed by a number of investigators in previous laboratory studies (Binks et al. 2008; Rosen and Solash, 1969). In this subsection of this chapter, the foam apparent viscosities are determined in a series of core flooding experiments where a variety of fluid systems (i. e. AOS 0.5 wt%, AOS 0.5 wt % + 0.15 wt %HPAM and AOS 0.5 wt % + 0.15 wt %AVS + 0.5 wt %N70K-T referred to as *Formula I*, *Formula II* and *Formula III*, respectively) and core plugs with different permeability ranges are used. The total injection flow rate (i.e. the sum of the liquid and gas flow rates) is kept constant at 2.0 ml/min (hence constant superficial velocity), while the foam quality varies from 10% to 95%. The influence of the foam quality on the apparent viscosity of the foam generated by varying formulations is illustrated in Fig. 4.27-4.29. Correspondingly, the experimental conditions and the results are summarized in Table 4.4. The details of the experimental procedure followed in conducting the measurements were presented in the previous chapter.

Minssieux (1974) investigated the foam apparent viscosity by means of Fann and Epprecht coaxial cylinder viscometer (i.e. static test) and concluded that in his work the foam apparent viscosity increased when the foam quality increased under the same shear rate. However, in a scenario where viscosities are determined from the core flooding experiments (i.e. dynamic test) different results are obtained. In other words, regardless of the foaming formulation and the rock permeability, the maximum foam apparent viscosity always exists under a specific foam quality known as the transition foam quality (Osterloh and Jante, 1992) which is indicated by the blue dash line in all the figures presented below. As for each foaming formulation, one of the intriguing features is that the transition foam quality is nearly independent of the rock permeability within the experimental accuracy. This observation matches the previous work of Alvarez et al. (2001) who suggested that the transition foam quality is a strong function of the foaming formulation and the overall flow rates in geometrically similar rock samples.

Another noticeable feature is that the foam generated by different foaming formulations all endowed with a greater apparent viscosity in higher permeability core plugs compared to their lower permeability counterparts. In a real life situation where the foam may be injected into a heterogeneous formation, the above mentioned feature, desirably, favours the foam

diversion flow into the lower permeability layers (Lee et al. 1991). Nonetheless, as evident from Figs. 4.27-4.29, the apparent viscosity differences in both of the higher and lower permeability core plugs becomes less obvious towards the two ends of the foam quality spectrum (the low foam quality regime (wet foam) at one end and the high foam quality regime (dry foam) at the other end), suggesting that the foam qualities which are near the transition foam quality (i.e. located in between the two ends of the spectrum) should be applied if the sweep efficiency in heterogeneous reservoirs need to be promoted to the highest possible extent.

In general, the apparent viscosity of the foam created by AOS/AVS/N70K-T is the greatest among the three formulations. This could be attributed to its well-balanced foamability and foam stability, which lead to the generation of the strongest foam under experimental conditions. Due to the dramatic loss of the foamability or stability, the other two formulae exhibit inferior thickening performance, though AOS/HPAM foam is thicker compared to the foam yielded by AOS alone.

Table 4.4 Summary of foam apparent viscosity measurement (50°C and 13.79 MPa)

Run No.	**1**	**2**	**3**	**4**	**5**	**6**
Formula	I	I	II	II	III	III
Core length (cm)	6.91	6.95	6.92	6.89	6.92	6.91
Core diam. (cm)	3.81	3.80	3.80	3.81	3.81	3.81
Porosity (%)	15.4	17.4	14.9	18.1	15.2	17.9
Perm. (mD)	148.65	449.68	149.79	452.12	148.67	452.12
Flow rate (min/L)	2.0	2.0	2.0	2.0	2.0	2.0
Transition foam quality (%)	55	59	70	77	87	80
Max. viscosity (mPa·s)	81.2	119.8	150.6	190.2	287.4	392.4

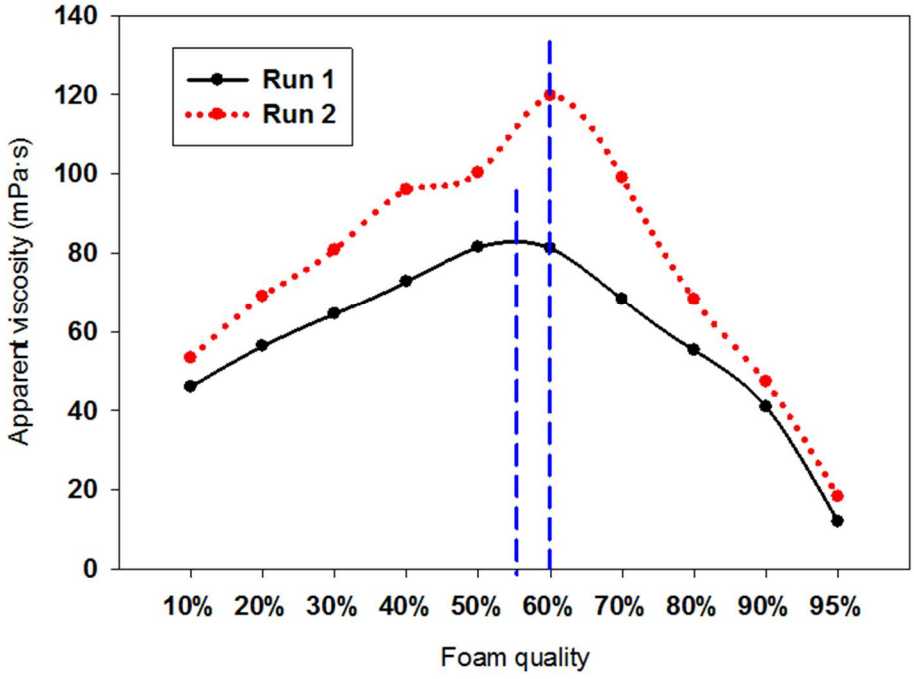

Fig. 4.27 The dependence of AOS foam viscosity on foam quality (The transition foam qualities were indicated by the blue dash lines)

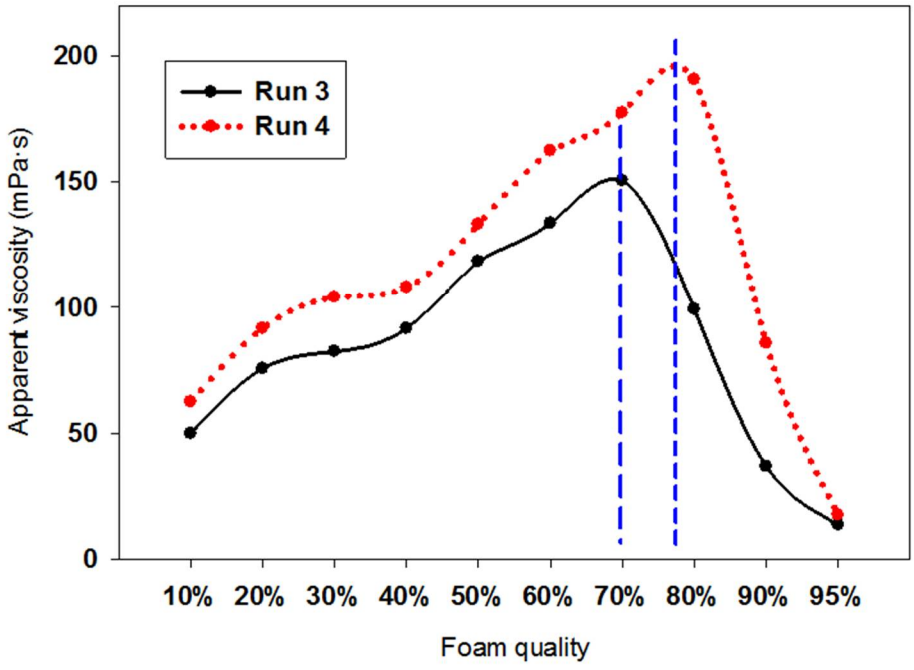

Fig. 4.28 The dependence of AOS/HPAM foam viscosity on foam quality (The transition foam qualities were indicated by the blue dash lines)

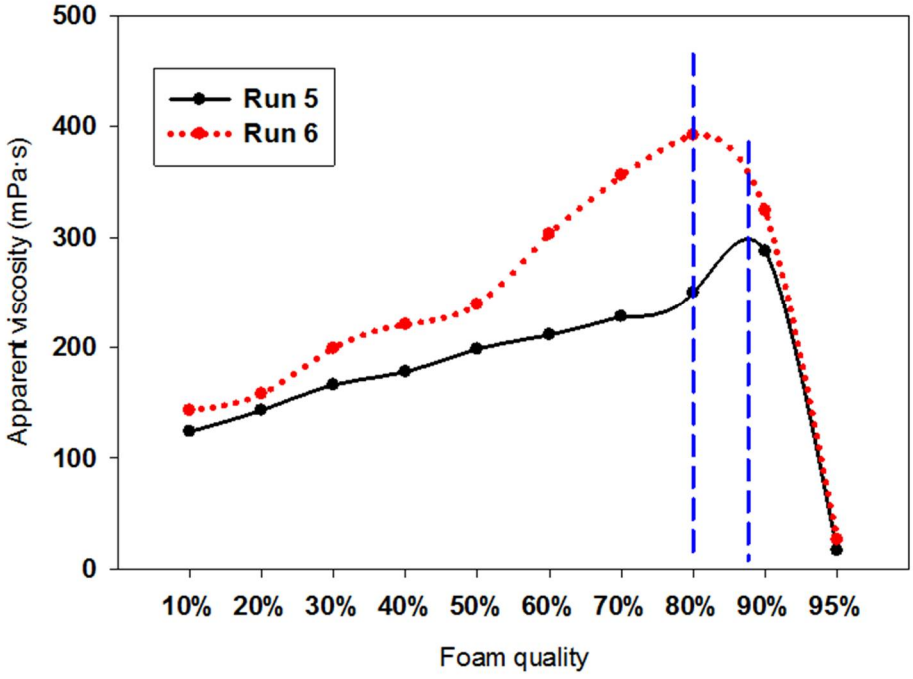

Fig. 4.29 The dependence of AOS/AVS/N70K-T foam viscosity on foam quality (The transition foam qualities were indicated by the blue dash lines)

4.2.3.3 Resistance Factor (RF) and Residual Resistance Factor (RRF)

As discussed in details earlier, RF can serve as a strong indication of the blocking ability, while RRF reveals the magnitude of the relative permeability reduction of the displacing fluid. To evaluate the dependence of RF and RRF on the foaming formulation and the foam injection strategy (i.e. direct foam injection with the aid of foam generator and co-injection of $CO_2$and foaming solution), six runs of foam flooding experiments using formulae I, II and III (Heading 4.2.3.2) in core plugs with a permeability of around 450 mD are carried out under 50°C and 13.79 MPa. The pressure drop histories during the foam flooding process are presented in figures 4.30-4.32. Some key experimental details and the end results of the experiments are listed in Table 4.5.

Apparently, as can be seen from the graphs presented in figures. 4.30-4.32, the foam injection scheme has a pronounced influence on the foam flow in a porous medium. As for all the three formulations investigated in this work, without any exception, the pressure differences between the inlet and outlet ends of the core plugs increases rapidly when the CO_2 foam is injected directly, which can be verified by the observation that steady state flow can be established after only 1.0-1.5 PV of foam injection. However, when it comes to the

simultaneous injection of CO_2 and the foaming solution, the increase in the pressure drop is more gradual, and greater amounts of fluids (2.0-3.0 PV) are required to be injected prior to reaching the plateau (i.e. steady state condition) . On the other hand, the differential pressures of simultaneous gas/solution injection drops dramatically once the chase brine is fed into a core plug. This can be explained by the fact that the foam production through the co-injection mode is not as efficient due to the insufficient contact time between CO_2 and the foaming solution in a relatively short core plug. As a consequence, it takes longer period of time to reach steady state flow which, then, can readily be affected by an externally induced disturbance such as the chase brine injection.

It can also be found that irrespective of the injection strategy, the variation between ΔP_2 (the steady-state pressure drop during the foam flow process) and ΔP_3 (the steady-state pressure drop during the chase brine) of Formula I is more appreciable in comparison with those of the other two foaming solutions, suggesting the considerable drop in blocking ability after the introduction of the chase brine. The excellent residual blockage in the cases of formulae II and III, very likely, can be attributed to the presence of polymers which are adsorbed onto the surface of flow channels (pores and pore-throats) when foams advanced in the porous medium. A significant portion of the adsorbed polymer can then be desorbed by the chase brine thickening it, while the rest of the adsorbed polymer remains on the surface diminishes the pore sizes or plugging up the pore-throats. In addition, the adsorbed surfactant can also dissolve into the chase brine and, possibly, result in the recreation of the foam stabilized by the desorbed polymer.

Through comparing the RF and RRF of these foaming formulations, it could be concluded that Formula III performs the best in terms of blocking ability as well as changing the relative permeability of the displacing phase. In general, extraordinary blocking ability leads to the improvement in the sweep efficiency, and the relative permeability modification promotes the displacement efficiency of the chase brine flood which, thereby, can be considered as an “extended foam flooding” in terms of its flow behaviour. Overall, the foam generated by foaming Formula III enables more regions in the core plugs to be explored during the displacement of foam and chase brine injections compared to its Formulae I and II counterparts under the same test conditions.

Table 4.5. Summary of the RF and RRF experiments (50°C and 13.79 MPa)

Run No.	1	2	3	4	5	6
Formula	I	I	II	II	III	III
Flow rate (min/L)	2.0	2.0	2.0	2.0	2.0	2.0
Foam quality (%)	75	75	75	75	75	75
Core length (cm)	6.90	6.93	6.91	6.87	6.89	6.91
Core diam. (cm)	3.80	3.80	3.81	3.81	3.81	3.81
Porosity (%)	18.4	17.5	17.9	17.7	18.1	17.6
Perm. (mD)	449.62	452.23	453.79	455.19	448.57	453.44
Injection mode	co-injection	pre-foamed	co-injection	pre-foamed	co-injection	pre-foamed
ΔP_1 (KPa)	21.3	23.4	22.7	22.7	24.1	23.4
ΔP_2 (KPa)	912.1	1112.8	1432.1	1734.7	2202.9	2951.6
ΔP_3 (KPa)	286.1	474.4	930.1	1216.2	1727.8	2516.6
RF	42.7	46.6	63.5	76.3	90.5	120.1
RRF	13.5	19.7	41.1	53.4	71.0	102.4

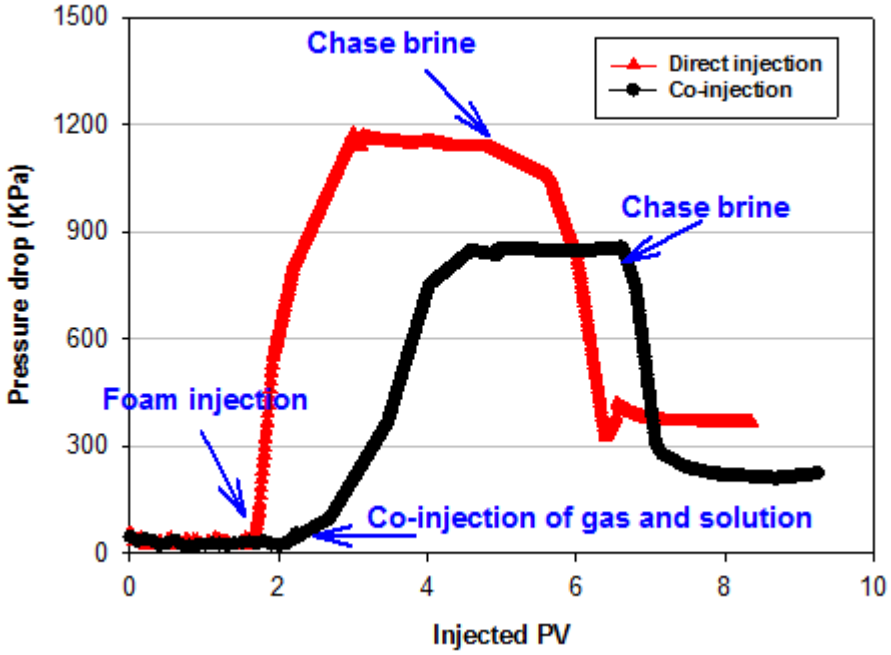

Fig. 4.30 Pressure drop history of AOS foam flooding (50°C and 13.79 MPa)

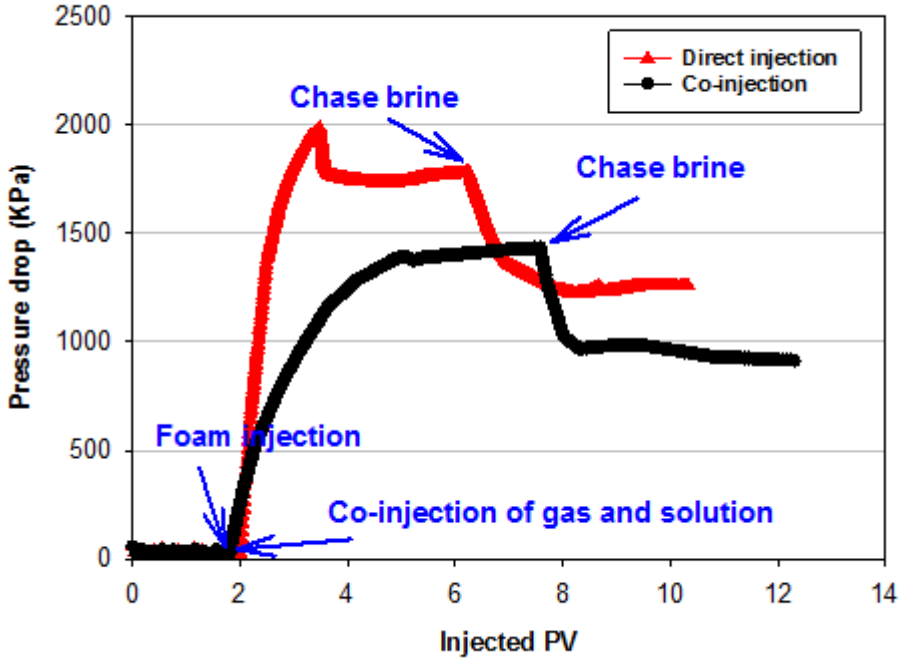

Fig. 4.31 Pressure drop history of AOS/HPAM foam flooding (50°C and 13.79 MPa)

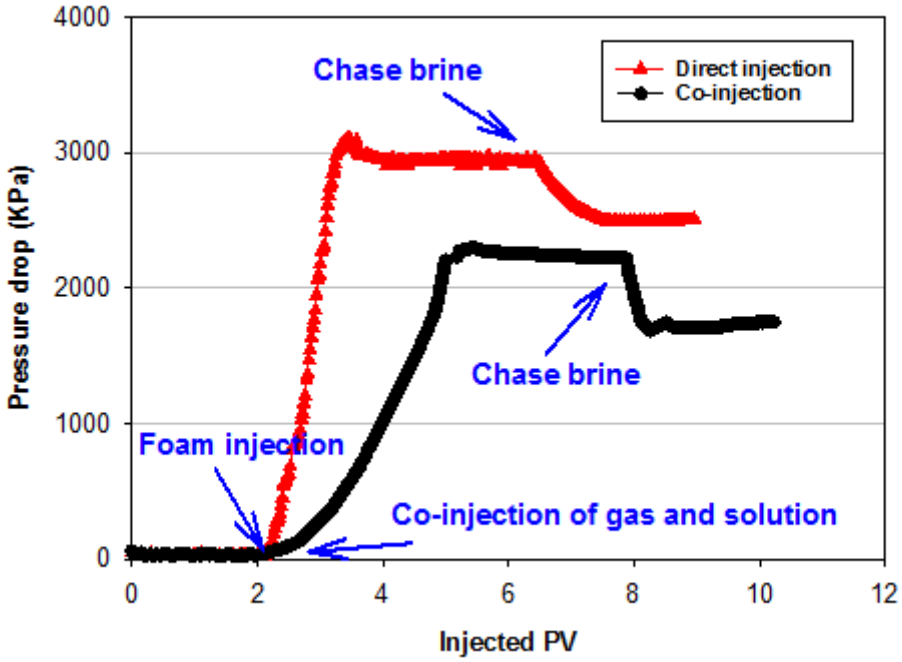

Fig. 4.32 Pressure drop history of AOS/HPAM/N70K-T foam flooding (50°C and 13.79 MPa)

4.2.3.4 Mobility Reduction Factor (MRF)

It is well known that the mobility reduction factor (MRF) reflects the extent of the promotion in the pressure gradient along the investigated core plug by replacing the brine being utilized in simultaneous injection of gas and liquid with the foaming solution. To assess the influences of the total gas/liquid flow rate (fixed gas/liquid ratio of 3:1) as well as the gas flow rate (fixed liquid flow rate at 1.0 ml/min) on the MRF, a series of core flood experiments using formulae I, II and III are conducted on core plugs with a permeability around 450 mD under 50°C and 13.79 MPa.

The MRFs of each formula are plotted as functions of the total injection rate in Fig. 4.33. The gas/liquid ratio is maintained at 3:1, while the overall flow rate varies from 4.0 ml/min to 12.0 ml/min. Apparently, as revealed by the data plotted in this figure, MRF is closely correlated with the total injection rate. With the flow rate rising, the MRF decreases continuously irrespective of the formulation used, although the extent of the loss is formula-

dependent. This can be attributed to the inadequate interaction between the gas and liquid phases in a relative short core plug, and larger total flow rate would lead to the less sufficient gas/liquid contact and thus fewer amount of in-situ foam. As for formulation I which contained no additives, it is found that there exists a "critical flow rate" (8.0 ml/min under this experimental condition) after which the MRF tend to remain constant as the overall flow rate increases further, indicating that the MRF is independent of the gas/liquid flow rate beyond this critical point. This behaviour may be thanks to the dynamic equilibrium of the foam formation: on one hand, the creation of the in-situ foam is hampered by the insufficient gas/liquid contact in the short porous medium; on the other hand, the increased injection rate enabled a large fraction of the absorbed surfactants to be desorbed into the solution and cause further foam generation. Nonetheless, it is not clear if this critical point exists universally regardless of the foaming agent type and concentration, thereby further investigation is required to verify the validity of this conclusion. With the presence of additives, formulations II and III do not displayed a similar trend within the investigated flow rate range, their MRFs, although larger than that of formulation I at identical gas/flow injection rate, decrease as the flow rate increases. The primary causes of this behaviour could be the unfavourable gas/liquid contact and the polymer viscosity loss due to the large shear force between the solution and porous medium at high flow rates. However, formulation III is less affected by the shear thinning owing to the existence of a 3D network associated with association effect compared to formulation II. It is noted that despite its highest capability to reduce the mobility among the three formulations, formulation III loses the advantage over the other two counterparts as the overall injection rate increases. As a consequence, it is reasonable to expect that these three formulations may exhibit similar if not same capability to reduce mobility with larger total flow rates in spite of the fact that the practical overall injection rate in reservoir scale, conventionally, is far less than 4.0 ml/min where formulation III exhibits superiority in terms of mobility reduction over the other two formulations.

The dependence of MRF of each formula on the gas flow rate is illustrated in Fig. 4.34. The liquid phase is fed into the core holder at the fixed rate of 1.0 ml/min with the CO_2 flow rate varying from 1.0 ml/min (foam quality of 50 %) to 9.0 ml/min (foam quality of 90 %). As can be clearly seen form Fig. 4.34, the gas flow rate imposes an evident effect on the MRF in a manner that is completely different from that of total flow rate with fixed gas/liquid ratio. It can be observed that the MRF reaches its peak value when the gas flows at an intermediate rate (5.0 ml/min) and the MRF decreases by differing percentages at relative low and high

gas flow rates regardless of the formulation. The MRF variations may stem from the various foam qualities which may lead to significantly different foam apparent viscosities. As discussed earlier, the capability of foams to modify the displacing phase flow is closely correlated with its apparent foam viscosity which turns out to be a strong function of the foam quality. Obviously, the foam apparent viscosity under 83.3 % foam quality (corresponding to the gas flow rate of 5.0 ml/min) is endowed with the greatest foam viscosity compared with that of 50 % and 90 % foam qualities (corresponding to gas flow rates of 1.0 ml/min and 9.0 ml/min, respectively). Furthermore, the total flow rate has considerable impact on the foam displacement, which was discussed in the previous section. Consequently, taking into consideration these two aspects, the foam possesses the least capability to control the displacing phase mobility if it flows at relative high rate. Among all formulations, formulation III exhibits a noticeable advantage in terms of reducing the CO_2 mobility, especially under intermediate and high gas flow rates.

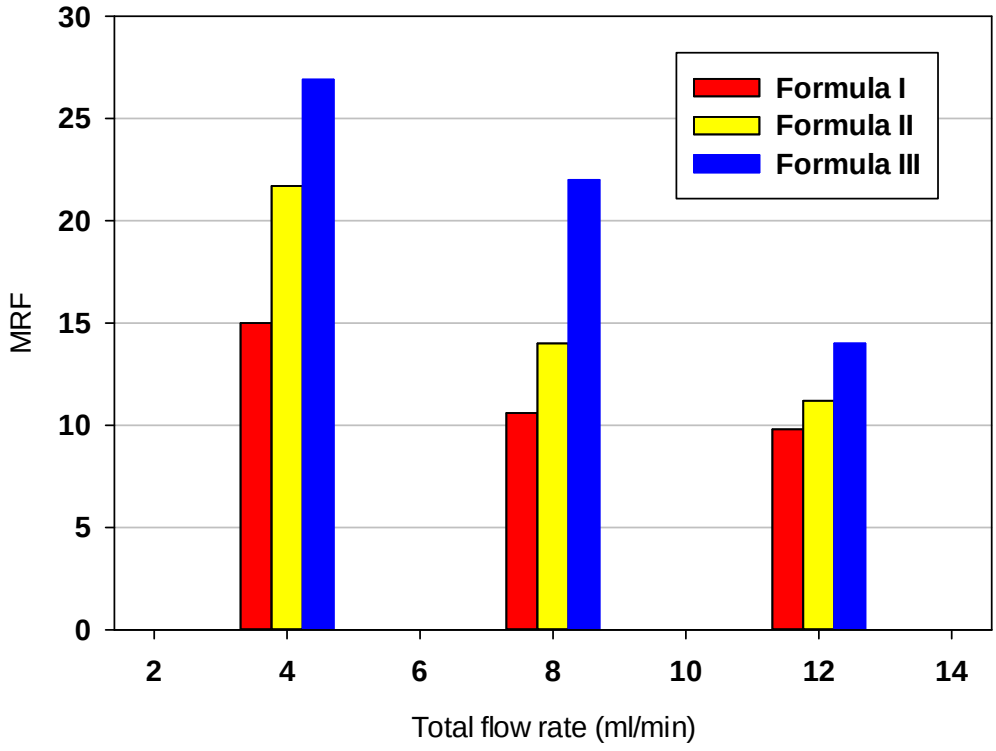

Fig. 4.33 The influence of total flow rate on mobility ratio factor (MRF) (gas/liquid ratio 3:1)

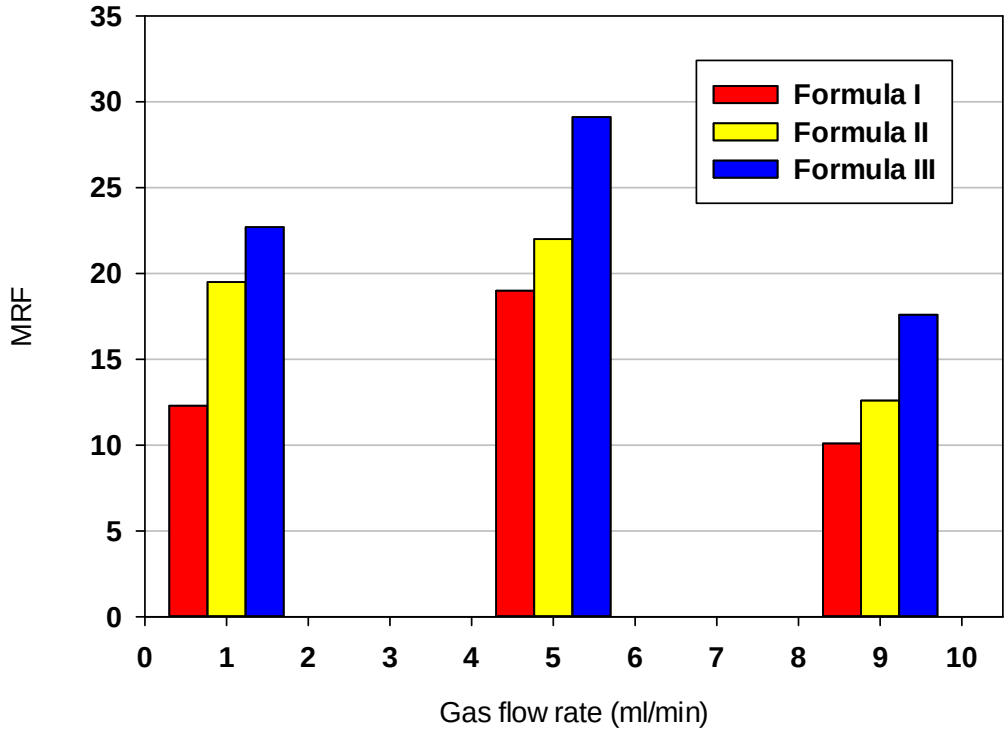

Fig. 4.34 The influence of gas flow rate on mobility ratio factor (MRF) (liquid flow rate 1.0 ml/min)

4.2.3.5 CO_2 Foam Flooding for Oil Displacement

The basic sample properties of porosity and permeability and the end results of the foam flooding experiments using various formulations are summarized in Table 4.6. As can be seen, the secondary water floods recover comparable percentages of the crude oil in each case. However, the tertiary displacement performances in the water-flooded core plugs are greatly different: the incremental tertiary oil recovery of Formula III is 12.5 % and 5.8% higher than that of formulae I and II, respectively, leading to the pronounced accumulative oil recovery differences.

As for Formula I, its apparent foam viscosity is fairly low due to the unfavourable gas/liquid ratio; furthermore, as stated before, its foam longevity is detrimentally affected because of the residual oil saturation. Consequently, the CO_2 foam induced by AOS alone cannot improve the oil recovery as significant as that of the CO_2 foam induced by AOS plus chemical additives. In the case of Formula II, it recovers more residual oil under the tertiary recovery process than AOS alone (Formula II) due to the presence of HPAM. However, to some extent, the polymer thermal degradation seems to hinder the positive influence of HPAM on the

performance of the CO_2 foam. Therefore, the foam is not as robust as it is supposed to be. Besides, the introduction of HPAM results in the reduction in the foamability, which also explains its deficiency in terms of the recovery.

Overall, Formula III is endowed with the best displacement performance. The strong synergism between AVS and N70K-T allows for the creation of the extraordinarily reliable lamellae and 3D network structure in the solution which in turn contributes to the foam's remarkable apparent viscosity and blocking ability. In other words, the sweep efficiency of the displacing phase would be improved substantially as a consequence of the excellent flowing performance of the foam in the porous media. This is mostly why, after water flooding, the CO_2 foam enhanced by AVS/N70K-T (formula III) yields the most recovery of the residual oil among the three cases.

Table 4.6 Summary of the oil recovery experiments (50℃ and 13.79 MPa)

Experiment	#1	#2	#3
Porosity (%)	18.7	17.8	18.6
Permeability (mD)	362.12	369.36	372.79
Formula	I	II	III
Gas/liquid ratio	3:1	3:1	3:1
Slug size (PV)	1.0	1.0	1.0
Initial oil saturation (%)	67.0	68.4	68.1
Water floods recovery (%)	33.8	34.6	33.4
Tertiary oil recovery (%)	27.2	32.9	39.7
Overall oil recovery (%)	61.0	67.5	73.1

4.3 Evaluation and Optimization of Chemical-Alternating-Foam (CAF) Flooding

The previous section described the development of a new foaming formulation for the CO_2 foam floods. The formulation is eventually determined to include 0.5 wt.% AOS + 0.15 wt.% AVS + 0.5 wt.% N70K-T. For simplicity, this specific formulation is referred to as a surfactant/polymer (S/P) combination, because N70K-T can be treated as a weak polymer. In this section, a novel CO_2-EOR method named CAF (chemicals-alternating-foam flooding) that uses the above developed formulation (S/P solution) is proposed and its behaviour is thoroughly assessed and optimized in an attempt to maximize its potential EOR performance.

4.3.1 Comparative Study of Direct Foam Injection, Co-injection of Gas/Liquid and CAF Flooding

As stated before, this work presents a new chemical EOR method called chemical-alternating-foam flooding (CAF) which combines the advantages of the foam and SP flooding, with the ultimate purpose of maximizing the EOR capability of the individual SP flooding and foam flooding. On one hand, the adsorbed surfactant in the foam flooding process can be compensated for by the SP solution through material exchange, then to some extent, the foaming ability of the proposed foaming formulation can be maintained if not enhanced; on the other hand, the polymer in the SP solution barely flows ahead of the surfactant as the polymer solution with a higher concentration is utilized in the foam flooding to boost the foam strength. So the polymer concentration gradient is established between the two floods to prevent the polymer from advancing ahead the surfactant in the SP flooding, leading to outstanding mobility control.

To assess the displacement efficiency of the combined SP/foam flooding or , as mentioned earlier, the chemicals-alternating-foam flooding (CAF), three modes (Mode A, Mode B and Mode C) where each of which utilizes 0.4 PV of CO_2 and 0.4 PV of surfactant/polymer (SP) are evaluated in this research. The composition of the SP solution was determined in earlier sections of this chapter: 0.5 wt. % AOS + 0.15 wt. % AVS + 0.5 wt. % N70K-T. The varying injection modes are illustrated in Fig. 4.35 and the corresponding descriptions are as follows:

1*) Mode A: direct foam injection*. 0.8 pore volume (PV) of foam consisting of 0.4 PV of CO_2 and 0.4 PV of SP solution is directly fed into a core sample with the assistance of a foam generator located ahead of the core holder.

2) *Mode B: co-injection of CO_2 and SP solution*. The CO_2 and SP solution are introduced alternately into a core plug by two cycles in order to create foam in-situ. In each cycle, 0.2 PV of CO_2 and 0.2 PV of SP solution are applied.

3) *Mode C: chemicals-alternating-foam flooding (CAF)*. Instead of CO_2, the foam is combined with SP solution and they are injected alternately, again by two cycles. In each cycle, 0.3 PV of foam (comprising 0.2 PV of CO_2 and 0.1 PV of SP solution) and 0.1 PV of SP solution are used.

The supercritical or dense CO_2 will be applied for all the experiments included in this section. The crude oil sample is sourced from an oil reservoir located in the North West Shelf of

Western Australia. Its minimum miscibility pressure (MMP) with CO_2 is estimated to be around 1500 ~ 1700 psi (Li et al., 2012). As described in the previous chapter, the oil sample is filtered before any use. Overall, two sets of core flooding experiments are carried out, one set is conducted under miscible condition (P= 2000 psi), while the other is performed when CO_2 is immiscible with the crude oil (P= 1200 psi).

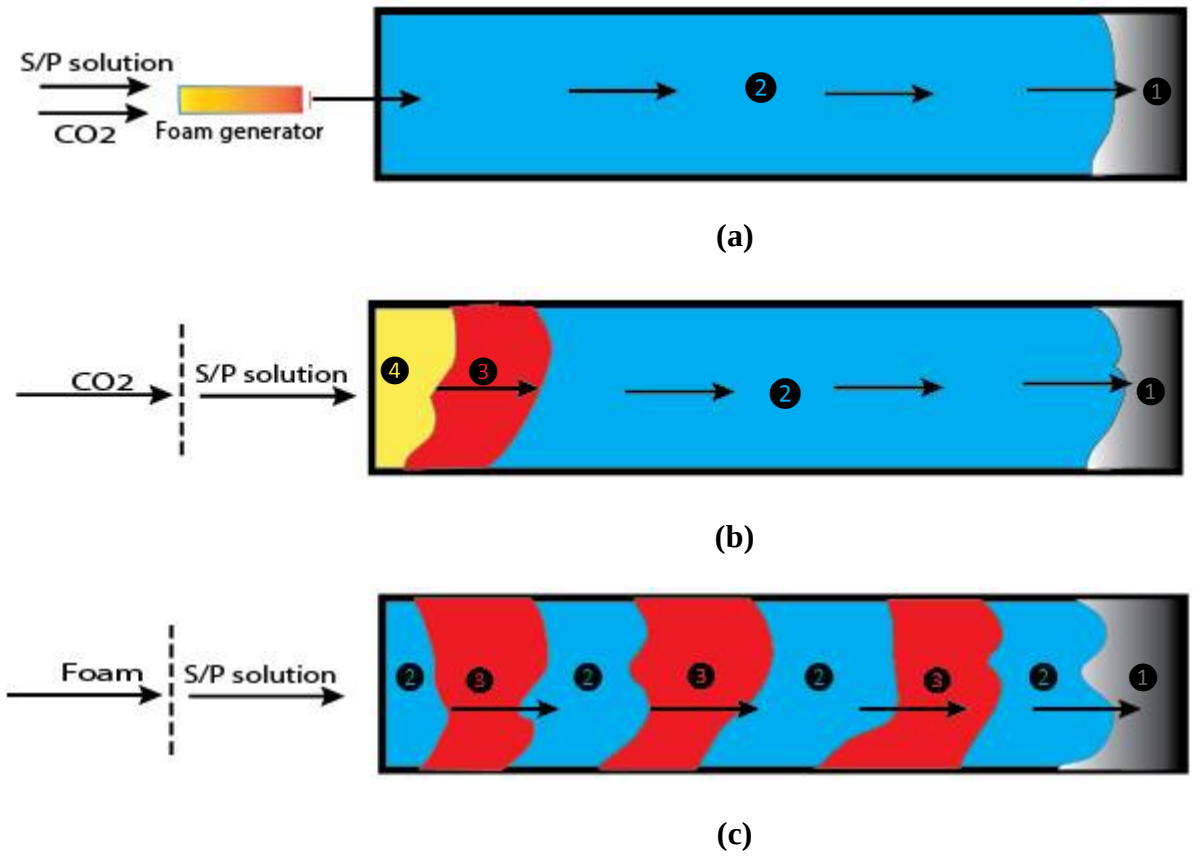

Fig. 4.35 The illustration of Mode A (a), Mode B (b) and Mode C (c) (Note: 1: oil bank 2: CO_2 Foam 3: SP solution 4: Dense CO_2)

4.3.1.1 Core Flooding Experiments under Miscible Condition

One set of experiments consisting of three runs (one run per each of the earlier mentioned three injection modes) are conducted under miscible condition. Apart from the way in which the supercritical CO_2 and chemicals are introduced into the core plug, the experimental conditions and procedures remain identical for the three experiments. The results of the experiments are summarized in Table 4.7.

Table 4.7 Summary of the core flooding results under miscible condition

(50 °C, 13.79 MPa)

Experiment	#1	#2	#3
Porosity (%)	18.4	18.1	18.6
Gas permeability (mD)	483.68	476.36	470.65
Brine permeability (mD	384.26	369.14	374.16
Tertiary mode	A	B	C
Total amount of gas and chemicals used	0.4 PV supercritical CO_2 + 0.4 PV SP solution	0.4 PV supercritical CO_2 + 0.4 PV SP solution	0.4 PV supercritical CO_2 + 0.4 PV SP solution
Injection scheme	0.8 PV foam[#]	(0.2 PV CO_2 + 0.2 PV SP solution) *2	(0.3 PV foam[#] + 0.1 PV SP solution) *2
Initial oil saturation (%)	69.4	67.8	70.1
Water floods recovery (%)	37.8	35.9	36.7
Tertiary oil recovery (%)	30.8	25.9	37.7
Max. pressure drop (KPa)	603.9	448.8	712.9
Overall oil recovery (%)	68.6	61.8	74.4

Note: The foam is produced with the assistance of a foam generator. The created foams are comprised of 0.4 PV supercritical CO_2 and 0.4 PV of the SP solution, and 0.3 PV of supercritical CO_2 and 0.1 PV of the SP solution in experiments #1 and #3, respectively.

4.3.1.1.1 Pressure Drop

The pressure drops across the core plugs during the secondary and tertiary recoveries of various injection modes are plotted in Figs. 4.36-4.38 as a function of PVs of fluids injected. As can be seen, irrespective of the injection mode, the differential pressure rises rapidly immediately after the commencement of the brine injection, indicating that the oil bank is moving towards the outlet end of the core holder. Nonetheless, the differential pressure decreases once 0.1 PV of brine is pumped. This can be attributed to the tendency of the floods for early brine breakthrough resulting from the density and viscosity differences between the brine and the crude oil and that the oil cannot be displaced evenly. After the brine breakthrough, the pressure drops tend to become steady until residual oil saturation is established. At this point, differing tertiary recovery methods are initiated.

In Mode A, the CO_2 foam is injected directly into the core plug with the assistance of a foam generator. As expected and can be seen from Fig. 4.36, the pressure drop increases dramatically reaching a maximum of 599.8 KPa. Two mechanisms may contribute to the tremendous increase in the pressure drop. Firstly, the foam possesses an extremely high apparent viscosity and thus is able to make the oil bank move forward. Secondly, the foam preferentially enters the wider pore channels and then blocks them, redirecting any further injected fluids into the relatively narrower pore channels which could not be reached in the preceding brine injection process. One noticeable phenomenon is the pressure drop fluctuations during the foam flooding process marked on Fig. 4.36. This may be attributed to the possible collapse and regeneration of the CO_2 foam in the porous medium. The chase brine is injected at the end of the foam injection in order to make full use of the CO_2 and chemicals which had already existed in the pores. Accordingly, the pressure drop increases at the beginning of the chase water-flood because of the blockage caused by the adsorbed polymer and recreated foam. With more chase brine being injected into the system, the blockage becomes less pronounced, which arise from the loss of chemicals. As a result, the pressure drop declines gradually until steady-state flow is attained.

When it comes to Mode B, as can be seen from Fig. 4.37, the pressure drop changes in a different manner. Compared to Mode A, the differential pressure increases relatively slowly but the fluctuations are more pronounced, reaching the maximum value of only 448.2 KPa, which is, very likely, an indication of the inadequate foam generation. This poor performance can be primarily caused by the insufficient interaction between CO_2 and SP solution, a consequence of their mobility difference. Another intriguing feature in the foam generation process is that, generally, the pressure drop increases when the CO_2 is introduced, while the injection of the SP solution is found to make the pressure drop to decrease. It can be seen from Fig.4.37 that this fluctuation takes place in both injection cycles, which validates the hypothesis that the foam creation in the porous medium is not instantaneous and it rather requires some amount of time for the foam creation and propagation to occur. Unlike Mode A, the differential pressure in Mode B continually decreases when chase water-flood is carried out. Again, this phenomenon reconfirms the low efficiency of the foam production in Mode B. To some extent, the adsorbed polymer and foaming agent which should facilitate the foam regeneration in the core plug are capable of prohibiting the decline of the pressure drop which, similar to Mode A, becomes relatively steady once 2.0 PVs of the chase brine is fed into the system.

In the case of Mode C, as can be seen in Fig. 4.38, the situation is completely different from those in modes A and B. It is found that the differential pressure across the core plug rises significantly once the foam injection phase begins. Although the introduction of the SP solution does cause the pressure drop to be unstable somehow, the pressure drop is able to reach a maximum of 689.5KPa at times but it mainly fluctuates around 551.6 KPa, indicating the oil bank keeps moving forward in the core sample during the foam and SP solution injection process. The distinguishing displacement performance of this mode may stem from the following reasons: (1) the foam stability is greatly improved because of the presence of the SP solution. The surfactant can assist in maintaining the foamability, while the polymer is helpful in terms of making the foam more robust; (2) the existence of the foam alleviates the problem of chromatographic separation of the SP solution; (3) the mass transfer between the foam and SP solution eases the chemicals loss to a great extent; (4) the synergism of the foam and chemicals aides the mobility reduction of the supercritical CO_2 and improves the displacement efficiency of the CO_2 flooding, considerably. In summary, the remarkable blockage resulted from Mode C injection can be largely attributed to the enhanced foam flooding as well as the modified SP flooding. As can be seen from Fig. 4.38, once the chase brine is introduced into the core sample, as expected, the differential pressure begins to decrease; nonetheless, compared to modes A and B, the decline is quite slow and gradual. As discussed earlier, the interaction between the CO_2 foam and SP solution in the porous medium was found to be quite strong, therefore, the residual resistance during the chase water-flood phase is evident and this prevents fast decrease of the differential pressure. The differential pressure becomes relatively steady once 2.2 PV of chase brine is injected, which means residual oil saturation had been attained at this stage.

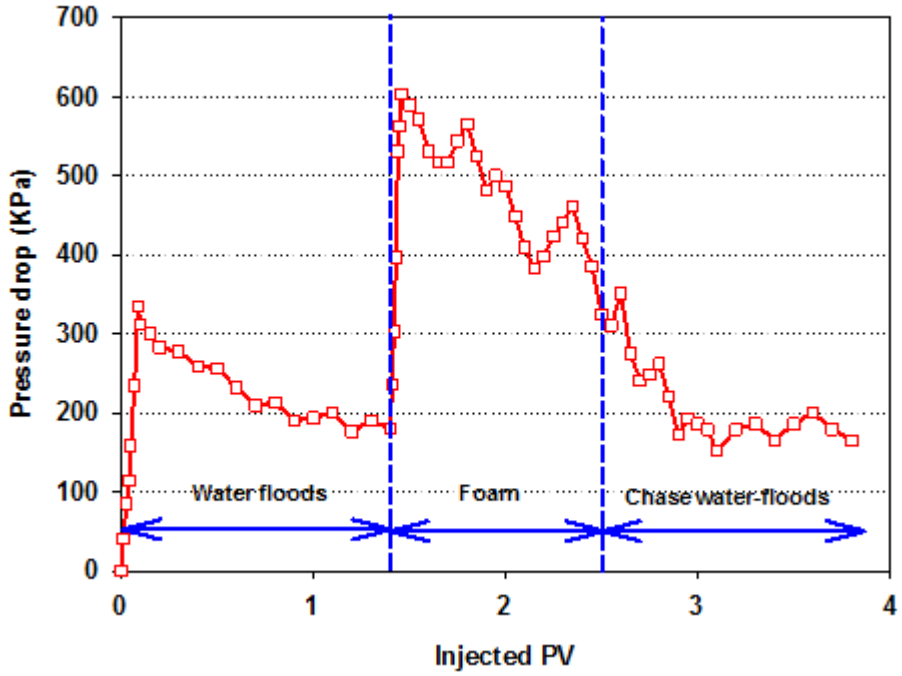

Fig. 4.36 The pressure drop history of Mode A under miscible condition (50 °C, 13.79 MPa)

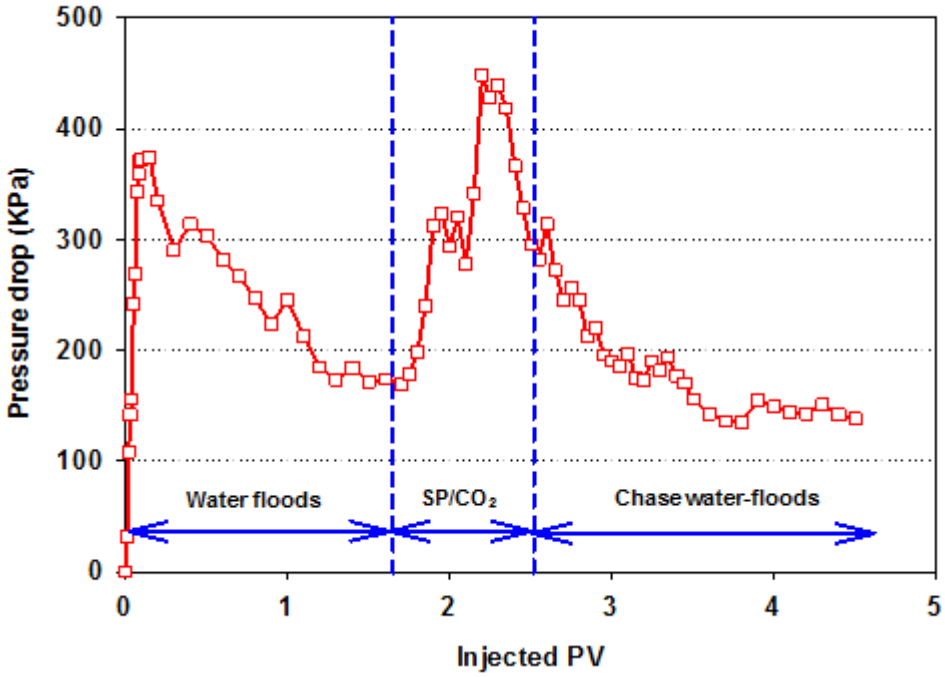

Fig. 4.37 The pressure drop history of Mode B under miscible condition (50 °C, 13.79 MPa)

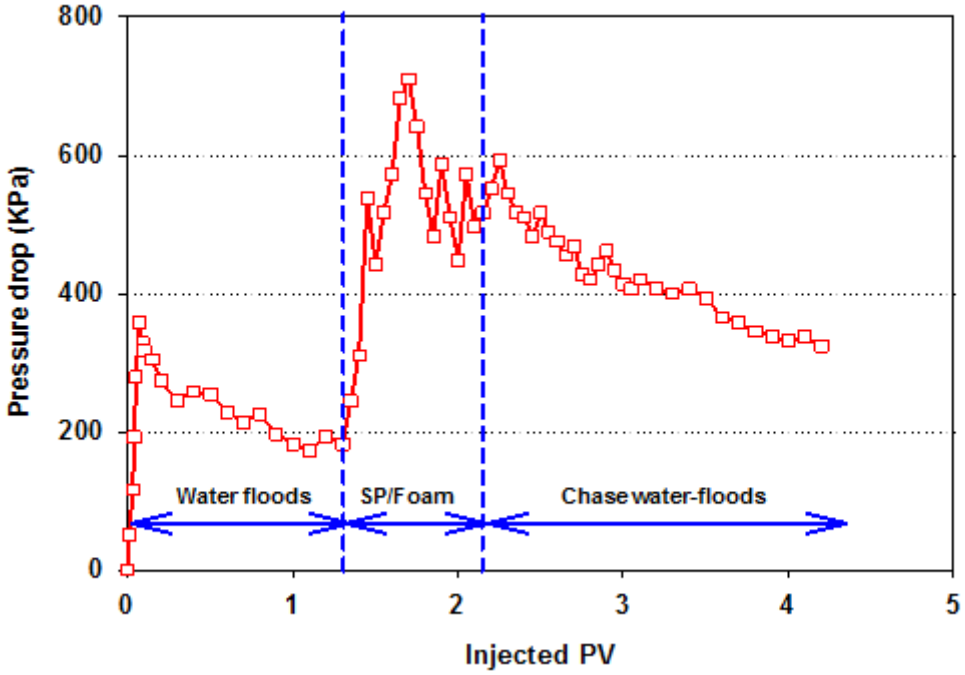

Fig. 4.38 The pressure drop history of Mode C under miscible condition (50 °C, 13.79 MPa)

4.3.1.1.2 Cumulative Oil Recovery and Water Cuts

The cumulative oil recoveries for the same core flooding experiments are presented in Figs.4.39-4.41As can be seen from Figs.4.39-4.41, prior to the tertiary floods, the brine floods (secondary recovery) recover, on average, around 36% of the initial oil in place before the water cut reaches 99%. At this point, the brine injection is stopped and various EOR methods comprising of either of modes A, B or C would commence. As illustrated in Table 4.7, the most amount of incremental oil (38.7%) is found to be produced by applying Mode C, followed by Mode A (32.8%), while the least amount (28.9%) is recovered by Mode B. Taking into consideration the secondary oil recovery figures, the cumulative oil recoveries (i.e. ultimate oil recoveries) of modes A, B and C would be 70.6%, 62.8% and 75.4% respectively.

In Mode A, direct foam which is created with the aid of the foam generator, is injected into the core plug resulting in a dramatic reduction in the mobility ratio of the flood. Accordingly, the displacement efficiency of the miscible CO_2 flooding is maximized. However, due to the

foam collapse caused by the oil invasion and the lamellae breakdown, and also because of the adsorption of the chemicals onto the rock surface, the foams become weak, especially during the chase water-flood phase. This phenomenon, with no doubts, would greatly affect the performance of the tertiary oil recovery stage. In Mode B, as stated before, the contact between the supercritical CO_2 and SP solution is inadequate, leading to the insufficient amount of foam production in the porous medium. Despite the relatively high performance of the foam flooding, the tertiary oil recovery of Mode B is the lowest among the three modes, indicating the detrimental impact imposed by this injection mode on the foam generation and eventual oil recovery. Under the miscible conditions, the alternative injection of the CO_2 foam and SP solution, namely Mode C, possesses the highest incremental recovery during the tertiary oil recovery stage. The combination of the foam flooding and SP flooding implemented in Mode C is capable of overcoming the problems existed in the direct foam injection (Mode A) through the synergism mechanism, and this may explain the tertiary oil recovery advantage of Mode C over that of Mode A.

With regards to the water cut, as can be seen from Figs.4.39-4.41, irrespective of the subsequent tertiary mode employed, the water breakthrough takes place after only 0.2-0.3 PV of brine injection. As mentioned earlier, this is a result of the unfavourable mobility ratio caused by the viscosity difference between the injected brine and crude oil. After the breakthrough, the water cut increases steeply and the crude oil can barely be recovered. At the end of the secondary brine injection, the water cut is nearly constant at 99%, indicating the establishment of residual oil saturation. At this point, the supercritical CO_2 and chemicals are fed into the system through various injection modes leading to considerable reductions in the water cut.

In Mode A, as illustrated in Fig. 4.40, the water cut decreases significantly to as low as 56% as the foam is directly injected. After the injection of around 0.2 PV of foam, however, the water cut begins to rise unceasingly even with the continuous foam injection. This phenomenon matches the fact that the oil production would eventually begin to decline at a certain point of the foam injection process owing to the pronounced foam collapse which would negatively impact on the blockage capability of the injected foam. Consequently, the water cut increases to 90% at the last stage of the direct foam flooding. When it comes to Mode B, as can be seen from Fig. 4.40, similar to that in the Mode A, the water cut goes down initially, but at a far lower rate. With the alternative injection of the supercritical CO_2 and chemicals, the water cut fluctuates dramatically, which again validates the low efficiency

of the foam generation by this mode of injection. The lowest water cut during this tertiary recovery process is only 68%, which is in good agreement with the less incremental oil production in comparison with that of Mode A. Moreover, the water production rate increases noticeably at the late stage of the CO_2 and chemicals injection and the water cut reaches 95% quickly. Afterwards, the water cut hardly changes and stays around 98% during the entire chase water-flood phase. In the case of Mode C, as evident from Fig. 4.41, the water cut again varies over time. Nevertheless, unlike in Mode B, the water production rate declines quickly as soon as the foam and SP solution are introduced resulting in a water cut as low as 48% which is the lowest post-secondary water cut achieved among all three modes of injection. Although somehow some degree of fluctuation in water cut still exists its extent is less evident than that of Mode B. Furthermore, it can be seen from Fig. 4.41 that this mode is endowed with the lowest overall average water cut among the three injection modes, reflecting its highest blocking capacity. As expected, the water cut increases by a great extent as the foam/SP solution injection ceases and the chase water-floods begins. However, compared to its other two counterpart modes, the water content of the production stream of this mode changes more slowly during the chase water-flood phase, which may be a resulted of the large relative permeability reduction of the chase brine. To summarise, the remarkable capability to control excessive water production validate the strong synergism arising from the combined use of the foam flooding and the SP flooding in Mode C.

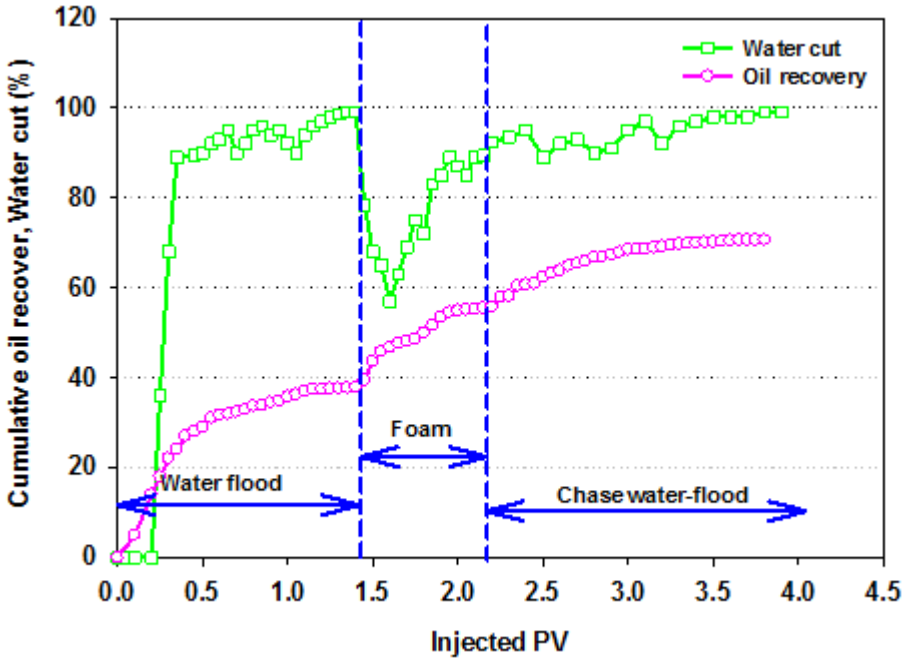

Fig.4.39 The water cut and cumulative oil recovery of Mode A under miscible condition (50 °C, 13.79 MPa)

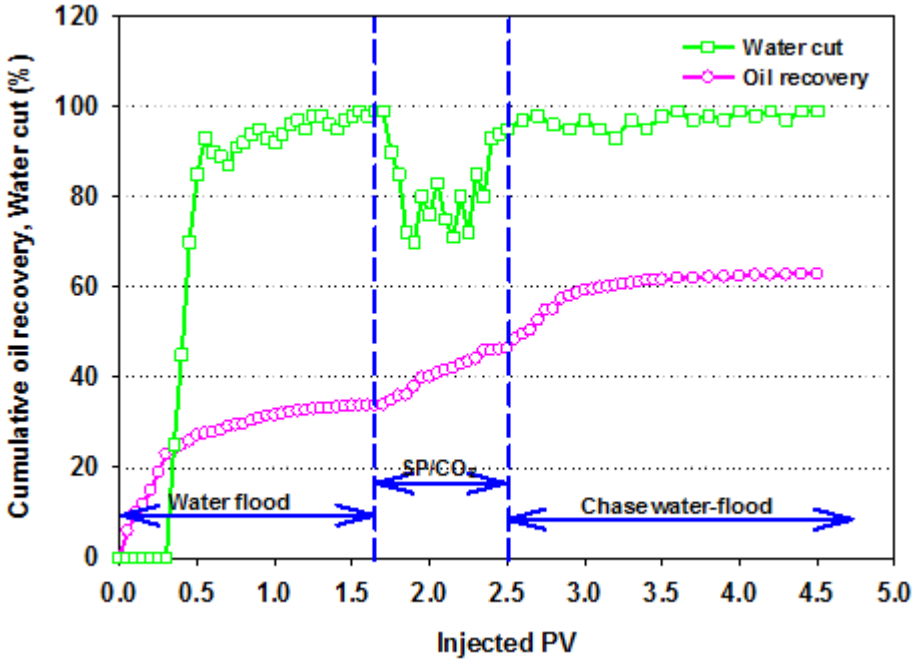

Fig.4.40 The water cut and cumulative oil recovery of Mode B under miscible condition (50 °C, 13.79 MPa)

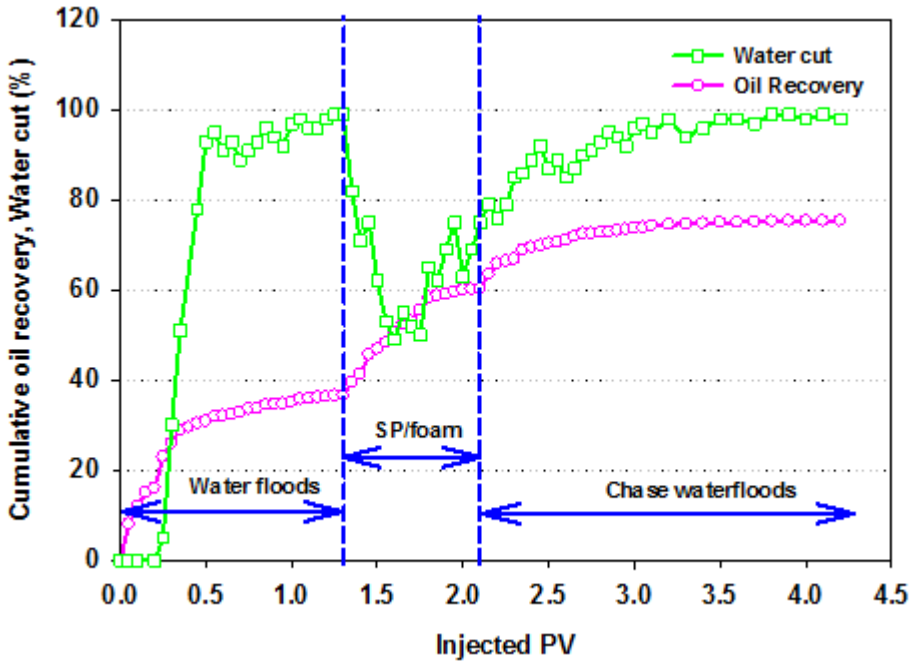

Fig.4.41 The water cut and cumulative oil recovery of Mode C under miscible condition (50 °C, 13.79 MPa)

4.3.1.2 Core Flooding Experiments under Immiscible Condition

In order to investigate the effect of injection pressure and hence the miscibility on the displacement performance, another set of core flooding experiments are conducted under immiscible conditions. Similar the earlier set of the experiments conducted under miscible condition, apart from the way in which the supercritical CO_2 and chemicals are introduced into the core plug, the experimental conditions and overall procedure remains consistent in all the experiments conducted in this set of experiments. A summary of the results obtained are presented in Table 4.8.

Similar to the experiments conducted under miscible condition, several important aspects of the results obtained from this new set of core-floods will be discussed in details in the upcoming sections of this chapter.

Table 4.8 Summary of the results of the core flooding experiments conducted under immiscible condition.

(50°C, 8.27 MPa**)**

Experiment	#4	#5	#6
Porosity (%)	18.1	17.6	18.3
Gas permeability (mD)	463.52	443.31	468.14
Brine permeability (mD)	369.51	354.69	373.77
Tertiary mode	A	B	C
Total amount of gas and chemicals used	0.4 PV supercritical CO_2 + 0.4 PV SP solution	0.4 PV supercritical CO_2 + 0.4 PV SP solution	0.4 PV supercritical CO_2 + 0.4 PV SP solution
Injection scheme	0.8 PV foam[#]	(0.2 PV CO_2 + 0.2 PV SP solution) *2	(0.3 PV foam[#] + 0.1 PV SP solution) *2
Initial oil saturation (%)	67.3	69.4	70.1
Water floods recovery (%)	33.8	34.5	31.4
Tertiary oil recovery (%)	24.2	20.9	30.7
Max. pressure drop (KPa)	421.9	411.6	637.1
Overall oil recovery (%)	58.0	55.4	62.1

4.3.1.2.1 Pressure Drop

This subsection presents a detailed discussion and interpretation of the pressure drop histories during the core flooding processes which were performed under immiscible condition. Such data are illustrated in Figs. 4.42-4.44. It is worth noting that the pressure behaviour and the corresponding mechanism behind it in the secondary water flooding phase of every experiment is very much the same as that observed in miscible condition experiments. Consequently, the focus of the discussion presented here would be on the differential pressure variations during the various tertiary injection modes applied.

As expected and evident from Fig. 4.42, the pressure drop substantially increases right after initiating the direct foam flooding (Mode A). However, it quickly decreases by a substantial amount as once only a small volume of CO_2 foam is injected. This is not something which was observed in the case of miscible condition injection. It is well known that the foam would break down once in contact with the crude oil even if the formula is well designed to make the foam oil-tolerant. As a result, the CO_2 could separate from the foam and become a

continuous phase and advance through the porous medium. It is no doubt that a partial CO_2 would enter the regenerated foam, yet most of it is released and is not capable of being miscible with the residual oil in place because of the relatively low pore pressure. Instead, the CO_2 can cause enhanced recovery by only swelling the oil and making it less viscous. However, under the conditions applied here the CO_2 mobility is much greater than that under the miscible condition, which explains the fast drop of the differential pressure. As apparent from Fig. 4.42, another intriguing feature is that the pressure drop across the core plug fluctuates noticeably during the chase water-flood phase. This behaviour is possibly because the more mobile CO_2 flowing in the pore channels allows the regeneration of the foam with the adsorbed surfactant, which slows down the decline of the pressure drop to some extent.

As can be seen from Fig. 4.43, Mode B injection seems to present an interesting scenario because it is found that its highest pressure drop during the alternating injection of supercritical CO_2 and chemicals is not much lower than that under miscible condition. This phenomenon is largely associated with the effect of the SP solution on supercritical CO_2: although the CO_2 can still escape from the ruptured foam and form a continuous phase, its mobility is greatly modified by the alternately injected SP solution, taking into consideration that the chemicals would not completely interact with the injected CO_2. Thus, it serves like a piston somehow to control mobility and make the immiscible CO_2 to advance relatively evenly.

When it comes to Mode C, the impact of the SP solution on CO_2 is still evident. However, it appears that the foam/SP synergism has become weaker than that under miscible condition. This would become clearer if the maximum as well as the average differential pressures are compared between the two conditions of miscible and immiscible. This may possibly arise from the foam instability caused by the lower pore pressure, although Mode C is still endowed with the best pressure behaviour (i.e. higher average differential pressure) among the three tertiary injection modes even under immiscible condition.

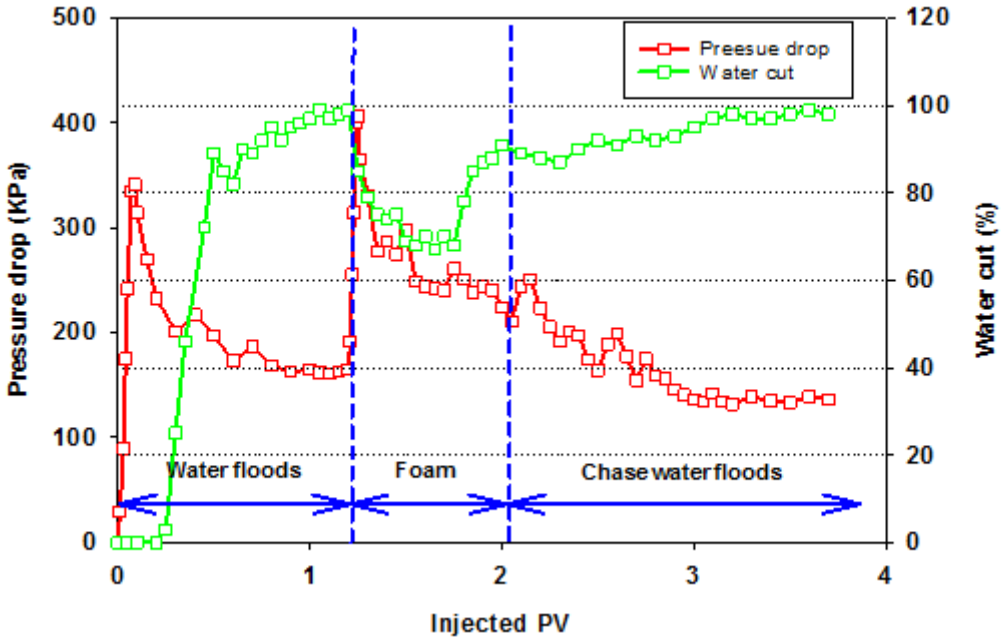

Fig. 4.42 The water cut and pressure drop history of Mode A under immiscible condition **(**50°C, 8.27 MPa**)**

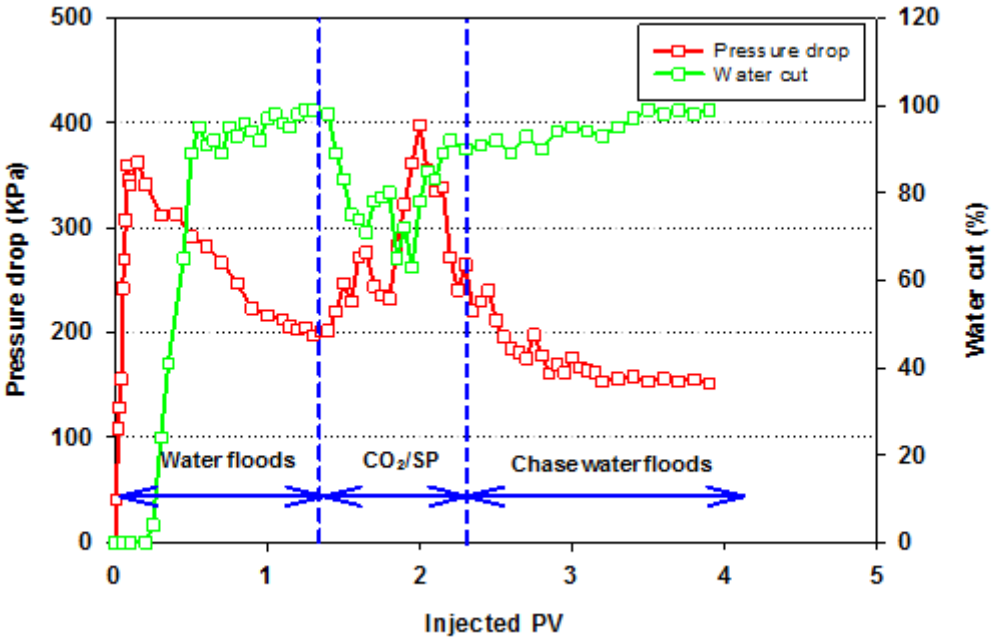

Fig. 4.43 The water cut and pressure drop history of Mode B under immiscible condition **(**50 °C, 8.27 MPa**)**

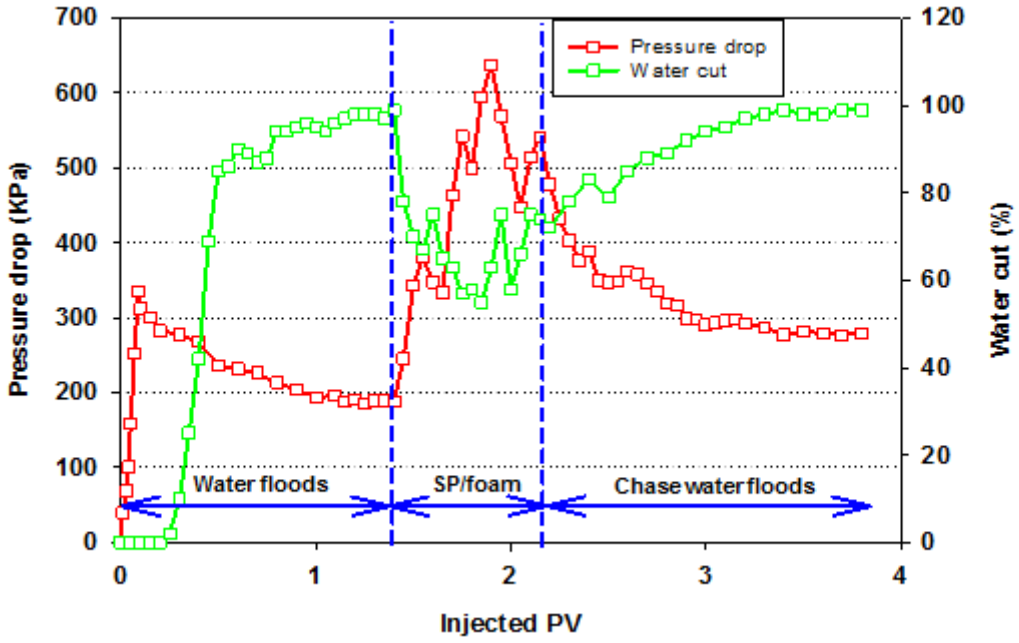

Fig. 4.44 The water cut and pressure drop history of Mode C under immiscible condition **(**50°C, 8.27 MPa**)**

4.3.1.2.2 Water Cut and Oil Recovery

The water cuts during the core flooding experiments are also presented in Fig. 4.42-4.44. Generally, regardless of the injection mode, the water content changes in a similar manner to that under the counterpart miscible conditions. That is, in general, the introduction of supercritical CO_2 and chemicals would significantly reduce the water production. On the other hand, it seems that the lower injection pressure negatively affects the water control performance of the various injection modes, making their water cuts not as low as the miscible condition injections. Nonetheless, Mode C produces the least amount of the water, while the water produced by modes A and B are comparable in the tertiary recovery phases.

As can be seen in Table 4.8, compared with the miscible condition experiments, due to the lower blocking ability of the injected fluids and higher water content in the effluents, the overall oil recoveries of all three modes have decreased by some extent. This is a reflection of the less encouraging displacement efficiency of the core flooding experiments conducted under immiscible condition. Furthermore, it is found that although Mode B still has the lowest total oil recovery, the oil recovery differences among the three modes has narrowed.

Especially for modes A and B which recover nearly the same amount of crude oil (if the data are evaluated within the accuracy of the measurement techniques) while their recovery factors differed under miscible condition. In agreement with its water production profile, Mode C yields the most oil among the three injection modes. However, as clearly illustrated in Fig. 4.45, its advantage in this regard over the other two modes is less evident under immiscible condition.

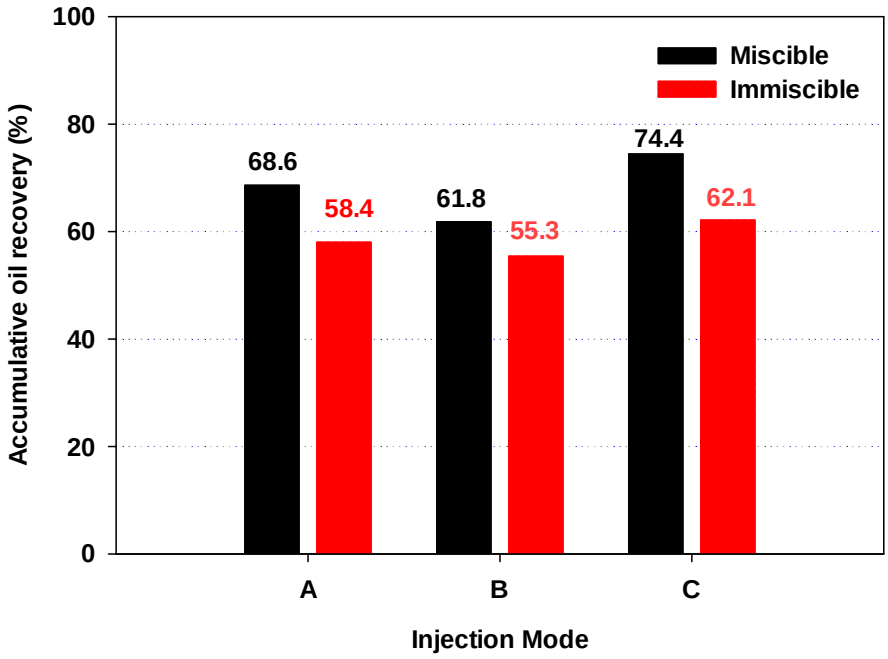

Fig. 4.45 Comparison of recovery factors under different injection modes and pressures (50°C)

4.3.2 Optimization of CAF Flooding

The data and results presented in this chapter so far have all revealed the high displacement efficiency of the CAF flooding over either the direct foam injection or the co-injection of gas and chemical solution assuming that the same amounts of CO_2 and chemicals are applied in every case. In this part of the chapter, a series of optimization studies have been conducted to maximize the displacement efficiency of the proposed CAF flooding in porous rocks. The total amount of the gas and chemicals involved in each experiment is maintained at 1.8 PV. The flood variables such as the foam quality, slug size and cycle number are assessed and adjusted to provide the CAF floods with the optimal displacement outcomes. All the core floods are carried out at 50°C and 13.78 MPa unless otherwise specified.

4.3.2.1 Effect of Foam Quality (gas/liquid ratio) on the Displacement Efficiency of CAF Flooding

The foam quality, which influences the foam rheological behaviour substantially, is considered to be a critical parameter in the foam flooding as well as the CAF flooding. In every core flood conducted to examine the effect of foam quality, the foam and the chemical slug are injected into a core plug in 3 cycles. In each cycle, the slug size of both the foam and the chemical are fixed at 0.3 PV. The foam quality ranges from 40% to 95% in different runs, as presented in Fig. 4.46. The experimental conditions and corresponding results are demonstrated in Table 4.9 and Fig. 4.47. With the gas fraction increasing, the amount of the produced foam would increase accordingly, which, as can be seen, boosts the overall displacement efficiency. It is noticeable that the tertiary oil recovery decreases once the gas/liquid ratio (foam quality) exceeds a certain value, which may indicate early gas breakthrough to have occurred in the foam slug due to the high mobility of the gas phase. Consequently, reliable foams cannot be obtained, even if the existence of the SP solution mitigates this issue to some extent. The recovery variation also can be explained with the varying foam apparent viscosity, as illustrated in Fig. 4.48. The maximum foam apparent viscosity is obtained under a specific foam quality known as the transition foam quality which is roughly 80% in this case. Neither low nor high foam qualities are capable of producing a thick foam. However, remarkable blockage is expected to be achieved around the transition foam quality. Consequently, more incremental oil is recovered compared to other CAF floods with the same amount of gas and chemicals injected.

Table 4.9 Summary of the results of the investigation performed on the foam quality of CAF flooding

(50°C, 13.78 MPa**)**

Run No.	1	2	3	4
Porosity	17.1%	17.0%	17.2%	17.1%
Permeability	404.31 mD	399.73mD	408.77 mD	401.63 mD
Chemical size in each cycle	0.3PV	0.3PV	0.3PV	0.3PV
Foam size in each cycle	0.3PV	0.3PV	0.3PV	0.3PV
Foam quality	40%	60%	80%	95%
Cycle number	3	3	3	3
Initial oil saturation	71.4%	70.5%	70.6%	71.0%
Recovery after water floods	40.2%	40.6%	40.5%	39.8%
Recovery by CAF floods	20.3%	37.1%	45.6%	25.2%
Cumulative oil recovery	60.5%	77.7%	86.1%	65.0%

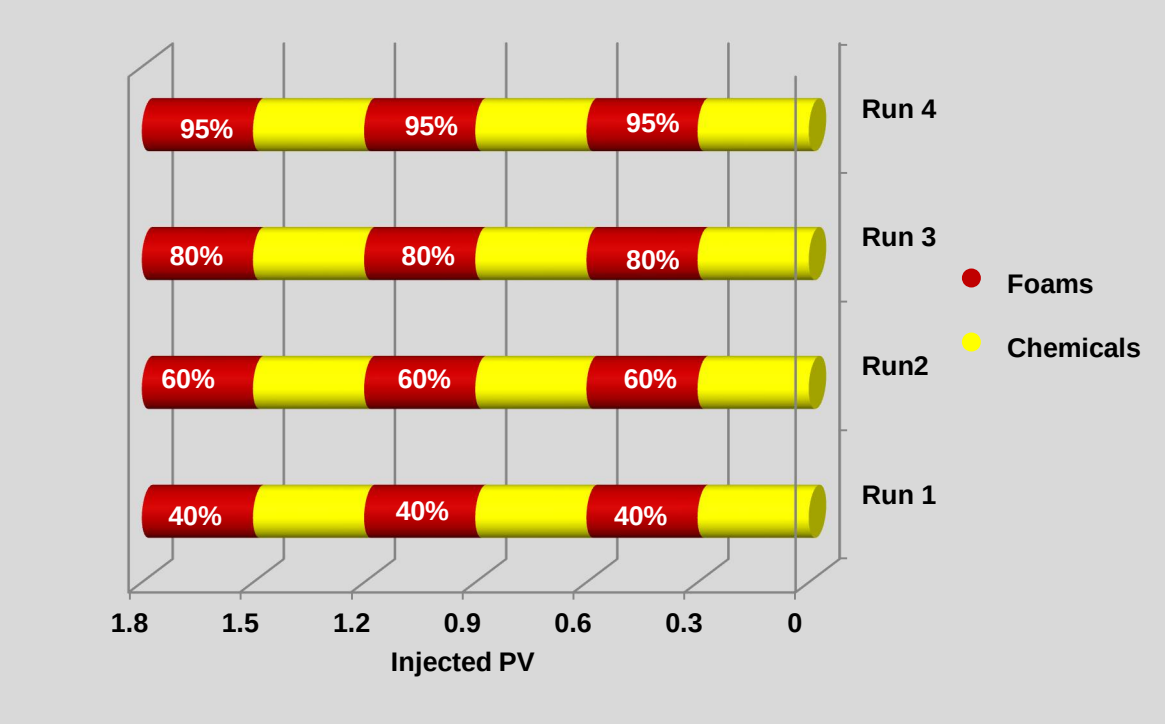

Fig. 4.46 Illustration of the CAF flooding with various foam qualities **(**50°C, 13.78 MPa**)**

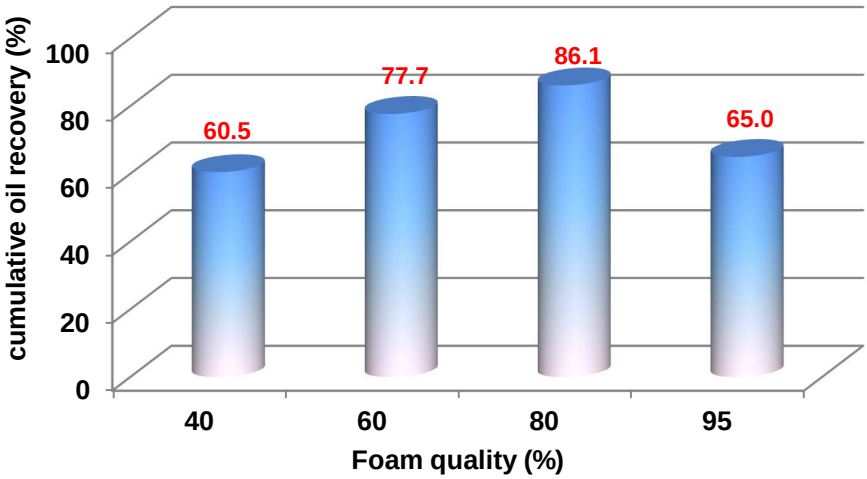

Fig. 4.47 Effect of the foam quality on the cumulative oil recovery **(**50°C, 13.78 MPa**)**

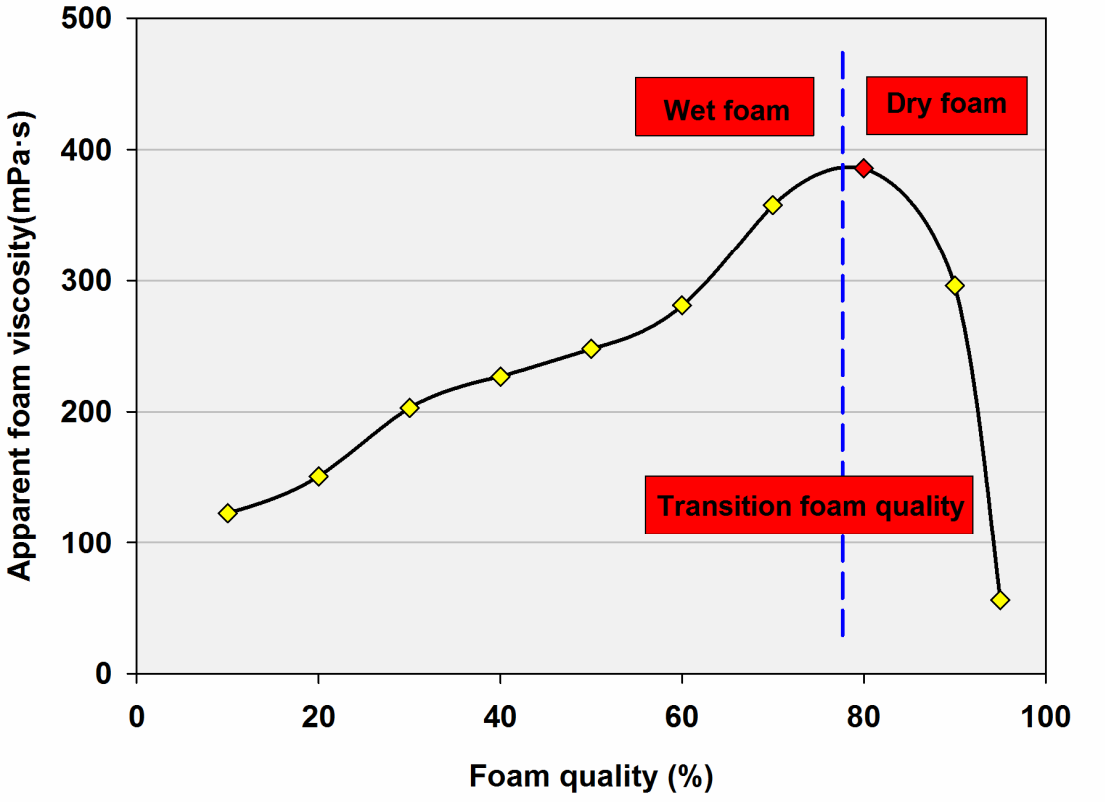

Fig. 4.48 Effect of the foam quality on the foam apparent viscosity.

4.3.2.2 The Effect of Slug Size on Displacement Efficiency

In the next step, core floods are carried out to investigate the dependence of the displacement efficiency on the foam and chemical slug sizes. The foam and the chemical slugs are injected into a core plug in three cycles, making the total amount of the foam and chemicals 0.6 PV for each cycle. The foam quality is kept at 80% for all the core floods, while the sizes of the foam and chemical slugs are varied in different runs, as presented in Fig. 4.49.

The results of the runs are summarised in Table 4.10 and Fig. 4.50. After comparing the outcomes of all the experiments, Run 3 is selected as the best injection strategy. The assessment results demonstrate that if the chemical and foam slugs are injected with the identical volumes for each cycle, it would be more beneficial compared to the other scenarios. This particular outcome is primarily attributed to the comprehensive interaction of the foam and chemical slugs. On one hand, if the foam slug size is greater than that of the chemical slug in one cycle (Run 1 and Run 2), the chemical slug is not capable of offering adequate stabilization and protection for the foam. As a consequence, the performance of the CAF flooding may be very much similar to that of the conventional foam flooding. On the other hand, if the amount of the chemical slug surpasses that of the foam slug in one cycle (Run 4 and Run 5), the foam slug is prone to be penetrated by the chemicals, which narrows the difference between the CAF flooding and chemical (surfactant/polymer) flooding. In both scenarios, the synergism of the foam and chemicals is negatively affected and accordingly the displacement performance of the CAF flooding is badly compromised.

Another intriguing feature of the results achieved is the varying recoveries of the cases where the foam and chemical slugs are not with the same size. It appears that the cases where the foam slug is larger (Run 1 and Run 2) produce more incremental oil compared to the cases where the chemical slug is larger (Run 4 and Run 5). This recovery variation is closely associated with the viscosity difference of the foam and the SP solution. As can be seen in Fig. 4.48, the foam viscosity at transition foam quality reaches up to 350 mPa·s, but as for the SP solution, the viscosity would be far lower at the given temperature and shear rate. Subsequently, more areas could be swept and more incremental oil is yielded by the foam-dominated floods (Run 1 and Run 2). Still, Run 3 with the identical size of the foam and chemical slugs performed the best among the experiments conducted. Its advantage over the others can be validated by Fig. 4.51 which shows the water cut variation during the CAF floods (the water cut reaches 99% after the secondary water floods and then the CAF and chase water floods are conducted). In other words, the outstanding performance of Run 3 is to

a great extent attributed to its remarkable capability to control water production, especially during the chase water flood.

Table 4.10 Summary of the results of the investigation performed on the slug size ratio of CAF flooding

(50°C, 13.78 MPa**)**

Run No.	**1**	**2**	**3**	**4**	**5**
Porosity	17.3%	17.0%	17.2%	17.2%	17.1%
Permeability	409.62 mD	402.73 mD	408.70 mD	415.63 mD	401.17 mD
Chemical size in each cycle	0.1PV	0.2PV	0.3PV	0.4PV	0.5PV
Foam size in each cycle	0.5PV	0.4PV	0.3PV	0.2PV	0.1PV
Foam quality	80%	80%	80%	80%	80%
Cycle number	3	3	3	3	3
Initial oil saturation	69.9%	69.4%	70.6%	69.1%	70.1%
Recovery after water floods	39.5%	40.2%	40.5%	39.9%	40.3 %
Recovery by CAF floods	32.4%	35.9%	45.6%	27.5%	20.5%
Cumulative oil recovery	71.9%	76.1%	86.1%	67.4%	60.8%

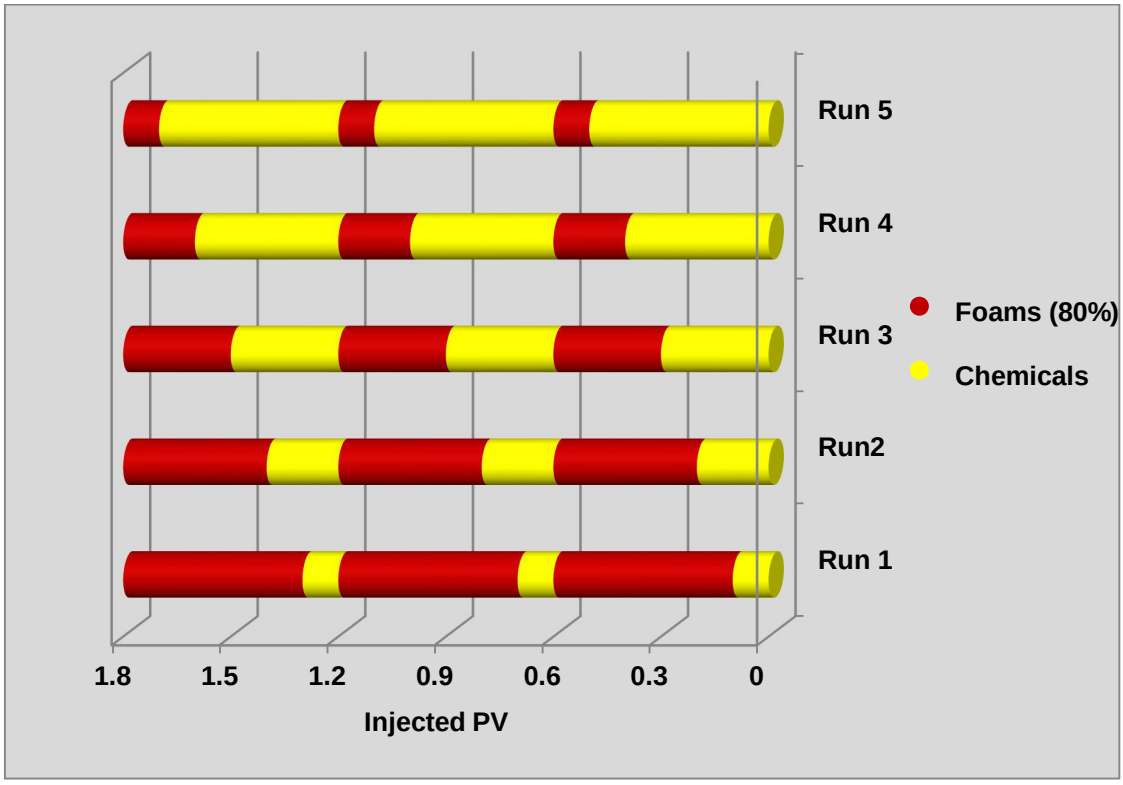

Fig.4.49 Illustration of the CAF flooding with various foam/chemical slug size ratios (50°C, 13.78 MPa)

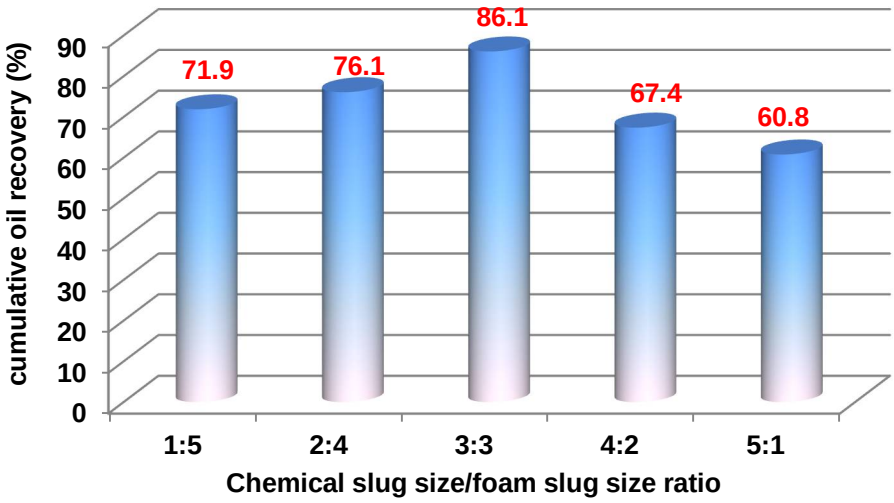

Fig. 4.50 Effect of the slug size ratio on the cumulative oil recovery of the CAF flooding (50°C, 13.78 MPa)

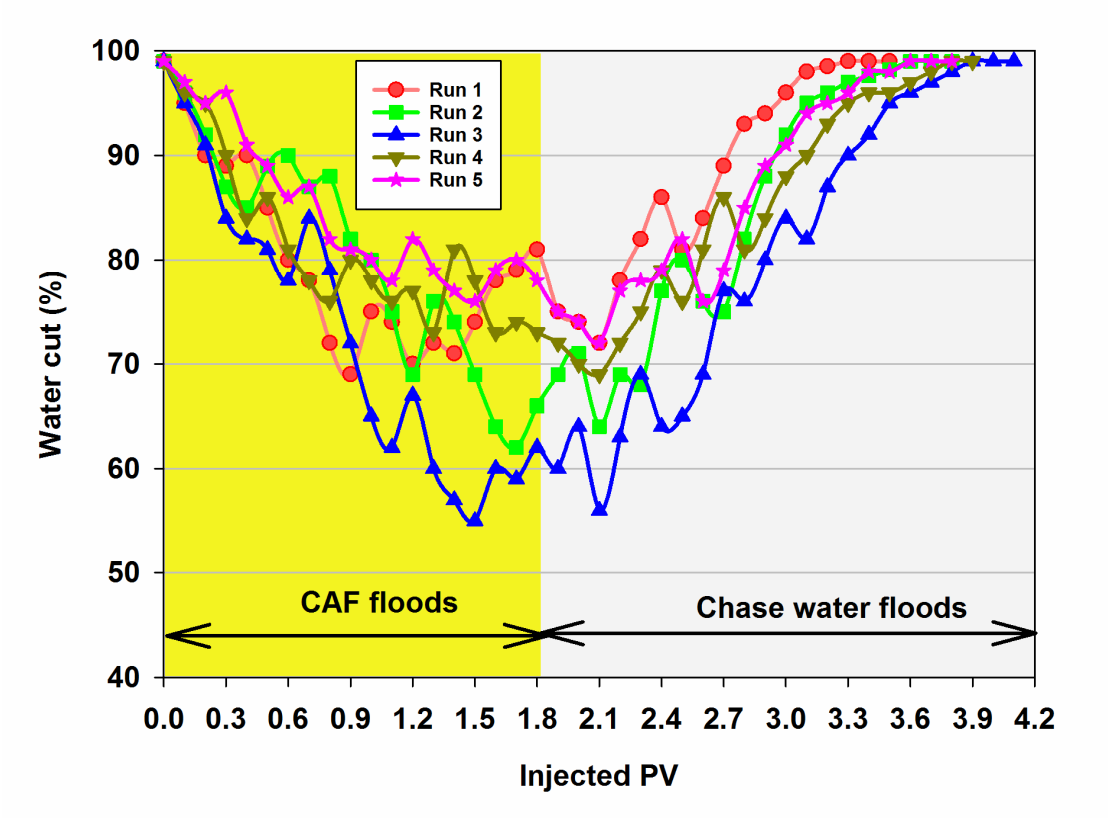

Fig. 4.51 The effect of the slug size ratio on the water cut in the CAF and chase water floods process **(**50°C, 13.78 MPa**)**

4.3.2.3 The Effect of the Injection Sequence on the Displacement Efficiency

The last part of the optimization work evaluates the influence of the injection sequence of the foam and chemical slugs on the displacement performance of the CAF flooding. Two core floods are carried out in this stage of the work. In every experiment, once the secondary water flooding is finalized, the foam and chemical slugs are injected into a core plug in 3 cycles with different sequences. In each cycle, 0.3 PV of foam and 0.3 PV of chemicals are included, as presented in Fig. 4.52.

The end results of the experiments are given in Table 4.11. Despite the identical foam quality, slug size ratio and cycle number in both experiments, their displacement efficiency is found to be, to some extent, dependent on the injection sequence of the foam and chemical slugs. Better performance is obtained in Run 1 with the chemicals being injected ahead of the foam, which is verified by its higher incremental oil recovery. The advantage of this injection sequence may be explained by a number of aspects of the injection process: 1) the polymer is capable of modifying the conformance, enabling the subsequent foam flood to sweep more areas; 2) the surfactant serves as the sacrificial agent and reduces the foaming agent loss of

the foam flooding; 3) the chemical flood prior to the foam injection decreases the oil saturation in the core plug, which is favourable for the foam longevity. However, as illustrated in Fig. 4.53, the recovery difference between the two experiments is not substantial, suggesting that the performance of the CAF flooding may not be a strong function of the injection sequence. To summarise, the injection sequence of the foam and chemical slugs may be expected to influence the performance of the CAF floods, but in a less noticeable manner compared to the other factors investigated earlier.

Table 4.11 Summary of the results of the investigation performed on the injection sequence of CAF flooding

(50°C, 13.78 MPa**)**

Run No.	1	2
Porosity	17.4%	17.1%
Permeability	408.75 mD	407.09 mD
Chemical size in each cycle	0.3PV	0.3PV
Foam size in each cycle	0.3PV	0.3PV
Foam quality	80%	80%
Initial injection slug	Chemical	Foam
Cycle number	3	3
Initial oil saturation	70.6%	70.1%
Recovery after water floods	40.5%	39.9%
Recovery by CAF floods	45.6%	40.5%
Cumulative oil recovery	86.1%	80.4%

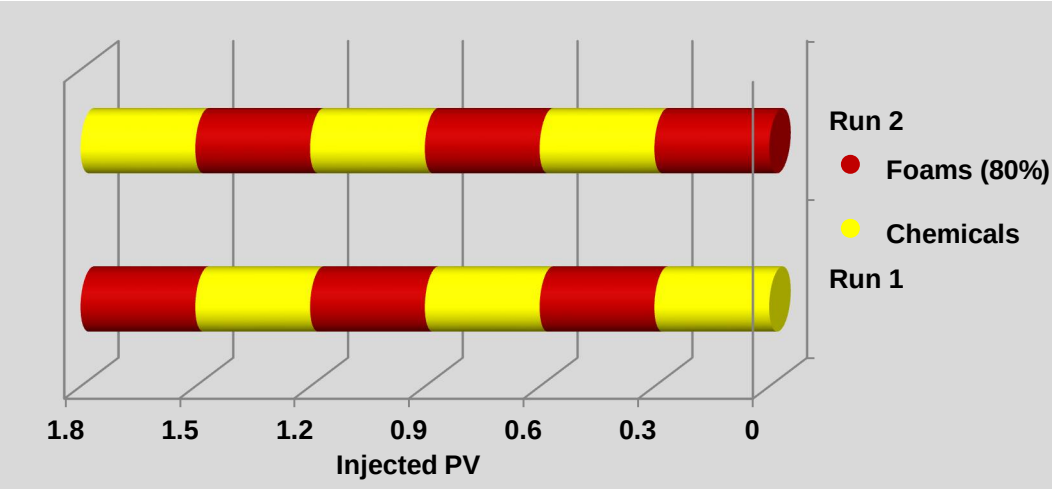

Fig. 4.52 Illustration of the CAF flooding with different injection sequence **(**50°C, 13.78 MPa**)**

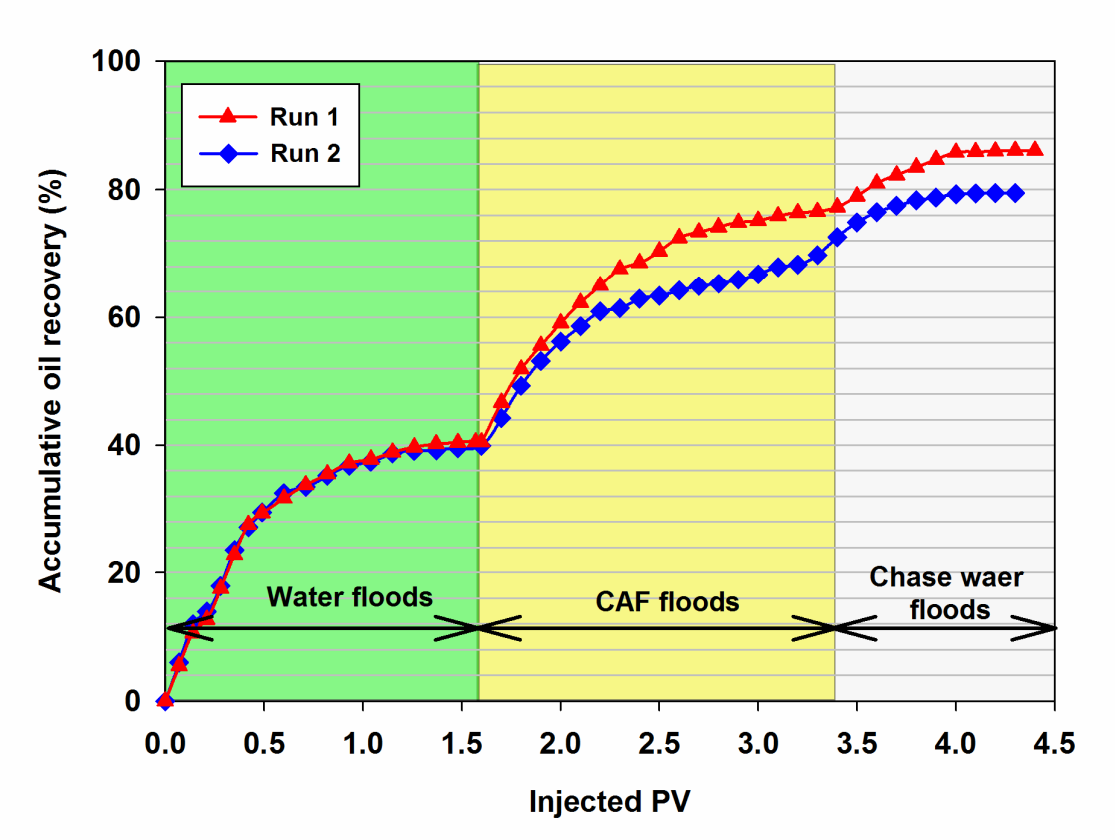

Fig. 4.53 Effect of the injection sequence on the accumulative oil recovery of the CAF flooding **(**50°C, 13.78 MPa**)**

References

Alvarez JM, Rivas HJ, Rossen WR, (2001). Unified model for steady-state foam behaviour at high and low foam qualities. SPE J. 6 (3): 325−333.

Binks BP, Kirkland M, Rodrigues JA, (2008). Origin of stabilization of aqueous foams in nanoparticle-surfactant mixture. Soft Matter, 4: 2373-2382.

Lee HO, Heller JP, Hoefer AMW, (1991). Change in apparent viscosity of CO_2 foam with rock permeability. SPE Reserv. Eng. 6 (04): 421-428.

Li H, Qin J, Yang D, (2012). An improved CO_2-oil minimum miscibility pressure correlation for live and dead crude oils. Ind. Eng. Chem. Res. 51: 3516−3523

Minssieux L, (1974). Oil displacement by foams in relation to their physical properties in porous media. J. Petrol. Technol, 01(26): 100-108.

Monsalve A, Schechter RS, (1984). The stability of foams: the stability of foams: Dependence of Observation on the Bubble Size Distribution. J. Colloid Interface Sci. 1 97(2): 327-335.

Osterloh WT, Jante MJJr, (1992). Effects of gas and liquid velocity on steady-state foam flow at high temperature. SPE/DOE Enhanced Oil Recovery Symposium, Tulsa, Oklahoma, US

Rosen MJ, Solash J, (1969). Factors affecting initial foam height in the Ross-Miles foam test. J. Am. Chem. Soc. 46(8): 399-402.

Sett S, Sahu RP, Pelot DD, Yarin AL, (2014). Enhanced foamability of sodium dodecyl sulfate surfactant mixed with superspreader trisiloxane-(poly)ethoxylate. Langmuir, 30 (49): 14765–14775.

Zhao J, Pu W, Li Y, Huang T, Wang C, (2014). Performance evaluation on a novel foaming formulation at elevated temperature and high salinity. Oilfield Chemistry, 32 (4): 65-69

Chapter 5 Summary, Conclusions and Recommendations

5.1 Summary

The international community's concern over fossil fuel supply and demand and global warming can be addressed with research and development into CO_2-EOR. This study proposes and examines a novel Chemical-Alternating-Foam (CAF) flooding scheme which couples chemical (surfactant and polymer) flooding with the conventional CO_2 foam flooding in an attempt to harness and combine the advantages of both of these two more common EOR techniques. Through systematic and thorough investigations, the CAF flooding has been found to be a viable and promising CO_2-EOR method.

This thesis has been organized in five chapters with Chapter 1 presented a brief background and the significance of CO_2-EOR as well as the research objectives.

Chapter 2 provided a comprehensive review of the developments made in the area of the CO_2-EOR related techniques, to date. The first part of this Chapter described the mechanisms, applications, strengths and faults of the widely acknowledged CO_2 flooding. Then the second part of this chapter mainly focused on a wide range of techniques formed around CO_2 flooding with the main objective of modifying the mobility ratio and controlling the injection profile with particular attention given to CO_2 foam flooding. In this chapter, the impediments to the wide application of the reviewed techniques are also provided and discussed in details.

Chapter 3 presented in details the properties of the experimental materials, such as the chemicals, crude oil and rock samples that are used in this research. Detailed experimental methodologies and procedures used were also provided in this chapter.

Chapter 4 described the development and assessment of a novel foaming formulation as well as the comparative and optimization study of the CAF floods which apply the proposed formulation. Furthermore, the interpretation, analysis and detailed discussion of the results obtained are included in this chapter.

Lastly, this chapter (Chapter 5) summarizes the research outcomes, and based on the experimental findings presented and discussed so far, several final conclusions are made. This chapter ends with a few recommendations for any future study built upon the results obtained in this research.

5.2 Conclusion

The chief conclusions which are derived from this experimental study and the corresponding interpretations and discussions are summarised as follows:

1. The development of a new foaming formulation for CO_2 foam floods:

- A number of commercially available surfactants were evaluated in terms of their foamability and foam stability through Warring blender method. The non-ionic candidates TMN-6, Triton X-100 and APG were not able to produce sufficient amounts of the CO_2 foams, though APG foam exhibited the longest lifetime than any other investigated surfactants.
- The amphoteric alternatives possessed both remarkable foamability and foam durability; however, their costly nature would hamper their large-scale field application.
- Anionic foaming agents AES and AOS had similarly outstanding foaming ability among the four assessed anionic products, but AOS had a far better foam longevity mainly due to its narrow distribution of bubble sizes. Therefore, AOS was selected as the foaming agent to be used in this study not only because of its comparable foamability and foam stability to its amphoteric alternatives but also due to its cost effectiveness.
- Compared to HPAM, AVS polymer had a higher capability to reduce surface tension, which was due to the introduction of hydrophobic as well as hydrophilic groups into the AVS molecules that were capable of adsorbing onto the gas/liquid interface.
- The addition of AVS into the foaming system could significantly enhance foam stability without lowering foamability to any great extent.
- The tertiary oil recovery of the CO_2 foam flooding enhanced by AVS was noticeable in both low and high permeability core plugs into which the foam was directly injected, exhibiting great potential for its application as an EOR agent.
- Regardless of the type and concentration, as may be expected, the addition of an additive or lamellae booster greatly promoted the foam longevity at the cost of foamability. However, the use of N70K-T in the AOS/AVS solution was found to greatly enhance the foam longevity without compromising foaming ability too much. Eventually, 0.5 wt % AOS + 0.15 wt% AVS + 0.5 wt% N70k-T was considered as the optimal foaming formulation that well balanced the foaming ability and foam stability.

- Despite the variations in the foaming formulation and rock permeability, the maximum foam apparent viscosity could be achieved under transition foam quality which seemed to be formulation dependent. As for each formulation, the apparent foam viscosity in the high permeability rock was larger than that in the low permeability rock under the same foam quality. However, the differences became less noticeable in low and high foam quality regions. It was noted that the apparent viscosity of the foam generated by AOS/AVS/N70K-T was the greatest among the three formulations, which could be attributed to its well-balanced foamability and foam stability giving rise to the generation of the strongest foam under the experimental conditions.
- Both of the resistance factor (RF) and residual resistance factor (RRF) could be correlated to the foam injection strategy. Compared to the simultaneous injection of the gas and foaming solution, direct injection of the foam with the assistance of the foam generator could produce foam more effectively in the porous medium leading to higher RF and RRF. In both of the foam injection modes, AOS/AVS/N70K-T foam possessed remarkable blocking and relative permeability modification abilities which facilitated the improvement of sweep efficiency of the foam and the chase brine displacement. Its superiority appeared to be associated with its unique 3D structure that gave rise to the flow resistance when advancing through the porous medium.
- The investigation on the mobility reduction factor (MRF) demonstrated that overall the injection rate (given gas/liquid ratio of 3:1) had evident effect on the MRF. As for the foaming formula without additives (AOS alone), a critical flow rate existed after which the MRF showed little variation. When it came to the formulae with additives (AOS/HPAM or AOS/HPAM/N70K-T), the MRF decreased as the total flow rate rose. In addition, AOS/HPAM/N70K-T displayed noticeable strength in terms of controlling the mobility, but the MRF's contribution among the formulations became less pronounced as the total injection rate increased. Furthermore, the gas flow rate (with a fixed liquid injection rate of 1.0 ml/min) also influenced the MRF. It was found that the MRF achieved the optimal value when the gas was flown at an intermediate rate, while it decreased at low and high gas flow rates irrespective of the formulation. This was attributed to the mixed effect of the foam quality and gas/liquid interface.

- After the water flooding under the secondary mode, CO_2 foam enhanced by AVS/N70K-T yielded higher enhanced oil recovery compared to the other two cases examined (AOS alone and AOS/HPAM). Its superior displacing performance was believed to be associated with the unique 3D structure that gave rise to the flow resistance when advancing through the porous medium.

2. Comparative study and evaluation of CAF flooding:

- Under an injection pressure which allowed the CO_2 and the crude oil to be completely miscible, the combined foam/SP flooding (CAF flooding) exhibited remarkable blocking ability which could be validated by its pressure behaviour during the core flooding. However, both of the direct foam flooding and the CO_2/SP flooding showed worse blocking ability either due to the foam instability or the low efficiency of the foam generation.
- Moreover, above the MMP, the CAF flooding possessed the best capacity of water control among the injection modes evaluated. Accordingly, its cumulative oil recovery was the highest making its advantage in this regard evident over its other two counterparts.
- Below the MMP, the CAF flooding still displayed the best performance with regards to the blocking ability, water cut control and improved oil recovery, but the differences were greatly narrowed as a consequence of the less pronounced synergism compared to that in the miscible condition
- The average water cuts of the direct foam flooding and CO_2/foam were close, resulting in nearly the same recovery factor below the MMP
- Based on the results achieved, it was suggested that the CAF flooding was more applicable to the reservoirs whose formation pressures were above the MMP. This injection mode was also found to be capable of significantly enhancing oil recovery below the MMP, but the displacement efficiency was not as encouraging as that above the MMP. Also it could not display evident advantage over the other two injection modes under the immiscible conditions.

3. Optimization study of the CAF flooding:

- Under the experimental conditions, 80% foam quality in the CAF flood was believed to be the optimal value.

- The assessment results demonstrated that it would be more beneficial if the chemical slug and foam slug were injected with identical volumes for each cycle.
- The injection sequence of the foam and chemical indeed influenced the CAF flooding performance, but in a less noticeable way compared to the other variables mentioned above.

4. Field scale implication

To date, the study on the CAF flooding is still in its preliminary stage. Extensive laboratory investigations have been conducted so far, however, numerical simulation along with the pilot test must be carried out if we intend to commercialize this novel CO2-EOR technology in the future. Consequently, such techniques are expected to come into the next research phase in the near future. In anticipation of the work suggested above, herein we briefly discuss the field scale application of the CAF flood investigated in this laboratory study:

- *Rock types*: The samples used in this research were sourced from sandstone reservoirs or quarried sandstone blocks. If similar investigation and evaluation could be done on other rock types, the application of CAF may be extended. For example, it is estimated that carbonate reservoirs hold around 60% of the world's oil. In the Middle East oil is predominately produced from heterogeneous carbonate fields. Such reservoirs are expected to be well suited candidates for CAF flooding. In general, the injected CO_2 dissolves in the formation brine and lowers the pH of the brine. Subsequently, the carbonate rock would be dissolved and the porosity and permeability may be favourably changed. From this point of view, CAF flood can possibly live up to the expectation of petroleum engineers, since high permeability is considered to be favourable to the foam flooding. However, as widely known, carbonate rocks tend to be highly heterogeneous on all scales, making reservoir characterisation and laboratory investigations very challenging As for the unconventional reservoir rock, such as shale, the CAF flood may encounter numerous geological and technique barriers as the ultralow permeability of such rocks poses a huge resistance for the chemicals to pass through.
- *Reservoir heterogeneity*: However, almost all the oil reservoirs exhibit some degree of heterogeneity in the real life. The CAF flood can to some extent control the profile and mitigate the adverse effects of the reservoir heterogeneity as this capability is a natural feature of both foam flooding and SP flooding. However, if fracture corridors

exist (primarily in carbonate reservoirs), the chemicals would preferentially flow through these highly conductive pathways and leave the target zone unswept. Of course, pre-treatment operations such as in-situ gel formation can be carried out before the implementation of the CAF flooding to minimize the influence of the existing fractures, but such operations can increase the overall cost of the EOR process. Another option is to increase the polymer concentration in the CAF flooding, since the polymer may, to some extent, block the fractures similar to the gel, but again the increase in the cost would be an issue.

- *Reservoir temperature*: There is no doubt that the performance of nearly all the categories of chemical flooding are strongly dependent on the reservoir temperature. Elevated reservoir temperature (above 85ºC) could be harmful to the applied polymer as they may undergo thermal degradation, so that the polymer could neither stabilize the foams nor modify the mobility ratio. When it comes to the foaming agent or the surfactant, high temperature effect is two folds. On one hand, extensive research has confirmed the significant activity loss of surfactant if the temperature increases to 85ºC. On the other hand, with increase in temperature, the surfactant loss due to the adsorption onto the reservoir rock would be intensified. Other chemicals or additives also suffer from high reservoir temperature. Most likely, the CAF floods would become ineffective in offshore reservoirs whose temperature are normally greater than 80ºC. Needless to say, the polymer and surfactant that are able to resist elevated temperature do exist, and the performance of CAF flooding would be enhanced if these chemicals are applied. Nonetheless, the overall operation cost will be the major concern when the chemicals applied in this research are to be replaced by the thermal-resist ones.
- *Brine salinity and composition*: In this research, except the additive, both the surfactant and polymer are ionic. The salinity and composition of the formation brine can always have significant impact on the performance of chemical floods through influencing the behaviour of the ionic chemicals used. Generally, high salinity negatively affects the effectiveness of both surfactant and polymer, lowering the foamability and foam stability simultaneously. Compared to Na^+, the Mg^{2+} and Ca^{2+} that are common in the formation brine of offshore reservoirs would be more detrimental. Unless special chemicals that possess salinity resistance are used in the CAF flooding, its application in the offshore reservoirs is not promising at this stage.

Again, if the chemical formulations of the CAF is to be altered, the cost needs to be acceptable in the industrial scale. In other words, affordable but effective surfactant and polymer agents need to be developed if we intend to employ CAF flood in reservoirs with high salinities.

- *Formation pressure*: As stated in the previous chapter, CO_2 is existed in the supercritical state in laboratory investigations performed in this work. If CO_2 is in gaseous or liquid phases, the performance of the CAF flood could be completely different. Therefore the reservoir pressure should be evaluated before the implementation of the results achieved here. Furthermore, the reservoir pressure can control the CO_2 miscibility with the crude oil, which in turn influences the displacement efficiency of the CAF flooding, indirectly. On the other hand, formation pressure has little effect on the behaviour of the surfactant and polymer, as validated by numerous other research works. In general, the CAF flooding may obtain greater recovery factor at higher formation pressures if the foam stability as well as the CO_2 miscibility are taken into account.

5.3 Recommendations

Needless to say, due to time and resources limitations, this research does not cover all the aspects related to the CAF floods. A few further characteristics of CAF flooding whose investigation may deepen the understanding of this proposed CO_2-EOR technique and thus deserve further investigations are listed below:

- The samples used in this work were all sandstone with permeabilities ranging from 100 mD to 400 mD. Since the rock type along with the rock permeability can impose pronounced impact on the CO_2-involved multiphase flow and thereby the outcomes of the CAF floods, further investigation on the carbonates and sandstones with a wider range of permeability are recommended.
- The composition, viscosity and API degree of the crude oil influences the CO_2 foam as well as the behaviours of the chemicals. The displacement performance of the CAF flooding, therefore, is largely dependent on the oil properties. As a result, it would be beneficial to use different oil samples to verify the broad applicability of the CAF floods.

- In this research, majority of the work was conducted at 50°C and 13.79MPa. The dependence of the EOR capability of the CAF floods on the temperature and pressure may be an interesting subject and deserves further study.
- Only fairly homogeneous rock samples were used during this study. In order to gain a more comprehensive perspective of the proposed CAF flooding, the effect of both vertical and areal heterogeneities on the multiphase flow and displacement performance of this new EOR technique should be evaluated.
- With the assistance of X-ray CT technology, visual observation of the multiphase flow during the flooding process could be achieved. Subsequently, the mechanisms behind the outstanding behaviour of CAF flooding may be better understood.
- Simulation study via commercial software such as CMG, Eclipse and Ansys, to some extent, may enable the prediction of the EOR potential of the CAF flooding in real field operations.